www.reanimatology.com
ISSN 2411-7110 (online)

GENERAL REANIMATOLOGY

SCIENTIFIC-AND-PRACTICAL JOURNAL

ОБЩАЯ РЕАНИМАТОЛОГИЯ

научно-практический журнал

Volume 22 Том 22

№ 3

Information from the AI Use Policy

Dear Authors,

Please note the following:

Beginning in August 2026, authors are required to disclose the use of AI tools during manuscript preparation when submitting manuscripts to the journal «General Reanimatology».

Information regarding the use or non-use of AI should be provided at the end of the «Materials and Methods» section, following the description of statistical data processing methods, under the subsection «Information on the Use of Artificial Intelligence».

This subsection specifies:

1. The AI model(s) and software version(s) used.
2. The sections of the article (including illustrations and references) and the technical tasks (such as style refinement, translation, etc.) in which AI was used.
3. The main instructions provided to the AI (the core prompts).

A copy (or copies) of the full prompt(s) must be provided upon request by the reviewer or editor if clarification of the logical structure of the AI-generated text is required.

The use of AI is not permitted in formulating the research and/or practical objectives of the work, discussing the results, or drawing conclusions.

If the authors prepared the article materials without the use of AI, the relevant subsection should state: «Artificial intelligence was not used in the preparation of this article».

Sincerely,
Editors of the «General Reanimatology» Journal

ISSN 1813-9779 (print) ISSN 2411-7110 (online)

GENERAL REANIMATOLOGY

OBSHCHAYA REANIMATOLOGIYA

Scientific-and-Practical Peer-Reviewed Journal
Since 2005

• Covers issues of critical care medicine
• Manuscripts in Russian and English are published free-of-charge
• Included in SCOPUS (since 2015), RINTs, RSCI, DOAJ, and other databases, as well as in the Official list of editions recommended for publication of dissertations (PhD, DSci) by the Russian Higher Attestation Commission

Registration certificate of the Journal «Obshchaya reanimatologiya» (General Reanimatology): ПИ № ФС77-18690, November 2, 2004, Federal Service for Supervision of Compliance with Legislation in the Sphere of Mass Communications and Protection of Cultural Heritage

Publication Frequency: 6 numbers per year.

Founder:

ОБЩАЯ РЕАНИМАТОЛОГИЯ

OBŜAÂ REANIMATOLOGIÂ

научно-практический рецензируемый журнал
Выходит с 2005 г.

• охватывает вопросы медицины критических состояний
• публикует рукописи на русском и английском языках бесплатно
• включен в базы данных SCOPUS (с 2015 г.), РИНЦ, RSCI, DOAJ и др. базы данных; Перечень изданий, рекомендованных ВАК для публикации результатов диссертационных работ

Свидетельство о регистрации: ПИ № ФС77-18690 от 02 ноября 2004 г. Печатное издание журнал «Общая реаниматология» зарегистрирован Федеральной службой по надзору за соблюдением законодательства в сфере массовых коммуникаций и охране культурного наследия.

Периодичность: 6 раз в год

Учредитель:

Publisher:
Federal Research and Clinical Center of Intensive Care Medicine and Rehabilitology, Moscow, Russia
Издатель:
Федеральный научно-клинический центр реаниматологии и реабилитологии (ФНКЦ РР), Москва, Россия

Supported by Russian Federation of Anesthesiologists and Reanimatologists
При поддержке Общероссийской общественной организации «Федерация анестезиологов и реаниматологов»

Artwork: Natalia V. Golubeva
Page-proof: Sergey V. Shishkov
Printing House:
Printed at LLC «Advanced Solutions». 19, Leninsky prospekt, build. 1, Moscow, 119071. www.aov.ru
Contacts:
25 Petrovka Str., Bldg. 2, 107031 Moscow, Russia.
Tel. +7-495-694-17-73.
E-mail: **journal_or@mail.ru;**
Web: **www.reanimatology.com**

Subscription:
Index 46338, refer to catalog of «Книга-Сервис»
Signed for printing: 30.06.2026

Оригинал-макет: Н. В. Голубева
Верстка: С. В. Шишков
Типография: отпечатано в ООО «Адвансед солюшнз». 119071, г. Москва, Ленинский пр-т, д. 19, стр. 1. www.aov.ru
Контакты с редакцией:
Россия, 107031, г. Москва, ул. Петровка, д. 25, стр. 2.
Тел.: +7-495-694-17-73.
E-mail: **journal_or@mail.ru;**
сайт: **www.reanimatology.com**

Подписка и распространение: индекс издания по каталогу «Книга-Сервис» — 46338.
Цена свободная
Подписано в печать: 30.06.2026

CONTENTS **СОДЕРЖАНИЕ**

https://doi.org/10.15360/1813-9779-2026-3-2698

Prognostic Index for Compensation of Reduced Heart and Lung Functions in Patients with Sepsis

Sergey A. Andreychenko[1,2], Dmitry O. Ovcharov[1]*, Konstantin V. Yatskov[3], Georgy N. Arbolishvili[3], Maxim A. Rakhmanov[2], Tatyana V. Klypa[1,2]

[1] Federal Scientific and Clinical Center for Specialized Types of Medical Care and Medical Technology, Federal Medical-Biological Agency of Russia, 28 Orekhovy bulvar, 115682 Moscow, Russia

[2] Academy of Postgraduate Education, Federal Scientific and Clinical Center for Specialized Types of Medical Care and Medical Technologies, Federal Medical and Biological Agency of Russia, Department of Anesthesiology and Resuscitation, 91 Volokolamskoe Highway, 125371 Moscow, Russia

[3] Moscow Clinical Science and Research Center 52, Moscow City Health Department 3 Pekhotnaya Str., 123182 Moscow, Russia

For citation: *Sergey A. Andreychenko, Dmitry O. Ovcharov, Konstantin V. Yatskov, Georgy N. Arbolishvili, Maxim A. Rakhmanov, Tatyana V. Klypa.* Prognostic Index for Compensation of Reduced Heart and Lung Functions in Patients with Sepsis.*Obshchaya Reanimatologiya = General Reanimatology.* 2026; 22 (3): 4–12. https://doi.org/10.15360/1813-9779-2026-3-2698 [In Russ. and Engl.]

***Correspondence to:** Dmitry O. Ovcharov, odo1306@inbox.ru

Summary

Magnitude of heart rate (HR) fluctuation during sepsis and septic shock can significantly impact tissue perfusion and organ dysfunction.

The aim of the study is to examine and compare the predictive characteristics of a composite index based on clinical parameters and demographic variables for early risk stratification of mortality in patients with sepsis.

Materials and Methods. In a multicenter retrospective cohort study, data from 257 patients with sepsis or septic shock were analyzed, including age, sex, height, weight, severity of illness, comorbidities, bedside hemodynamic and respiratory monitoring parameters upon admission to the ICU, and 3 hours after the initiation of intensive therapy, as well as treatment outcomes. Statistical characteristics of the generated Prognostic Index for Compensation of Reduced Cardiorespiratory Function (PICRCF) were assessed, calculated as the ratio of the product obtained by multiplying heart rate by respiratory rate and by age to the product obtained by multiplying of diastolic blood pressure by body surface area (BSA). To identify clinical and laboratory predictors of fatal outcomes, all patients were divided into two groups: survivors and those who died during treatment.

Results. The hospital mortality rate in the analyzed patient sample was 48%. Differences were found between those who died and those who survived in terms of age, scores on the Glasgow (RR), heart rate (HR), and blood pressure (BP), as well as PICRCF values both upon admission ((PICRCF 0) and after 3 hours of intensive care ((PICRCF 3). Notably, (PICRCF 3 demonstrated the highest discriminative performance among all studied predictors (AUC 0.800; 95% CI 0.744–0.855) with a cutoff value of 1.1 (sensitivity 69%, specificity 85%). In the Cox proportional hazards model, (PICRCF 3 was the only independent predictor of mortality (OR 1.313 (95% CI 1.062–1.623), $p=0.012$). Additionally, PICRCF values were associated with the number of days without organ replacement support.

Conclusion. The indicators reflecting the state of the cardiovascular and respiratory systems, indexed according to anthropometric and age characteristics, have several advantages over standard prognostic scales in the early risk stratification of patients with sepsis. The simplicity, accessibility, and rapid measuring of the components for calculating PICRCF allow for dynamic assessment of the patient's condition from the first minutes of admission to the ICU.

Keywords: predictive compensation index; reduced heart and lung function; mortality prediction in sepsis; sepsis; ICU

Conflict of interest. The authors declare no conflict of interest.

Information about the authors:
Sergey A. Andreychenko: https://orcid.org/0000-0002-3180-3805
Dmitry O. Ovcharov: https://orcid.org/0009-0000-9373-4887
Konstantin V. Yatskov: https://orcid.org/0000-0003-0125-9068
Georgy N. Arbolishvili: https://orcid.org/0000-0002-2252-3975
Maxim A. Rakhmanov: https://orcid.org/0009-0008-3524-2698
Tatyana V. Klypa: https://orcid.org/0000-0002-2732-967X

Introduction

Sepsis and septic shock are life-threatening complications, and intensive care for these conditions is aimed at restoring and maintaining adequate tissue perfusion [1]. The substrate for the deterioration of patient's condition is usually a combination of hemodynamic disturbances, the primary one being a decrease in vasomotor tone. In this context, vasoplegia has the most pronounced effect on diastolic blood pressure (DBP) compared to systolic blood pressure (SBP) or mean arterial pressure (MAP) [2].

However, DBP should not be assessed in isolation from heart rate (HR). A generalized infection activates the sympathetic nervous system, leading

to the release of endogenous catecholamines and tachycardia. This biological mechanism is aimed at compensatory maintenance of cardiac output and vascular tone [3]. Nevertheless, persistent tachycardia contributes to increased myocardial oxygen consumption and may exacerbate coronary hypoperfusion [4]. Furthermore, prolonged sympathetic activation promotes the development of autonomic nervous system dysfunction [5].

The degree of changes in the combination of increased HR and decreased DBP can be assessed using the diastolic shock index (DSI). Several studies have demonstrated that opposing pathophysiological deviations in DBP and HR may indicate severe cardiovascular dysfunction, where increasing tachycardia is unable to compensate for diastolic hypotension. This allows the DSI to be used as a clinically significant predictor of adverse outcomes in a wide range of critical conditions [6–8].

In addition to arterial hypotension, tachycardia is associated with a number of clinical and demographic parameters. Although there is no evidence of a direct correlation, there is likely a certain inverse relationship between HR and body surface area (BSA) [9]. In turn, BSA, in addition to its wide clinical application as a biometric unit for standardizing physiological parameters, can also be directly applied for prognostic purposes. The predictive value of BSA has been confirmed in patients with acute kidney injury, congestive heart failure, and sepsis [10–12].

During cardiorespiratory testing, which allows for an objective assessment of exercise tolerance, maximum HR is of particular clinical significance, as it decreases proportionally with the patient's age [13]. Thus, the prognostic significance of HR varies across different age groups [14].

Respiratory rate (RR) is a well-known parameter for assessing the condition not only of the respiratory system but also of the entire body as a whole. RR is associated with clinical deterioration and mortality in various patient cohorts [15]. At the same time, RR and HR are also interrelated in a certain way and can be used to predict mortality in critically ill patients [16].

We hypothesized that the combination of the listed clinical and demographic parameters could serve as a simplified equivalent of the functional status of the cardiovascular and respiratory systems in patients in the intensive care unit (ICU).

The aim of the study is to investigate and compare the predictive characteristics of a composite index based on clinical and demographic paramters for early risk stratification of mortality in patients with sepsis.

Materials and Methods

A multicenter retrospective cohort study was conducted at the ICU of the Central Clinical Hospital of Russian Railways-Medicine, the ICU of the Federal Scientific and Clinical Center of the Federal Medical and Biological Agency of Russia (FSCC FMBA), and ICU No. 8 of the Moscow Clinical Research Center of Hospital No. 52 of the Moscow City Health Department. The study included all patients with sepsis and/or septic shock hospitalized between January 2023 and December 2024. The criteria for «sepsis» and «septic shock» were defined in accordance with the Third International Consensus (Sepsis-3) [17]. The study was approved by the local ethics committee of the Federal Scientific and Clinical Center of the Federal Medical Biological Agency (Protocol No. 8_2023 dated September 12, 2023).

Patients who did not undergo invasive blood pressure monitoring, who were readmitted to the ICU, or who died within the first 3 hours after sepsis verification were excluded.

For analysis, data from electronic and/or paper medical records, including clinical and demographic characteristics of patients (age, sex, height, weight), assessment of severity of condition and comorbidities upon admission to the ICU (Glasgow Coma Scale (GCS), SOFA, APACHE II, Charlson Comorbidity Index), types of therapeutic modalities utilized (respiratory support and rate of mechanical ventilation (MV), vasopressor support, renal replacement therapy (RRT), as well as duration of treatment in the ICU, and outcome). Assessment of bedside vital signs was performed in two stages: the first upon the patient's admission to the ICU (BP_0, HR_0, RR_0); the second — 3 hours after initiation of intensive care (BP_3, HR_3, RR_3).

When processing missing readings median values were imputed, as their maximum proportion for each variable was less than 5%.

The Dubois formula was used to calculate BSA. DSI was calculated as the ratio of HR to DBP. We also assessed the statistical characteristics of a new indicator, named the prognostic index of compensation for reduced cardiorespiratory function (acronym «PICRCF»), calculated using the formula: PICRCF = (HR × RR × age / DBP × BSA) / 1000. For patients on mechanical ventilation, the default RR was set to 50. This figure was chosen based on the maximum rank value for RR in the APACHE II scale.

The hypothesis was that the predictive value of the composite PICRCF index would be higher than the predictive values of its components when used individually.

To identify clinical and laboratory predictors of mortality, all patients were divided into groups of survivors and those who died during treatment.

Statistical analysis of the data was performed using IBM SPSS Statistics 31.0.0.0 (IBM Corporation, USA). Continuous variables were expressed as the median and quartiles (*Me* [*Q1*; *Q3*]) and analyzed using the Mann–Whitney *U* test. Categorical variables were presented as absolute numbers and

percentages and analyzed using Pearson's χ^2 test or Fisher's exact test. Cox univariate regression was used to assess the association between mortality and indicators differing between groups. Variables with a *p-value*< 0.1 were included in a Cox proportional hazards multivariate regression model to identify independent predictors of in-hospital mortality. The assumption of proportional hazards for each predictor was assessed using log-log survival plots and analysis of partial (Schoenfeld) residuals over follow-up time. ROC analysis was performed to determine the cutoff point for the identified predictors. The optimal cutoff value, providing the best balance between sensitivity and specificity, was determined using the Youden index. The strength of the relationship between variables was assessed using Spearman's rank correlation coefficient. Two-sided *p-value*< .05 were considered statistically significant.

Sample adequacy was determined based on the «10 events per variable» (EPV) rule for Cox multivariate regression. Based on the estimated hospital mortality rate for sepsis in low- and middle-income countries of 40% [18], the minimum cohort size was 175 individuals. To account for an expected 20% rate of missing data (a conservative estimate based on a preliminary analysis of the local database), the target number of observations was increased to 219.

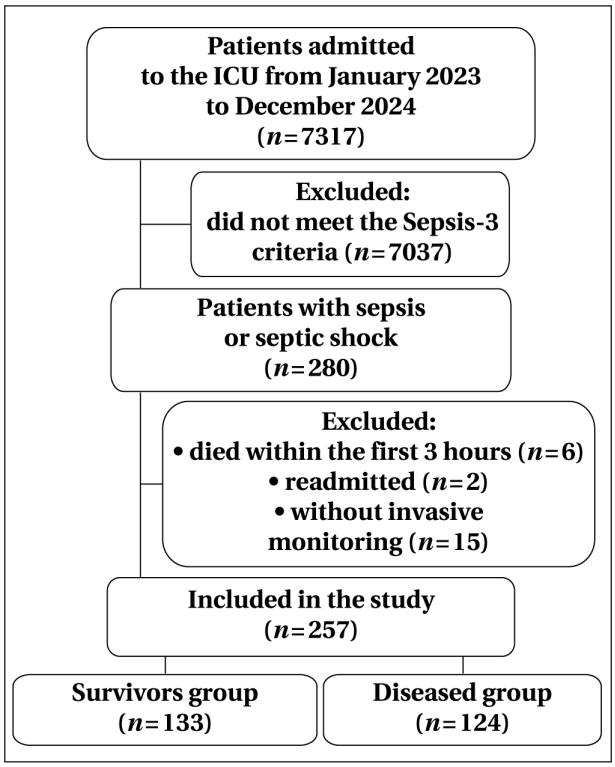

Fig. 1. Flowchart of patient selection for the study.

Results

The final study model included 257 patients (exceeding the minimum calculated sample size, n=219; Fig. 1).

In-hospital mortality was 48% (Table 1).

A comparison of parameters between surviving and deceased patients revealed significant differences in age, GCS, SOFA, APACHE II scores, and the Charlson Comorbidity Index (p< 0.001). Deceased patients also had lower BSA values and were more frequently diagnosed with AF upon admission to the ICU. No differences in gender distribution were observed. When comparing bedside monitoring, baseline HR_0 and RR_0 were higher in the group of deceased patients, while SBP_0 and MAP_0 were higher in the group of survivors. After 3 hours of intensive care, differences between the groups in hemodynamic and respiratory parameters persisted and became apparent, including in SBP3 levels. Baseline values of combined calculated indices (DSI_0 and $PICRCF_0$) also differed and were higher in the group of deceased patients (p< 0.001). After 3 hours of targeted intensive care, a similar trend persisted for DSI_3 and $PICRCF_3$.

The need for vasopressor support, MV, and RRT was higher in the group of deceased patients (p< 0.001).

After testing for multicollinearity among the clinically significant parameters differing between surviving and deceased patients, a univariate Cox regression analysis was performed (Table 2). Of the 7 variables included in the Cox proportional hazards multivariate model, only $PICRCF_3$ was statistically significantly associated with the risk of death in patients with sepsis (OR 1.313 (95% CI 1.062–1.623), p=0.012).

Among the early predictors of mortality studied, $PICRCF_3$ had the highest discriminatory power with an AUC of 0.800 (95% CI 0.744–0.855), a cutoff value of 1.1, with a sensitivity of 69% (95% CI 60–77%) and a specificity of 85% (95% CI 78–91%). The positive predictive value was 81% (95% CI 72–88%), and the negative predictive value was 74% (95% CI 67–81%). Furthermore, the predictive value of $PICRCF_3$ exceeded that of $PICRCF_0$ (Fig. 2, *b*).

In the correlation analysis, $PICRCF_3$ was also associated with the number of vasopressor-free days (*rho*=–0.5), ventilator-free days (*rho*=–0.5), and RRT-free days (*rho*=–0.3) (all p< 0.001).

Discussion

A hyperdynamic circulatory pattern with increased cardiac output and low systemic vascular resistance is the most typical course of sepsis and septic shock. However, prolonged sympathetic hyperactivation can lead to myocardial dysfunction characterized by a significant deterioration in hemodynamics in the context of tachycardia [19]. This relationship between heart rate and mortality can be described by a *U*-shaped curve. Thus, during sepsis, both very low and very high heart rates increase the risk of death [20]. However, international

Table 1. Clinical, demographic, laboratory, and diagnostic parameters of deceased and surviving patients with sepsis ($n = 257$).

Parameters	Parameter values in the groups		p
	Survivors, $n = 133$	Diseased, $n = 124$	
Age, years	64 [54–72]	71 [58–77]	< 0.001
Male, *n* (%)	71 (53.4)	73 (58.9)	0.376
BMI, kg/m²	27.0 [24.1–31.6]	25.1 [22.5–29.4]	0.006
BSA, m²	1.91 [1.79–2.07]	1.82 [1.69–1.97]	0.001
GCS, scores	15 [15–15]	15 [12–15]	< 0.001
SOFA, scores	6 [4–8]	8 [6–11]	< 0.001
APACHE II, scores	19 [16–24]	24 [20–29]	< 0.001
Charlson Index, scores	6 [4–9]	9 [6–12]	< 0.001
Prevalence of AF on admission to the ICU, *n* (%)	17 (12.8)	34 (27.4)	0.003
CVP, cm H_2O.	4 [1–8]	5 [2–7]	0.487
Treatment results			
HR_0, beats per minute	95 [80–110]	101 [86–119]	0.002
HR_3, beats per minute	90 [78–102]	100 [86–117]	< 0.001
Respiratory rate 0, breaths per minute	18 [17–20]	19 [18–22]	0.002
RR_3, breaths per minute	18 [16–20]	18 [17–21]	0.006
SBP_0, mm Hg	117 [98–130]	105 [90–128]	0.062
SBP_3, mm Hg	120 [102–130]	110 [95–125]	0.003
DBP_0, mm Hg	66 [56–75]	60 [51–70]	0.004
DBP_3, mm Hg	65 [59–73]	60 [54–69]	< 0.001
MAP_0, mm Hg	83 [71–93]	75 [65–87]	0.007
MAP_3, mm Hg	83 [73–92]	76 [68–87]	< 0.001
DSI_0	1.4 [1.2–1.7]	1.7 [1.3–2.1]	< 0.001
DSI_3	1.4 [1.1–1.6]	1.7 [1.4–2.0]	< 0.001
$PICRCF_0$	0.9 [0.7–1.1]	1.3 [0.9–1.9]	< 0.001
$PICRCF_3$	0.8 [0.6–1.0]	1.4 [1.0–1.9]	< 0.001
Length of treatment in the ICU, days	6 [3–11]	7 [2–15]	0.546
MV rate, *n* (%)	39 (29.3)	124 (100)	< 0.001
RRT rate, *n* (%)	40 (30.1)	93 (75.0)	< 0.001
Frequency of vasopressor support, *n* (%)	94 (70.7)	124 (100)	< 0.001

Note. BMI — body mass index; BSA — body surface area; GCS — Glasgow Coma Scale; AF — atrial fibrillation; CVP — central venous pressure; ICU — intensive care unit; MV — mechanical ventilation; RRT — renal replacement therapy; HR, RR — heart rate, respiratory rate; SBP, DBP, MAP — systolic blood pressure, diastolic blood pressure, mean arterial pressure; DSI — diastolic shock index; PICRCF — prognostic index of compensation for reduced heart and lung function; subscript indices: 0 — on admission, 3 — after 3 hours of intensive care. SOFA — Severe Organ Failure Assessment; APACHE II — acute physiology and chronic health evaluation.

Table 2. Cox regression analysis accounting for variables associated with in-hospital mortality.

Variable	Univariate Cox regression		Multivariate Cox regression	
	OR (95% CI)	p	OR (95% CI)	p
BMI	0.974 (0.949–1.000)	0.054	0.991 (0.963–1.020)	0.549
GCS	0.964 (0.915–1.016)	0.172		
SOFA	1.025 (0.969–1.085)	0.392		
APACHE II	1.044 (1.018–1.071)	< 0.001	1.016 (0.982–1.050)	0.373
Charlson M.index	1.049 (1.006–1.093)	0.024	1.030 (0.984–1.078)	0.206
AF on admission	1.336 (0.898–1.987)	0.153		
HR_0	1.007 (1.000–1.015)	0.062	1.002 (0.992–1.013)	0.660
RR_3	0.990 (0.939–1.045)	0.725		
DBP_0	0.994 (0.982–1.005)	0.286		
MAP_3	0.982 (0.968–0.996)	0.010	0.993 (0.973–1.013)	0.496
DSI_3	1.669 (1.250–2.230)	< 0.001	1.105 (0.642–1.902)	0.719
$PICRCF_3$	1.522 (1.291–1.795)	< 0.001	1.313 (1.062–1.623)	0.012

Note. See the notes for Table 1 for an explanation of abbreviations.

guidelines for the intensive care of sepsis specify a particular level of MAP to guide treatment strategy, without indicating target HR values [21]. This approach is likely flawed and requires revision in light of the body of evidence from recent clinical trials.

The shock index, first proposed more than half a century ago! and calculated as the ratio of HR to MAP, is a simple and informative hemodynamic parameter for the early diagnosis of shock and hypoperfusion [22]. Numerous studies have demonstrated its prognostic value, including in patients with sepsis [23]. Subsequently, several variations of the index were proposed to expand the capabilities of assessing hemodynamic status — the so-called modified shock index (ratio of HR to MAP), as well as the diastolic and age-adjusted shock indices (the product of age and the ratio of HR to SBP). All of these modifications have also been vali-

dated for identifying patients with sepsis and an increased risk of death [24, 25, 6]. Furthermore, when comparing the variations of the indices with one another, the age-adjusted shock index demonstrated the highest prognostic accuracy [26]. Thus, it can be concluded that adding an age component improves the discriminatory characteristics of hemodynamic predictors of mortality in sepsis.

In the mammalian phylogenetic series, an allometric relationship is observed between an increase in body size and a decrease in heart rate. Within the human population, this relationship is nonlinear and varies depending on lifestyle, constitutional characteristics, and the state of autonomic regulation [27]. Nevertheless, several studies have demonstrated an association between stroke volume and BSA [28], as well as an inverse correlation between height and resting HR in healthy volunteers [29]. Furthermore, the increase in survival with increased BSA in patients with sepsis can also be explained by the «obesity paradox». Patients with larger BSA (and, as a rule, with increased body weight) have greater reserves of fat and muscle mass, which serve as reservoirs of energy and amino acids [30]. Thus, high BMI values serve, to a certain extent, as markers of the body's greater physiological reserves.

We developed the PICRCF formula based on literature data regarding the association of HR, age, RR, diastolic BP, and BSA with mortality. The direction of these associations determined the distribution of components between the numerator and denominator: factors associated with an increased risk of mortality were placed in the numerator, and those associated with a reduced risk — in the denominator. Thus, PICRCF represents a modification of the age-adjusted DSI, adjusted for RR and BSA. This indexing allowed for further improvement of the predictive characteristics of the developed indicator with minimal complication of the calculation formula.

The combination of clinical-demographic, respiratory, and hemodynamic data from bedside monitoring associated with HR, as presented in this study, allows for the effective prediction of an adverse treatment outcome in patients with sepsis upon admission to the ICU. Furthermore, the results indicate that the discriminatory ability of the prognostic index calculated based on these indicators increases when they are reassessed after the completion of the initial phase of intensive care, which is consistent with published data [31].

From a practical standpoint, this allows for rapid bedside stratification of patients based on readily available clinical parameters. For example, during sepsis, a decrease in diastolic BP from 60 to 40 mm Hg accompanied by an increase in HR from 90 to 125 beats per minute and RR from 20 to 24 breaths per minute in an average 40-year-old patient who is 170 cm tall and weighs 69 kg is associated with a 31% increase in the risk of in-hospital mortality. However, for an 80-year-old patient with identical anthropometric characteristics, such changes in hemodynamic and respiratory parameters and the need for only mechanical ventilation will increase the risk of an adverse outcome by 62%. Thus, the predictive value of PICRCF, in addition to statistical characteristics that exceed standard prognostic

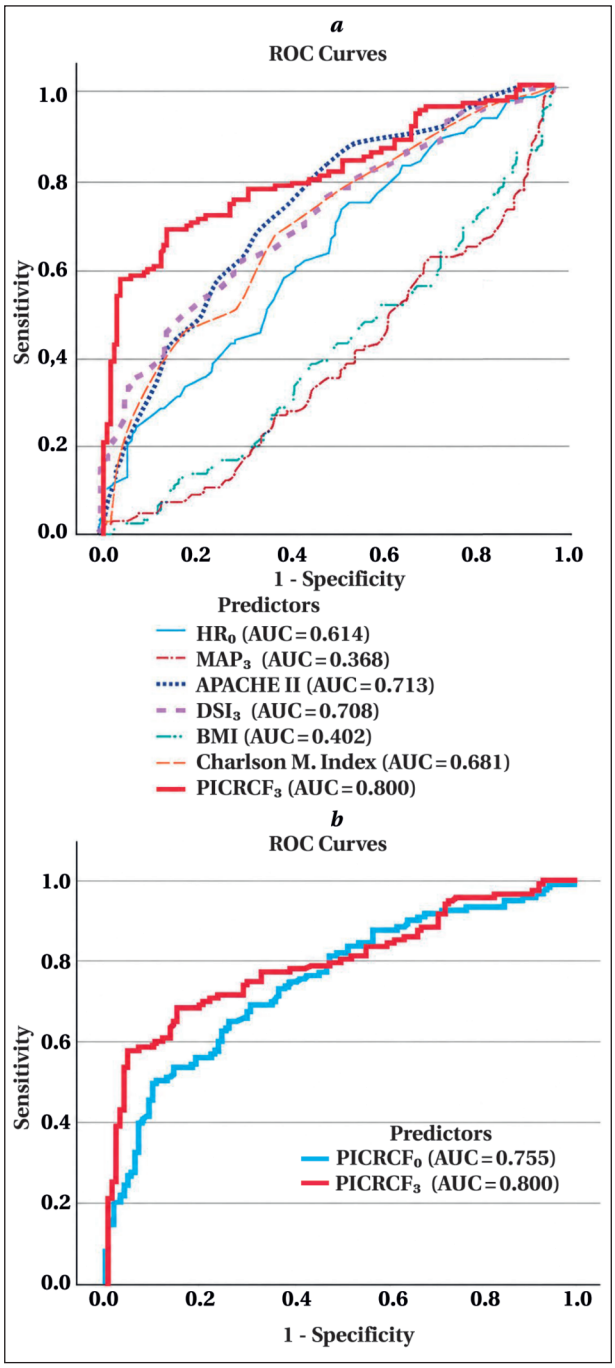

Fig. 2. ROC curves for predictors of in-hospital mortality in patients with sepsis (a) and the PICRCF score before and after 3 hours of intensive care (b).
Note. PICRCF indices: 0 –on admission; 3 – after 3 hours of intensive care. For a, b – all p<0.05.

scales, lies in the ability to identify high-risk patients early, optimize resource allocation, and individualize intensive care.

The study's limitations should be noted. First, due to the retrospective nature of the analysis, data on the types and doses of vasopressors were not taken into account. Nevertheless, a study by Y. Shen et al. [20] demonstrated that in patients with sepsis, mortality is associated with tachycardia regardless of norepinephrine use. Second, the exclusion of patients in an agonal state, as well as those readmitted to the ICU, may have limited the diagnostic value of the results obtained due to selection bias. Nevertheless, the deterioration in vital signs among patients with sepsis — resulting from decompensated multiple organ failure following delayed transfer to the ICU and subsequent death — could also have significantly skewed the results. Third, the current study did not analyze parameters of advanced hemodynamic and laboratory monitoring. However, there is evidence of a variable effect of tachycardia on in-hospital mortality depending on the cardiac index [32] or serum lactate concentration [33]. Fourth, patients with cardiac arrhythmias were not excluded from the study. AF was recorded in 20% of patients upon admission to the ICU. In the tachysystolic variant of AF, PICRCF index values may have been overestimated, thereby distorting the true assessment of disease severity. Fifth, the PICRCF index was assessed at limited time points — upon admission and after 3 hours — which allows for characterization primarily of the early stage of sepsis. The absence of follow-up measurements makes it impossible to assess the prognostic significance of the index at later time points and its dynamics against the backdrop of ongoing intensive care, which requires further prospective studies. Sixth, a fixed RR value was used to calculate PICRCF in patients on mechanical ventilation, which may have limited the accuracy of assessing the respiratory component's contribution to the index value. However, the need for mechanical ventilation in sepsis is an independent predictor of poor outcome, as it reflects the severity of multiple organ failure [34]. Since critical deviations in RR (both tachypnea and bradypnea) in patients with sepsis are an indication for mechanical ventilation, the actual RR in patients on mechanical ventilation loses its independent prognostic value. Similarly to the widely accepted and validated APACHE II scale, where the maximum score for RR is assigned upon reaching the threshold of respiratory decompensation ($\geqslant$50 per minute) and does not increase further, reflecting a «ceiling effect» of risk, the continuous value of RR in patients on MV in the PICRCF index serves as a standardized marker of disease severity. This approach, which treats RR as a continuous variable (rather than introducing the dichotomous variable «mechanical ventilation» into the model), allowed us to include in the analysis patients who were on mechanical ventilation from the very first hours of treatment in the ICU, highlighting the severity of their condition without reducing the index's discriminatory power or complicating the calculation formula. An additional physiological rationale is the proven nonlinear (J-shaped) relationship between in-hospital mortality and RR in critically ill patients [35], which confirms the appropriateness of a threshold-based, rather than a linear interpretation of extreme RR values. Finally, the PICRCF formula was developed using the a priori method, without internal validation. Thus, despite the multicenter nature of the study, external validation of the PICRCF index on an independent cohort of patients is necessary prior to its clinical implementation.

The body of data presented allows us to conclude that vital signs reflecting the state of the cardiovascular and respiratory systems, indexed to account for anthropometric and age-related characteristics, offer a number of advantages in early risk stratification in patients with sepsis. Unlike dichotomous and rating scales, the index-based approach allows for continuous bedside assessment of parameters, making it possible to account for even minor changes in physiological parameters. Recording a set of minimal deviations in the functioning of the respiratory and cardiovascular systems in patients with sepsis may be clinically significant, indicating the onset of decompensated organ dysfunction. Furthermore, the numerical scoring format of the calculated index is not subject to subjectivity, unlike assessments of skin mottling (livedo reticularis) or capillary refill time. The simplicity, accessibility, and speed of measuring the components used to calculate PICRCF enable dynamic assessment of patient's condition from the very first minutes of admission to the ICU, which is crucial for the timely identification of the severity of sepsis.

Conclusion

The PICRCF index, based on a combination of cardiovascular and respiratory parameters, as well as demographic and anthropometric characteristics, offers advantages over standard prognostic scales in patients with sepsis. The predictive value of this index 3 hours after the start of intensive care was the highest among the early predictors of mortality studied in this research, with an AUC of 0.800 (95% CI 0.744–0.855), a cutoff value of 1.1, with a sensitivity of 69% and a specificity of 85%. In addition, PICRCF index values were associated with the number of days without organ replacement support.

References

1. *Багненко С. Ф., Горобец Е. С., Гусаров В. Г., Дехнич А. В., Дибиров М. Д., Ершова О. Н., Замятин М. Н., с соавт.* Клинические рекомендации «Сепсис (у взрослых)». *Вестник анестезиологии и реаниматологии*. 2025; 22 (1): 80–109. *Bagnenko S. F., Gorobets E. S., Gusarov V. G., Dekhnich A. V., Dibirov M. D., Ershova O. N., Zamyatin M. N., et al.* Clinical guidelines «Sepsis (in adults)». *Messenger of Anesthesiology and Resuscitation=Vestnik Anesthesiologii i Reanimatologii*. 2025; 22 (1): 80–109. (in Russ.).
DOI: 10.24884/2078-5658-2025-22-1-81-109.
2. *Ramasco F., Nieves-Alonso J., García-Villabona E., Vallejo C., Kattan E., Méndez R. et al.* Challenges in septic shock: from new hemodynamics to blood purification therapies. *Jf Pers Med*. 2024*;* 14 (2): 176.
DOI: 10.3390/jpm14020176.
PMID: 38392609.
3. *Belfiore J., Taddei, R. & Biancofiore, G.* Catecholamines in sepsis: pharmacological insights and clinical applications — a narrative review. *J Anesth Analg Critl Care*. 2025*;* 5 (1): 17.
DOI: 10.1186/s44158-025-00241-2.
PMID: 40176108.
4. *Morelli A., Singer M., Ranieri V. M., D'Egidio A., Mascia L., Orecchioni A., Piscioneri F., et al.* Heart rate reduction with esmolol is associated with improved arterial elastance in patients with septic shock: a prospective observational study. *Intensive Care Med*. 2016*;* 42: 1528–1534.
DOI: 10.1007/s00134-016-4351-2.
PMID: 27101380.
5. *Carrara M., Bollen Pinto B., Basell G., Bendjelid K., Ferrario M.* Baroreflex sensitivity and blood pressure variability can help in understanding the different response to therapy during acute phase of septic shock. *Shock*. 2018*;* 50: 78–86.
DOI: 10.1097/SHK.0000000000001046.
PMID: 29112634.
6. *Ospina-Tascón G. A., Teboul J. L., Hernandez G., Alvarez I., Sánchez-Ortiz A. I., Calderón-Tapia L. E., Manzano-Nunez R., et al.* Diastolic shock index and clinical outcomes in patients with septic shock. *Ann. Intensive Care*. 2020; 10: 41.
DOI: 10.1186/s13613-020-00658-8.
PMID: 32296976.
7. *Paiva M., Carvalho R. A., Brizido C., Bello A. R., Lima M. R., Domingues M., Pereira J. C., et al.* Diastolic shock index: a novel prognostic parameter unveiling insights into vasodilatory cardiogenic shock. *Eur Heart J*. 2024*;* 45 (1): ehae666.1734.
DOI: 10.1093/eurheartj/ehae666.1734.
8. *Owattanapanich N., Boonchana N.* Diastolic shock index: its importance and application in critically ill patients: a narrative review. *Clin CritCare*. 2025; 33: Article ID e250005.
DOI: 10.54205/ccc.v33.270310.
9. *de Simone G., Devereux R. B., Kimball T. R., Roman M. J., Palmier V., Celentano A., Daniels S. R.* Relation of heart rate to left ventricular dimensions in normotensive, normal-weight children, adolescents and adults. *Ital Heart J*. 2001; 2: 599–604. PMID: 11577834.
10. *Lin S., Yang X.* Body surface area is a predictor of 90-day all-cause mortality in critically ill patients with acute kidney injury. *Injury* 2024*;* 55 (6): 111544.
DOI: 10.1016/j.injury.2024.111544.
PMID: 38626586.
11. *Chang H., Liao L., Wang W., Pinhu L.* Body surface area as a prognostic predictor in patients with sepsis. 2022. License CC BY 4.0.
DOI: 10.21203/rs.3 rs-1888518/v1.
12. *Zafrir B., Salman N., Crespo-Leiro M. G., Anker S. D., Coats A. J., Ferrari R., Filippatos G., et al.* Body surface area as a prognostic marker in chronic heart failure patients: results from the heart failure registry of the Heart Failure Association of the European Society of Cardiology. *Eur J Heart Fail*. 2016*;* 18 (7): 859–868.
DOI: 10.1002/ejhf.551. PMID: 27198159.
13. *Nes, B. M., Janszky I., Wisløff U., Støylen A., Karlsen T.* Age-predicted maximal heart rate in healthy subjects: the HUNT Fitness Study. *Scand J Med Sci Sports*. 2013*;* 23: 697–704.
DOI: 10.1111/j.1600-0838.2012.01445.x.
PMID: 22376273.
14. *Lupón J., Domingo M., de Antonio M., Zamora E., Santesmases J., Díez-Quevedo C., Altimir S., et al.* Aging and heart rate in heart failure: clinical implications for long-term mortality. *Mayo Clin Proc*. 2015*;* 90: 765–772.
DOI: 10.1016/j.mayocp.2015.02.019.
PMID: 26046411.
15. *Aglen S. A. S., Simonsen H. F., Sjøset T. E., Jammer I.* Respiratory rate as a predictor of clinical deterioration and mortality: a scoping review. *Acta Anaesthesiol. Scand*. 2025*;* 69 (8): e70113.
DOI: 10.1111/aas.70113.
PMID: 40828518.
16. *Zhang T. Y., Du Y. J., Hou Y. Z., Du Q., Dou H. R., Gao X. M.* Heart/breathing rate ratio [HBR] as a predictor of mortality in critically ill patients. *Heliyon*. 2024*;* 10 (10): e31187.
DOI: 10.1016/j.heliyon.2024.e31187.
PMID: 38803872.
17. *Singer M., Deutschman C. S., Seymour C. W., Shankar-Hari M., Annane D., Bauer M., Bellomo R. et al.* The third international consensus defi-

nitions for sepsis and septic shock (Sepsis-3). *JAMA*. 2016; 315 (8): 801–810.
DOI: 10.1001/jama.2016.0287.
PMID: 26903338.

18. *La Via L, Sangiorgio G., Stefani S., Marino A., Nunnari G., Cocuzza S., La Mantia I., et al.* The global burden of sepsis and septic shock. *Epidemiologia (Basel)*. 2024; 5 (3): 456–478.
DOI: 10.3390/epidemiologia5030032.
PMID: 39189251.
19. *Shvilkina T., Shapiro N.* Sepsis-induced myocardial dysfunction: heterogeneity of functional effects and clinical significance. *Front Cardiovasc Med*. 2023; 10: 1200441.
DOI: 10.3389/fcvm.2023.1200441.
PMID: 37522079.
20. *Shen Y., Wang J., Cao Q., Wu Y., Wang Q., Wang N., Shao M.* Maximum heart rate and mortality in sepsis patients: a retrospective cohort study. *Intern Emerg Med*. 2025; 21 (2): 621–630.
DOI: 10.1007/s11739-025-03960-0.
PMID: 40358822.
21. *Evans L., Rhodes A., Alhazzani W., Antonelli M., Coopersmith C. M., French C., Machado F. R., et al.* Surviving sepsis campaign: international guidelines for management of sepsis and septic shock 2021. *Intensive Care Med*. 2021; 47: 1181–1247.
DOI: 10.1007/s00134-021-06506-y.
PMID: 34599691.
22. *Allgöwer M., Burri, C.* «Schockindex». *Dtsch Med Wochenchr*. 1967; 92 (43): 1947–1950.
DOI: 10.1055/s-0028-1106070. PMID: 5299769.
23. *Jouffroy R., Pierre Tourtier J., Gueye P., Bloch-Laine E., Bounes V., Debaty G., Boularan J., et al.* Prehospital shock index to assess 28-day mortality for septic shock. *Am J Emerg Med*. 2020; 38: 1352–1356.
DOI: 10.1016/j.ajem.2019.11.004.
PMID: 31836349.
24. *Torabi M., Moeinaddini S., Mirafzal A., Rastegari A., Sadeghkhani N.* Shock index, modified shock index, and age shock index for prediction of mortality in Emergency Severity Index level 3. *Am J Emerg Med*. 2016; 34: 2079–2083.
DOI: 10.1016/j.ajem.2016.07.017.
PMID: 27461887.
25. *Yu T., Tian C., Song J., He D., Sun Z., Sun Z.* Age shock Index is superior to shock index and modified shock index for predicting long-term prognosis in acute myocardial infarction. *Shock*. 2017; 48: 545–550.
DOI: 10.1097/SHK.0000000000000892.
PMID: 28481840.
26. *Jouffroy R., Gille S., Gilbert B., Travers S., Bloch-Laine E., Ecollan P., Boularan J., et al.* Relationship between shock index, modified shock index, and age shock index and 28-day mortality among patients with prehospital septic shock. *J Emerg Med*. 2024; 66: 144–153.
DOI: 10.1016/j.jemermed.2023.11.010.
PMID: 38336569.
27. *Dewey, F. E., Rosenthal, D., Murphy, D. J., Froeliche V. F., Ashley, E. A.* Does size matter? *Circulation*. 2008; 117: 2279–2287.
DOI: 10.1161/CIRCULATIONAHA.107.736785.
PMID: 18443249.
28. *Jegier W., Sekelj P., Auld P. A. M., Simpson R., McGregor M.* The relation between cardiac output and body size. *Heart*. 1963; 25: 425–430.
DOI: 10.1136/hrt.25.4.425.
PMID: 14045321.
29. *Infeld M., Avram R., Wahlberg K., Silverman D. N., Habel N., Lustgarten D. L., Pletcher M. J., et al.* An approach towards individualized lower rate settings for pacemakers. *Heart Rhythm O2*. 2020; 1 (5): 390–393.
DOI: 10.1016/j.hroo.2020.09.004.
PMID: 33604585.
30. *Yeo H. J., Kim H. L., So M. W., Park J. M., Kim D., Cho W. H.* Obesity paradox of sepsis in long-term outcome: the differential effect of body composition. *Intensive Crit Care Nurs*. 2025; 87.
DOI: 10.1016/j iccn.2024.103893.
PMID: 39608164.
31. *Lee K. J., Kim Y. K., Jeon K., Ko R.-E., Suh G. Y., Oh D. K., Lim S. Y. et al.* Shock indices are associated with in-hospital mortality among patients with septic shock and normal left ventricular ejection fraction. *PLoS One* 2024; 19 (3): e0298617.
DOI: 10.1371/journal.pone.0298617.
PMID: 38470900.
32. *Ngan C., Zeng X., Lia T., Yin W., Kang Y.* Cardiac index and heart rate as prognostic indicators for mortality in septic shock: a retrospective cohort study from the MIMIC-IV database. *Heliyon*. 2024; 10 (8): e28956.
DOI: 10.1016/j.heliyon.2024.e28956.
PMID: 38655320.
33. *Na S. J., Oh D. K., Park S., Lee Y. J., Hong S.-B., Park M. H., Ko R.-E., et al.* The association between tachycardia and mortality in septic shock patients according to serum lactate level: a nationwide multicenter cohort study. *J Korean Med Sci*. 2023; 38 (40): e313.
DOI: 10.3346/jkms.2023.38.e313.
PMID: 37845786.
34. *Mohamed A. K. S., Mehta A. A., James P.* Predictors of mortality of severe sepsis among adult patients in the medical intensive care unit. *Lung India*. 2017; 34 (4): 330–335.
DOI: 10.4103/lungindia. lungindia_54_16.
PMID: 28671163.
35. *Zhang K., Shi Y., Han Y., Cai T. Y., Gu F. M., Gu Z. X., Zhang T., et al.* J-shaped association between respiratory rate and in-hospital mor-

tality in acute myocardial infarction patients complicated by congestive heart failure in intensive care unit. *Dose Response*. 2024; 22 (4): 15593258241303040.
DOI: 10.1177/15593258241303040.
PMID: 39629219.

Received 21.03.2026
Accepted 13.05.2026
Online First 08.06.2026

https://doi.org/10.15360/1813-9779-2026-3-2674

Inhalation Effect of Heated Helium-Oxygen Mixture and Nitric Oxide on Gas Exchange Parameters in Patients with Polytrauma and Pulmonary Contusion

Yuri E. Kostyrya[1,2]*, Nikolay I. Gulyaev[1], Roman E. Lakhin[3], Anna F. Kostyrya[4]

[1] National Medical Research Center for High Medical Technologies — A. A. Vishnevsky Central Military Clinical Hospital, Ministry of Defense of the Russia, 1 Novy township, Krasnogorsk Urban District, 143420 Moscow Region, Russia
[2] Clinical Hospital, Medical and Sanitary Unit, Ministry of Internal Affairs of Russia for Moscow, 3a Novaya Ipatovka Str., 127299 Moscow, Russia
3 S. M. Kirov Military Medical Academy, 6 Academician Lebedev Str., B, 194044 St. Petersburg, Russia
[4] Moscow City Oncology Hospital No. 62, Moscow City Health Department, 27 Istra Township, Krasnogorsk Urban District, 143515 Moscow Region, Russia

For citation: *Yuri E. Kostyrya, Nikolay I. Gulyaev, Roman E. Lakhin, Anna F. Kostyrya.* Inhalation Effect of Heated Helium-Oxygen Mixture and Nitric Oxide on Gas Exchange Parameters in Patients with Polytrauma and Pulmonary Contusion. *Obshchaya Reanimatologiya = General Reanimatology.* 2026; 22 (3): 13–20. https://doi.org/10.15360/1813-9779-2026-3-2674 [In Russ. and Engl.]

***Correspondence to:** Yuri E. Kostyrya, urry.k@yandex.ru

Summary

The heated helium-oxygen mixture (t-He/O_2, heliox) reduces resistance in the airways and improves ventilation in affected zones of the lungs. Inhaled nitric oxide (NO) is a selective pulmonary vasodilator that lowers pressure in the pulmonary artery and enhances the ventilation-perfusion matchig, which also contributes to the optimization of oxygenation.

The aim of the study is to assess the efficacy and safety of adding inhaled NO, t-He/O_2, and their combination to standard respiratory therapy in patients with polytrauma and pulmonary contusion.

Materials and Methods: We conducted an open prospective randomized study. 186 patients were divided into 4 groups: the NO group (n=43), the t-He/O_2 group (n=49), the t-He/O_2 + NO group (n=48), and the control group (oxygen therapy, O_2, n=46). The respiratory therapy course lasted 12 days. We assessed the dynamics of computed tomography (MSCT) signs of pulmonary contusion, as well as the arterial blood gas (ABG) parameters (PaO_2, $PaCO_2$, SaO_2, lactate, pH) on days 1, 4, 8, and 12.

Results. The most remarkable improvements were documented in the combination therapy group (t-He/O_2 + NO). By day 12, this group showed a statistically significant 69% reduction in the extent of lung injury on MSCT (p=0.018), an increase in PaO_2 to 95.1 mm Hg (p< 0.001), a decrease in $PaCO_2$ to 35.8 mm Hg (p< 0.001), and a reduction in lactate to 1.38 mmol/L (p=0.0025). The same parameters in the monotherapy groups NO or t-He/O_2 also markedly improved compared to the control group (O_2). No therapy-related adverse events were reported.

Conclusion. Employment of inhaled t-He/O_2 and NO, especially in combination, as a part of the total care plan of patients with polytrauma and pulmonary contusion, contributes to a significant improvement in gas exchange and regression of radiographic signs of lung tissue injury. Thereby, described method is recommended for early respiratory therapy in intensive care units.

Keywords: helium-oxygen mixture; heliox; inhaled nitric oxide; polytrauma; pulmonary contusion; respiratory therapy; blood gas composition

Highlight. A 12-day respiratory therapy course with inhaled NO and heated helium-oxygen mixture accelerates recovery from pulmonary contusion and improves gas exchange parameters in patients with polytrauma.

Conflict of interest. The authors declare no conflict of interest.

Information about the authors:
Yuri E. Kostyrya: https://orcid.org/0009-0006-1037-8607
Nikolay I. Gulyaev: https://orcid.org/0000-0002-7578-8715
Roman E. Lakhin: https://orcid.org/0000-0001-6819-9691
Anna F. Kostyrya: https://orcid.org/0009-0001-0453-4910

Introduction

Polytrauma remains one of the leading causes of mortality and disability among working-age individuals, representing a significant medical and social issue, particularly for the healthcare system of law enforcement agencies [1–5]. A distinctive pathophysiological feature of polytrauma is the syndrome of mutual buffering, where the simultaneous presence of two or more injuries causes a disproportionate worsening of patient's overall health status due to destructive synergy between co-occurring conditions [3–6]. Pulmonary contusion,

as a common component of polytrauma, is an independent risk factor for the development of acute respiratory failure (ARF), prolongs the duration of mechanical ventilation (MV), and increases overall mortality [2–5, 7, 8].

The mainstay of respiratory support for a pulmonary contusion is respiratory therapy aimed at optimizing oxygenation and ventilation. The search for adjunctive methods that can improve gas exchange and shorten the time needed for lung function recovery is an important issue in intensive care.

Helium-oxygen mixture (heliox), due to helium's low density, reduces resistance in the airways and improves ventilation in areas with turbulent flow, which could theoretically be beneficial in the edema and obstruction accompanying pulmonary contusion [9–13]. Thermal modification of the heated heliox, namely heating it immediately before inhalation to 70–90°C, may further improve the rheological properties of sputum and mucociliary clearance. Inhaled nitric oxide (iNO) is a selective pulmonary vasodilator that reduces pulmonary artery pressure and improves ventilation-perfusion matching, thereby also helping optimize oxygenation [14–17].

Numerous studies have confirmed that nitric oxide (NO) is a fundamental regulator of metabolic processes in all living organisms, exhibiting a wide range of biological effects. These findings have helped elucidate the mechanisms by which NO functions in biological systems. The physicochemical properties of neutral NO molecules, which are produced in the human body through enzymatic synthesis, explain their dual action on target organs. NO molecules can both regulate and exert cytotoxic effects on cells and tissues [16, 18–21].

NO is a key mediator involved in a wide range of biochemical processes that are critically important for regulating physiological functions at the cellular level. Its role in signaling, both intercellular and intracellular, helps maintain the body's homeostasis. In particular, in the cardiovascular system, NO induces vasodilation by activating an endothelium-dependent mechanism of relaxation of vascular smooth muscle [8, 17, 18, 20].

The main effect of inhaled nitric oxide on the body is its direct action on the vessels of the pulmonary circulation, through which various mechanisms of improved gas exchange are effectuated. In addition, its direct regulatory effect on the smooth muscle of the bronchial tree helps reduce resistance to the gas mixture flowing through it [14–17]. The advantage of heated heliox in pathological bronchoconstriction lies in its very low viscosity and high flowability, which ensure a high capacity to penetrate the alveoli and provide a direct thermal effect [9–13].

Despite the well-established effects of helium-oxygen mixtures and nitric oxide individually, data on simultaneous use of both — especially in combination of iNO with heated heliox — in patients with traumatic lung injury are limited.

The aim of the study: to evaluate the efficacy and safety of adding inhaled nitric oxide (NO), heated heliox, and their combination to standard respiratory therapy in patients with polytrauma and pulmonary contusion.

Materials and Methods

An open-label, single-center, interventional, prospective, randomized clinical study was conducted in the intensive care units of the National Medical Research Center for High Medical Technologies — A. A. Vishnevsky Central Military Clinical Hospital of the Russian Ministry of Defense (A. A. Vishnevsky NMRC HMT) from September 2023 to May 2025. The study was approved by the Ethics Committee of A. A. Vishnevsky NMRC HMT (research project «Helium,» protocol No. 14/23 dated July 20, 2023; research project «Helium+», protocol No. 2/25 dated February 27, 2025).

Totally 15,846 patients with multiple trauma were subjected to chest MSCT screening upon admission to the medical facility. Of these, 468 patients had lung injury as the predominant problem in the setting of polytrauma, manifested as pulmonary contusion and respiratory failure without signs of inflammation. A total of 192 patients meeting the inclusion criteria were selected for the study (all men; mean age 31 ± 7 years). Of these, 186 completed the study protocol in full, and 6 patients were excluded because of emerging inflammatory changes in pulmonary tissue in four, and acute kidney injury requiring renal replacement therapy in two patients (Fig. 1).

Inclusion criteria: patients of both genders aged 18–65 years with a confirmed diagnosis of polytrauma and pulmonary contusion (based on emergency chest MSCT), signs of respiratory failure ($SaO_2 \leqslant 95\%$, $PaO_2 \leqslant 80$ mm Hg), who signed informed consent.

Exclusion criteria: isolated chest trauma; bacterial pneumonia at admission; severe organ pathology (renal dysfunction with a glomerular filtration rate below 30 mL/min/1.73 m², need for hemodialysis, liver failure with signs of cytolysis, decompensated diabetes mellitus, oncologic or hematologic diseases); need for extracorporeal membrane oxygenation (ECMO); and participation in other clinical trials.

Group allocation: 186 patients who met the inclusion criteria were randomized using sealed envelopes into 4 groups:

Group 1 (NO), $n = 43$: standard of care + NO inhalations at a dose of 30 ppm via the Tianox device (AIT-NO-O1, according to Technical Specifications TU 32.50.21-001-07623615-2017), twice a day for 20 minutes each session.

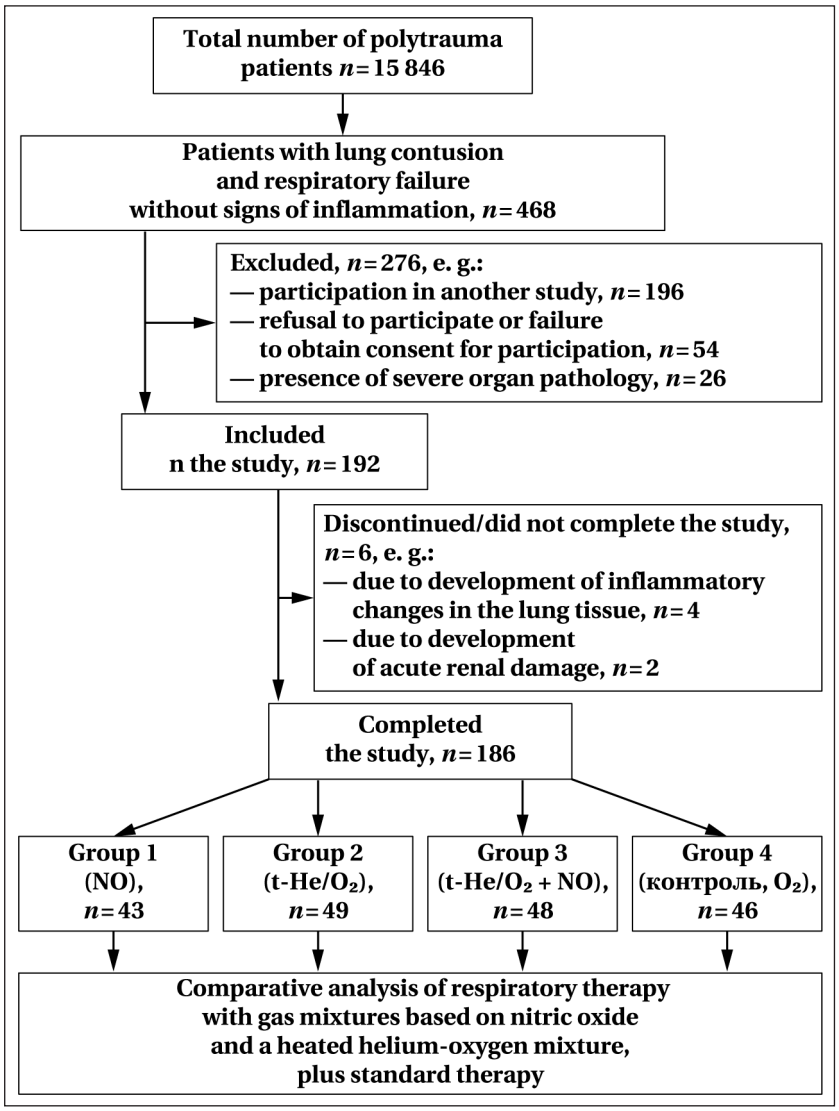

Fig. 1. Flowchart of patient selection for the study.

Group 2 (t-He/O_2, heated heliox), $n=49$: standard of care plus inhalations of heated helium-oxygen mixture (65–75% He, 25–35% O_2, temperature 70–90°C) administered via the Heliox Extreme device (RZN 2016/3988, TU 9444-001-0116489960-2015) twice daily for 20 minutes.

Group 3 (t-He/O_2 + NO), $n=48$: standard of care + co-inhalations (t-He/O_2 + NO) according to the same regimen.

Group 4 (control, O_2), $n=46$: standard of care plus oxygen therapy via a Venturi mask (O_2 flow rate of 6 L/min) twice daily for 20 minutes.

Standard therapy in all groups was administered in accordance with current clinical guidelines and included adequate pain management, respiratory support when indicated, antibacterial therapy, and infusion therapy.

Measured parameters. The study's primary endpoint was the change in PaO_2 (arterial oxygen partial pressure) by day 8 of therapy. In addition to PaO_2, changes in several arterial blood gas (ABG) parameters ($PaCO_2$, SaO_2, lactate, pH) and MSCT-based extent of pulmonary lesion resolution were assessed. Evaluations were performed at baseline (day 1) and on days 4, 8, and 12 of therapy. The severity of lung contusion was assessed using a modified classification: CT-1 (mild), CT-2 (moderate), and CT-3 (severe) [8].

Sample size justification. The sample size was calculated for the primary endpoint, namely the change in PaO_2 (arterial oxygen partial pressure) by day 8 of therapy. Based on a retrospective analysis of medical records of patients with polytrauma and pulmonary contusion at our center, the minimum clinically meaningful between-group difference was set at 12 mm Hg. The standard deviation (*SD*) of PaO_2 in the study population was 7.0 mm Hg.

The statistical calculation was performed using G*Power software (version 3.1.9.7, Universität Düsseldorf, Germany) for a one-way analysis of variance (ANOVA) with four groups. The following values were considered statistically significant: significance level $\alpha=0.05$ (two-sided), statistical power $(1–\beta)=0.80$, and expected effect size Cohen's $f=0.50$ (corresponding to a ratio of the difference in means to the standard deviation, $\triangle/SD \approx 12/7=1.71$, converted to f for four groups).

To control Type I error in multiple pairwise comparisons, we used the Bonferroni correction: the number of comparisons among the four groups was 6, so the adjusted significance level was $\alpha\_adj = 0.05 / 6 \approx 0.0083$.

Calculation result: the minimum required sample size was 21 patients per group. Taking into account possible attrition (about 10% due to the development of inflammatory changes, acute kidney injury, and other reasons), the planned group size was set at 23 patients.

In fact, after randomization and the exclusion of 6 patients, each group included 43 to 49 patients, which was 1.9–2.1 times more than the calculated minimum. Statistical power was calculated for a one-way analysis of variance (ANOVA) with four groups, a total sample size of $n=192$, a significance level of $\alpha=0.05$, and Cohen's $f=0.50$, using G*Power software (version 3.1.9.7, Universität Düsseldorf,

Table 1. Anthropometric, clinical, and laboratory parameters of patients.

Parameters	Parameter values in the groups				*p*
	NO, *n* = 43	t-He/O_2, *n* = 49	t-He/O_2 + NO, *n* = 48	O_2 *n* = 46	
Age, years	32 ± 7	30 ± 6	30 ± 7	32 ± 6	0.779
Gender, m	43 (100%)	49 (100%)	48 (100%)	46 (100%)	0.999
Height, cm	175 ± 6	174 ± 5	175 ± 7	173 ± 7	0.741
Weight, kg	76.8 ± 6.8	77.4 ± 8.1	75.9 ± 8.6	77.2 ± 7.6	0.861
Body mass index, kg /m²	25.6 ± 4.8	24.9 ± 5.3	25.1 ± 4.9	25.8 ± 5.6	0.863
BMI > 25kg/m²	12 (28%)	16 (32%)	17 (35%)	14 (30%)	0.902
HR, bpm	92 ± 14	86 ± 12	88 ± 15	90 ± 14	0.668
Pulmonary lesion MSCT (on admission)*, scores	1.96 (1.45–2.47)	1.92 (1.36–2.56)	2.0 (1.39–2.61)	1.94 (1.33–2.55)	0.675
PaO_2 (on admission) mm Hg	72.1 ± 6.9	74.3 ± 9.7	73.1 ± 8.4	72.8 ± 8.8	0.807
$PaCO_2$ (on admission) nm Hg	47.2 ± 6.8	48.4 ± 7.6	48.3 ± 7.7	47.0 ± 7.5	0.850
SaO_2 (on admission), %	91.6 ± 1.4	92.3 ± 2.1	91.9 ± 1.9	92.0 ± 2.2	0.780
Lactate level (on admission), mmol/L	4.12 ± 0.78	3.86 ± 1.12	3.92 ± 0.84	4.01 ± 1.22	0.766
pH (on admission)	7.33 ± 0.07	7.32 ± 0.07	7.32 ± 0.07	7.33 ± 0.07	0.886
ISS1					
extremities*	2.3(1–4)	2.4(1–4)	2.3(1–4)	2.4(1–4)	0.950
head*	2.6(1–4)	2.5(1–4)	2.5(1–4)	2.6(1–4)	0.953
neck*	0.3(0–1)	0.2(0–1)	0.3(0–1)	0.3(0–1)	0.841
face*	0.2(0–1)	0.2(0–1)	0.2(0–1)	0.3(0–1)	0.841
chest*	9(9–9)	9(9–9)	9(9–9)	9(9–9)	0.999
abdomen*	2.8(1–4)	2.6(1–4)	2.7(1–4)	2.8(1–4)	0.964
external* and other trauma	2.2(1–4)	2.4(1–4)	2.3(1–4)	2.0(1–4)	0.790

Note. Data in Tables 1 and 2 are presented as *M* ± *SD*, where *M* is the arithmetic mean and *SD* is the standard deviation. ISS1 — severity of combined injury by body region according to the Injury Severity Score (ISS), scores. * — Data are presented as *Me*, the median, (*Q1–Q3*) — lower and upper quartiles.

Germany) for the specified parameters. Power was approximately 1.00 (or 100%). Even after applying the Bonferroni correction, statistical power remained very high (99%), ensuring the reliability of the conclusions for all planned between-group comparisons.

Statistical analysis was performed using IBM SPSS Statistics for Windows, Version 22.0 (IBM Corp., Armonk, NY, USA) and Microsoft Excel LTSC MSO (16.0.14332.20761) (Microsoft Corp., Redmond, Washington 98052-6399, USA). The normality of distributions was assessed using the Shapiro–Wilk test and Pearson's χ^2 test. Variables that followed a normal distribution were described using arithmetic means *(M)*, standard deviations *(SD)*, and 95% confidence intervals (95% CI). In cases of non-normal distribution of quantitative data, they were described using the median *(Me)* and the lower and upper quartiles *(Q1–Q3)*. Continuous numerical data from independent samples were compared using Student's *t*-test, while paired samples were compared using the *t*-test for dependent observations. Differences between groups involving variables with non-normally distributed data were assessed using the Mann–Whitney *U* test and the Wilcoxon signed-rank test. Proportions in groups and categorical variables were compared using Pearson's chi-square test or Fisher's exact test (when the outcome frequency was less than 10%). Differences in group mean values were assessed using analysis of variance (ANOVA). The results of multiple comparisons were adjusted using Tukey's method for pairwise mean differences and a significance-level correction (Bonferroni adjustment). As a quantitative measure of effect when comparing relative measures, odds ratios *(ORs)* were used, with 95% confidence intervals calculated. Differences were considered statistically significant at $p < 0.05$.

Generative artificial intelligence. No generative AI technologies were used in creating this article.

Results

Baseline characteristics of the groups: patients' baseline demographic, clinical, and laboratory parameters were comparable in all four groups ($p > 0.05$), confirming the validity of the randomization (Table 1). All patients were male, which was related to epidemiology of polytrauma. Patients' mean age was 31 ± 7 years. Moderate lung contusion (CT-2) predominated, accounting for 77% of cases.

Dynamics of MSCT findings: on day 12 of follow-up, the most remarkable reduction in the volume of pulmonary involvement was observed in the combination therapy group t-He/O_2+NO (69% decrease from baseline, $p = 0.018$) and in the t-He/O_2 group (62% decrease, $p = 0.044$). In the NO group, the regression was 54% ($p = 0.09$), and in the O_2 control group, 42% ($p = 0.230$) (Fig. 2).

Dynamics of ABG panel parameters. SaO_2: by day 4, SaO_2 had increased significantly in all study groups compared with the control group ($p < 0.05$), reaching its highest value in the t-He/O_2+NO group (96.6%). By day 12, SaO_2 had stabilized at 97.4% in

Table 2. Dynamics of monitored ABG parameters over 12 days of therapy.

Parameters, day	Parameter values in the groups			
	NO, $n=43$	t-He/O_2, $n=49$	t-He/O_2 + NO, $n=8$	O_2 $n=46$
SaO_2, %				
1st	91.6±1.4	92.3±2.1	91.9±1.9	92.0±2.2
4th	95.6±1.1*	96.1±1.3*	96.6±1.1*	94.0±2.2
8th	96.1±1.3	97.8±1.1	98.9±0.7	94.7±1.9
12th	96.6±1.4	98.8±0.8	99.1±0.8	95.0±2.8
p, 1-e and 12th	$p<0.001$	$p<0.001$	$p<0.001$	$p=0.285$
PaO_2, mm Hg				
1-e	72.1±6.9	74.3±9.7	73.1±8.4	72.8±8.8
4th	82.7±5.9	85.8±6.3	86.7±5.6	81.3±7.1
8th	88.1±6.9	95.3±4.5	95.1±4.4	82.8±4.8
12th	92.8±5.1	97.1±1.9	98.3±0.9	90.1±8.2
p, 1-e and 12th	$p<0.001$	$p<0.001$	$p<0.001$	$p=0.036$
$PaCO_2$, mm Hg				
1st	47.2±6.8	48.4±7.6	48.3±7.7	47.0±7.5
4th	43.2±5.8	42.4±4.6	40.9±6.1	45.2±6.5
8th	39.2±3.2	36.4±2.6	36.1±2.1	42.4±6.1
12th	37.2±4.1	36.1±2.3	35.9±2.7	39.8±4.5
p, 1-e and 12th	$p=0.015$	$p<0.001$	$p<0.001$	$p=0.110$
Arterial blood lactate, mmol/L				
1st	4.12±0.78	3.86±1.12	3.92±0.84	4.01±1.22
4th	2.66±0.62*	2.12±0.68*	2.06±0.74*	3.1±1.18
8th	1.78±0.84	1.54±0.91	1.48±0.88	2.45±1.32
12th	1.82±0.96	1.36±0.85	1.38±0.84	2.34±1.14
p, 1st and 12th	$p=0.017$	$p=0.003$	$p=0.003$	$p=0.144$
Arterial blood pH				
1st	7.33±0.07	7.32±0.07	7.32±0.07	7.33±0.07
4th	7.36±0.07	7.36±0.07	7.36±0.07	7.36±0.07
8th	7.39±0.07	7.40±0.07	7.40±0.07	7.35±0.07
12th	7.38±0.07	7.42±0.07	7.43±0.07	7.36±0.07
p, 1st and 12th	$p=0.481$	$p=0.155$	$p=0.116$	$p=0.667$

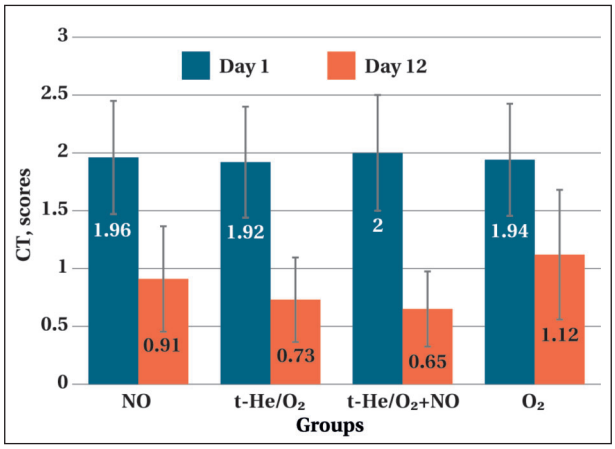

Fig. 2. Changes in CT findings of pulmonary contusion in the groups.

the study groups vs 95.0% in the control group (Table 2).

PaO_2. A significant increase in PaO_2 by day 8 was observed in all groups; however, the increase was most remarkable in the t-He/O_2 and t-He/O_2+NO groups (to 95.3 and 95.1 mmHg, respectively; $p<0.001$), exceeding the values in the control group (82.8 mmHg, $p=0.040$) (Table 2).

$PaCO_2$. A statistically significant decrease in $PaCO_2$ by day 8 was observed in the t-He/O_2 group (36.4 mm Hg, $p=0.027$) and the t-He/O_2+NO group (36.1 mm Hg, $p=0.030$). No significant changes were observed in the control group ($p=0.110$) (Table 2).

Lactate. By day 4, all study groups showed a significant decrease in lactate compared with baseline ($p<0.05$), whereas the change in the control group was not significant ($p=0.443$). By day 12, lactate concentrations in the t-He/O_2 and t-He/O_2 + NO groups reached 1.36 and 1.38 mmol/L, respectively, which was lower than in the control group (2.34 mmol/L) (Table 2).

pH. No intergroup differences were found in the dynamics of arterial blood pH ($p>0.05$), although there was a trend toward faster physiological recovery to normal reference ranges in the groups treated with t-He/O_2 (Table 2).

Safety. Throughout the entire follow up period, no adverse events related to NO or t-He/O_2 inhalation therapy were reported. The highest methemoglobin level recorded was 1%.

Discussion

The results of the study show that adding respiratory therapy with inhalations of NO and, in particular, with heated helium-oxygen mixture to standard of care in patients with polytrauma and pulmonary contusion leads to a significantly greater improvement in gas exchange parameters compared with oxygen therapy alone.

The greatest effectiveness of the heated heliox + NO combination can be explained by its impact on different links in the pathogenesis of respiratory failure in pulmonary contusion. Inhaled NO, as a selective vasodilator, presumably improved perfusion in ventilated lung areas, thereby reducing shunting [16, 22–24]. Heated heliox, by lowering breathing mixture density and possibly through the mucolytic effect of warmed, humidified gas, may have helped improve gas flow distribution and patency of the distal airways, reducing areas of hypoventilation [11–13, 20, 25]. The synergistic combination of these effects probably led to the fastest improvement of PaO_2, $PaCO_2$, and lactate values to normal ranges in group 3.

Similar effects were reported in a systematic review and meta-analysis [26] that included 8 studies with a total of 1,097 patients with pneumonia, showing that adding He/O_2 to standard therapy may improve oxygenation regardless of the He/O_2 inhalation protocol used. During the COVID-19 pandemic, He/O_2 inhalation improved oxygenation, helping to shorten the duration of oxygen therapy and reduce mortality [9, 10, 27]. The use of He/O_2 inhalation in preoperative preparation reduces the incidence of postoperative complications [25].

An important finding is the significant reduction in lactate levels in all study groups by day 4. Since hyperlactatemia in critically ill patients often reflects tissue hypoperfusion and oxygen debt, its rapid decline during use of the studied methods may indicate improved peripheral oxygenation and overall hemodynamics, which is consistent with the known effects of NO on microcirculation [9, 14, 17].

The complete absence of adverse events is consistent with the literature indicating the high safety of both low-dose inhaled NO [8, 18, 24] and heliox therapy [9, 11, 27] when used short-term in patients without severe pulmonary hypertension.

The limitations of this study include its open-label design, which is related to the technical characteristics of the equipment used, as well as its single-center setting, which may limit the generalizability of the results. A promising direction is to conduct multicenter studies using blinding to assess the impact of these methods on more hard endpoints: duration of mechanical ventilation, length of ICU stay, and all-cause mortality.

Clinical relevance: the proposed respiratory support methods are low-cost, noninvasive, and can be rapidly deployed in hospital settings and military field medical facilities. Their use may help stabilize polytrauma patients more quickly, shorten intensive care stays, and improve outcomes, which is of great importance for medical support in emergency zones.

Conclusion

Adding inhalations of either nitric oxide (30 ppm) or heated helium-oxygen mixture to standard respiratory therapy in patients with polytrauma and pulmonary contusion leads to a significant improvement in gas exchange parameters (PaO_2, SaO_2, $PaCO_2$), as well as a more rapid reduction in arterial blood lactate, compared with standard oxygen therapy.

The combined use of heated heliox and nitric oxide inhalations shows the most pronounced positive effect on gas exchange dynamics and on the resolution of CT signs of contusion-related lung injury, indicating a possible synergistic effect between the two methods.

All inhalation treatments demonstrated a favorable safety profile when used over a 12-day treatment course.

References

1. *Агаджанян В. В., Устьянцева И. М., Пронских А. А., Кравцов С. А., Новокшонов А. В., Агаларян А. Х., Милюков А. Ю., с соавт.* Политравма. Неотложная помощь и транспортировка. Новосибирск: Наука; 2008: 320. *Agadzhanyan V. V., Ustyantseva I. M., Pronskikh A. A., Kravtsov S. A., Novokshonov A. V., Agalarian A. Kh., Milukov A. Y., et al.* Polytrauma. Emergency aid and transportation. Novosibirsk: Nauka; 2008: 320.
2. Военная анестезиология и реаниматология. Национальное руководство. Щеголев А. В. (ред). М.: ГЭОТАР-Медиа; 2026: 912. ISBN 978-5-9704-9771-5. Military фnesthesiology and кesuscitation. National Guidelines. Shchegolev A. V. (ed). Moscow: GEOTAR-Media; 2026: 912. ISBN 978-5-9704-9771-5. (in Rus.).
3. *Крюков Е. В., Язенок А. В., Зайцев А. А., Говердовский Ю. Б., Агафонов П. В., Фурсова Е. Н.* Особенности патологии органов дыхания у раненых в условиях современного вооруженного конфликта. *Военно-медицинский журнал*. 2025; 346 (10): 4–10. *Kryukov E. V., Yazenok A. V., Zaitsev A. A., Goverdovsky Yu. B., Agafonov P. V., Fursova E. N.* Features of respiratory pathology in the wounded in the conditions of a modern armed conflict. *Military Medical Journal=Voenno- Meditsinskiy Zhurnal*. 2025; 346 (10): 4–10. (in Russ.).
   DOI: 10.52424/00269050_2025_346_10_4.
4. *Тришкин Д. В., Крюков Е. В., Агафонов П. В., Аланичев А. Е., Базилевич С. Н., Барсуков А. В., Башарин В. А., с соавт.* Военно-полевая терапия. Национальное руководство. М.: ГЭОТАР-Медиа; 2023: 736. *Trishkin D. V., Kryukov E. V., Agafonov P. V., Alanichev A. E., Bazilevich S. N., Barsukov A. V., Basharin V. A., et al.* Military field therapy. National guidelines. M.: GEOTAR-Media; 2023: 736. (in Russ.). ISBN 978-5-9704-8023-6.
   DOI 10.33029/9704-8023-6-VPT-2023-1-736.
5. *Язенок А. В., Паценко М. Б., Чеховских Ю. С., Агафонов П. В., Говердовский Ю. Б., Загородников Г. Г., Головко К. П.* Структура висцеральной патологии на этапе оказания специализированной медицинской помощи — в военно-медицинской организации центрального подчинения в условиях современного военного конфликта. *Военно-медицинский журнал*. 2025; 346 (12): 4–10. *Yazenok A. V., Patsenko M. B., Chekhovskikh Yu. S., Agafonov P. V., Goverdovsky Yu. B., Zagorodnikov G. G., Golovko K. P.* The structure of visceral pathology at the stage of providing specialized medical care in a centrally subordinate military medical organization during a modern military conflict. *Military Medical Journal=Voenno-Meditsinskiy Zhurnal*. 2025; 346 (12): 4-10. (in Russ.).
   DOI 10.52424/00269050_2025_346_12_4.
6. *Бойко И. В., Зафт В. Б., Лазаренко Г. О.* Организация экстренной медицинской помощи пострадавшим с политравмой на этапах медицинской эвакуации. *Медицина неотложных состояний*. 2013; 2 (49): 77–84. УДК: 616-001.756-083.98. *Boyko I. V., Zaft V. B., Lazarenko G. O.* Organization of emergency medical care for patients with polytrauma at the stages of medical evacuation. *Emergency Medicine= Neotlozhnaya Meditsina*. 2013; 2 (49): 77–84. (in Russ.). UDK: 616-001.756-083.98.
7. *Евдокимов В. И., Алексанин С. С., Рыбников В. Ю., Мясников А. А., Глухов В. А.* Наукометрический анализ статей по применению газовых дыхательный смесей в экстремальной медицине. *Медико-биологические и социально-психологические проблемы безопасности в чрезвычайных ситуациях*. 2024; 3: 104–123. *Evdokimov V. I., Aleksanin S. S., Rybnikov V. Yu., Myasnikov A. A., Glukhov V. A.* Scientometric analysis of articles of respiratory gas mixtures and their application in emergency medicine. *Medical, biological, and socio-psychological problems of safety in emergency situations*. 2024; 3: 104–123. (in Russ.).
   DOI: 10.25016/2541-7487-2024-0-3-104-123.
8. *Чучалин А. Г.* Респираторная медицина в 3 томах. М.: ГЭОТАР-Медиа. 2017;1: 640. *Chuchalin AG.* Respiratory Medicine in 3 volumes. M.: GEOTAR-Media. 2017;1: 640. (in Russ.).
9. *Шогенова Л. В., Петриков С. С., Журавель С. В., Гаврилов П. В., Уткина И. И., Варфоломеев С. Д., Рябоконь А. М., с соавт.* Термическая гелий-кислородная смесь в лечебном алгоритме больных с COVID-19. *Вестник РАМН*. 2020; 75 (5S): 353–362. *Shogenova L. V., Petrikov S. S., Zhuravel S. V., Gavrilov P. V., Utkina I. I., Varfolomeev S. D., Ryabokon A. M., et al.* Thermal helium-oxygen mixture as part of a treatment protocol for patients with COVID-19. *Annals of the Academy of Medical Sciences =Vestn Ross Acad Med Nauk*. 2020; 75 (5S): 353–362. (in Russ.). DOI: 10.15690/vramn1412.
10. *Смирнова М. И., Антипушина Д. Н., Драпкина О. М.* Возможные варианты применения гелиево-кислородной смеси при острой респираторной патологии и в условиях пандемии COVID-19. *Профилактическая медицина*. 2020; 23 (7): 78–84. *Smirnova M. I., Antipushina D. N., Drapkina O. M.* Possible options for the use of helium-oxygen mixture in acute respiratory pathology and in the context of the COVID-19 pandemic. *Russian Journal of Preventive Medicine =Profilakticheskaya Meditsina*. 2020; 23 (7): 78–84. (in Russ.). DOI: 10.17116/profmed20202307178.
11. *Beurskens, C. J., Wosten-van Asperen, R., Preckel, B., Juffermans N. P.* The potential of heliox as a therapy for acute respiratory distress syndrome in adults and children, a descriptive review. *Respiration*. 2015; 89 (2): 166–174.
   DOI:10.1159/000369472. PMID: 25662070.
12. *Chiappa G. R., Queiroga F. Jr., Meda E., Ferreira L. F., Diefenthaeler F., Nunes M., Vaz M. A., et al.* Heliox improves oxygen delivery and utilization during dynamic exercise in patients with chronic obstructive pulmonary disease. *Am J Respir Crit Care Med*. 2020; 395: 1004–1010. DOI: 10.1164/rccm.200811-1793OC. PMID: 19299497.
13. *Colebourn C. L., Barber V., Young J. D.* Use of helium-oxygen mixture in adult patients presenting with exacerbations of asthma and chronic obstructive pulmonary disease: a systematic review. *Anaesthesia*. 2007; 62 (1): 34–42. DOI: 10.1111/j.1365-2044.2006.04897.x. PMID: 17156225.
14. *Царева Н. А., Неклюдова Г. В., Ярошецкий А. И., Нуралиева Г. С., Куркиева Ф. Т., Шмидт А. Е., Су-*

ворова О. А. с соавт. Исследование эффективности и безопасности высоких доз ингаляционного оксида азота у пациентов с внебольничной пневмонией: пилотное исследование. *Пульмонология.* 2024; 34 (3): 417–426. *Tsareva N. A., Neklyudova G. V., Yaroshetsky A. I., Nuralieva G. S., Kurkieva F. T., Schmidt A. E., Suvorova O. A., et al.* Efficacy and safety of high doses of inhaled nitric oxide in patients with community-acquired pneumonia: a pilot study. *Pulmonology=Pulmonologiya*. 2024; 34 (3): 417–426. (in Russ.).
DOI: 10.18093/0869-0189-2024-34-3-417-426.

15. *Чучалин А. Г., Зайцев А. А., Куликова Н. А., Лиходий В. И., Давыдов Д. В.* Ушиб легкого: клинические рассуждения. *Пульмонология*. 2023; 33 (3): 408–413. *Chuchalin A. G., Zaitsev A. A., Kulikova N. A., Likhodiy V. I., Davydov D. V.* Pulmonary contusion: clinical reasoning. *Pulmonology=Pulmonologiya*. 2023; 33 (3): 408–413. (in Russ.).
DOI: 10.18093/0869-0189-2023-33-3-408-413.
16. *Bath P. M., Coleman C. M., Gordon A. L., Lim W. S., Webb A. J.* Nitric oxide for the prevention and treatment of viral, bacterial, protozoal and fungal infections. *F1000Res*. 2021; 10: 536.
DOI: 10.12688/f1000research.51270.2.
PMID: 35685687.
17. *Dweik R. A.* Exhaled nitric oxide analysis and applications. Literature review. UpToDate. Mar 07, 2023. URL: https://www.uptodate. com/contents/exhaled-nitric-oxide-analysis-and-applications.
18. *Ванин А. Ф.* Позитивное (регуляторное) и негативное (цитотоксическое) действие динитрозильных комплексов железа в живых организмах. *Биохимия*. 2022; 87 (11): 1739–1760. *Vanin A. F.* Positive (regulatory) and negative (cytotoxic) effects of iron dinitrosyl complexes in living organisms. *Biochemistry = Biokhimiia*. 2022; 87 (11): 1739–1760. (in Russ.). DOI: 10.31857/S0320972522110173.
19. *Калашникова Т. П., Арсеньева Ю. А., Каменщиков Н. О., Подоксенов Ю. К., Кравченко И. В., Чубик М. В., Карпова М. Р., с соавт.* Антибактериальное действие оксида азота на возбудители госпитальной пневмонии (экспериментальное исследование). *Общая реаниматология*. 2024; 20 (3): 32–41. *Kalashnikova T. P., Arsenyeva Yu. A., Kamenshchikov N. O., Podoksenov Yu. K., Kravchenko I. V., Chubik M. V., Karpova M. R., et al.* Antibacterial effect of nitric oxide on the causative agents of hospital-acquired pneumonia (experimental study). *General Reanimatology = Obshchaya Reanimatologiya*. 2024; 20 (3): 32–41. (in Russ. &Eng.).
20. *Чучалин А. Г.* Оксид азота — молекула XXI века. *Пульмонология*. 2024; 34 (3): 326–333. *Chuchalin A. G.* Nitric axide — a molecule of the 21st century. *Pulmonology=Pulmonologiya*. 2024; 34 (3): 326–333. (in Russ.). DOI: 10.18093/0869-0189-2024-34-3-326-333.333.
21. *Fink J. B.* Helium-oxygen: an old therapy creates new interest. Feb 7, 2007. Chron. Pulm. Dis. respiratorytherapy. com [сайт]. Текст: электронный. (дата обращения: 20.01.2026)
22. *Tejero J., Shiva S., Gladwin M. T.* Sources of vascular nitric oxide and reactive oxygen species and their regulation. *Physiol Rev*. 2019; 99 (1): 311–379.
DOI: 10.1152/physrev.00036.2017. PMID: 30379623.
23. *Zhao Y., Vanhoutte P. M., Leung S. W.* Vascular nitric oxide: beyond NOS. *J Pharmacol Sci*. 2015; 129 (2): 83–94.
DOI: 10.1016/j. jphs.2015.09.002. PMID: 26499181.
24. *Костыря Ю. Е., Гуляев Н. И., Агафонов П. В., Юркин А. К.* Исследование эффективности и безопасности оксида азота в ранней респираторной реабилитации пациентов с политравмой и ушибом легких. *Вестник Российской военно-медицинской академии*. 2026; 28 (1): 65–73 *Kostyrya Yu. E., Gulyaev N. I., Agafonov P. V., Yurkin A. C.* Study of nitric oxide effectiveness and safety in early respiratory rehabilitation of patients with polytrauma and pulmonary contusion. *Bulletin of the Russian Military Medical Academy= Vestnik Rossiyskoy Voenno-Meditsinskoy Akademii*. 2026; 28 (1): 65–73 (in Russ.).
DOI: 10.17816/brmma697540.
25. *Лянгазов А. П., Габитов М. В., Скрипкин Ю. В., Молчанов И. В., Гребенчиков О. А.* Влияние предоперационной подготовки гелий-кислородной смесью на частоту легочных осложнений у пациентов с ХОБЛ и раком легкого. *Общая реаниматология*. 2026; 22 (1): 4–13. *Lyangazov A. P., Gabitov M. V., Skripkin Yu. V., Molchanov I. V., Grebenchikov O. A.* The effect of preoperative preparation with helium-oxygen mixture on the incidence of pulmonary complications in patients with COPD and lung cancer. *General Reanimatology= Obshchaya Reanimatologiya*. 2026; 22 (1): 4–13. (in Russ. &Eng.).
DOI: 10.15360/1813-9779-2026-1-2606.
26. *Лахин Р. Е., Шаповалов П. А., Щеголев А. В., Козлов К. В., Жданов А. Д.* Эффективность использования кислородно-гелиевой смеси в интенсивной терапии пневмоний у взрослых пациентов: систематический обзор и метаанализ. *Вестник интенсивной терапии им. А. И. Салтанова*. 2022; 2: 52–69. *Lakhin R. E., Shapovalov P. A., Shchegolev A. V., Kozlov K. V., Zhdanov A. D.* The effectiveness of oxygen-helium mixture in the intensive care of pneumonia in adult patients: a systematic review and meta-analysis. *Ann Crit Care =Vestnik Intensivnoy Terapii im A. I. Saltanova*. 2022; 2: 52–69. (in Russ.).
DOI: 10.21320/1818-474X-2022-2-52-69.
27. *Лахин Р. Е., Жданов А. Д., Щеголев А. В., Жданов К. В., Салухов В. В., Зверев Д. П., Козлов К. В.* Применение кислородно-гелиевой газовой смеси «ГелиОкс» для лечения дыхательной недостаточности у пациентов с новой коронавирусной инфекцией COVID-19 (рандомизированное одноцентровое контролируемое исследование). *Журнал им. Н. В. Склифосовского «Неотложная медицинская помощь»*. 2021; 10 (3): 430–437. *Lakhin R. E., Zhdanov A. D., Shchegolev A. V., Zhdanov K. V., Salukhov V. V., Zverev D. P., Kozlov K. V.* Oxygen-helium gas mixture «Heliox» for the treatment of respiratory failure in patients with the new coronavirus infection COVID-19 (randomized single-center controlled trial). *Russian Sklifosovsky Journal «Emergency Medical Care» = Zhurnal im. N. V. Sklifosovskogo «Neotlozhnaya Meditsinskaya Pomoshch»*. 2021; 10 (3): 430–437. (in Russ.).
DOI: 10.23934/2223-9022-2021-10-3-430-437.

Received 09.02.2026
Accepted 13.05.2026

https://doi.org/10.15360/1813-9779-2026-3-2608

The Neuroprotective Effects of Lithium Chloride in a Model of Photochemically Induced Stroke

Georgy S. Klimenkov[1], Vladimir T. Dolgikh[1], Mikhail V. Gabitov[1]*, Yuri V. Skripkin[2], Oleg A. Grebenchikov[1]

[1] V. A. Negovsky Research Institute of General Reanimatology, Federal Research and Clinical Center of Intensive Care Medicine and Rehabilitology, Ministry of Education and Science of Russia, 25 Petrovka Str., Bldg. 2, 107031 Moscow, Russia
[2] M. F. Vladimirsky Moscow Regional Research Clinical Institute 61/2 Shchepkin Str., 129110 Moscow, Russia

For citation: *Georgy S. Klimenkov, Vladimir T. Dolgikh, Mikhail V. Gabitov, Yuri V. Skripkin, Oleg A. Grebenchikov.* The Neuroprotective Effects of Lithium Chloride in a Model of Photochemically Induced Stroke. *Obshchaya Reanimatologiya* = *General Reanimatology.* 2026; 22 (3): 21–27. https://doi.org/10.15360/1813-9779-2026-3-2608 [In Russ. and Engl.]

***Correspondence to:** Mikhail V. Gabitov, mgabitov@fnkcrr.ru

Summary

The aim of the study was to investigate the neuroprotective properties of lithium chloride in a model of photochemically induced stroke in rats.

Materials and Methods. The experimental work was conducted in the organoprotection laboratory for critical conditions at the V. A. Negovsky Research Institute of General Reanimatology, Federal Research and Clinical Center of Intensive Care Medicine and Rehabilitology. The study included 32 outbred Wistar rats, randomized into 2 equal groups: the NaCl (control) group, treated with physiological saline solution, and the LiCl group, which received a 4.2% lithium chloride solution (63 mg/kg). The solutions were administered intravenously 120 minutes after inducing a stroke. The ischemic stroke model was generated using photochemically induced thrombosis in cerebral sensorimotor cortex vessels. Neurological deficit was assessed using the «limb placement test». Ischemic lesion volume was measured using MRI (7 Tesla). Immunohistochemical analysis included markers for NeuN (survived mature neurons), Cas-3 (neuronal apoptosis), and Iba-1 (microglial activation). Statistical analysis was performed using the Shapiro–Wilk test, Student's *t*-test, and the Mann–Whitney *U* test with significance at $p < 0.05$.

Results. Lithium chloride infusion resulted in a 30% reduction in the ischemic lesion volume compared to the control group ($p = 0.0236$). The LiCl group showed an increase in signal intensity (relative units, RU) in the NeuN-positive neurons in the penumbra (80 RU vs 41 RU in the control group, $p = 0.0001$), a 25% decrease in signal intensity in Cas-3-positive cells ($p = 0.0008$), and a 58% decrease in signal intensity in Iba-1-positive cells ($p < 0.0001$). Neurological deficit in the LiCl group was less detectable (NaCL vs LiCl: 9,8 ± 1,2 vs 12,5 ± 1,5 scores, respectively, $p < 0.0001$).

Conclusion. Lithium chloride demonstrated significant neuroprotective properties in a model of ischemic stroke, reducing the volume of damage and favoring the suppression of apoptosis and inflammation. The findings validate the potential of lithium chloride as a therapeutic agent for treatment of ischemic stroke, owing in particular to ability to modulate key pathogenic mechanisms of the disease. The results underscore the need for further clinical research to assess the efficacy and safety of lithium in medical practice.

Keywords: lithium; neuroprotection; ischemic stroke; acute cerebrovascular accident; NeuN; Cas-3; Iba-1

Conflict of interest. The authors declare no conflict of interest.

Information about the authors:
Georgy S. Klimenkov: https://orcid.org/0009-0006-5853-7961
Vladimir T. Dolgikh: https://orcid.org/0000-0001-9034-4912
Mikhail V. Gabitov: https://orcid.org/0009-0005-9615-6118
Yuri V. Skripkin: https://orcid.org/0000-0002-6747-2833
Oleg A. Grebenchikov: https://orcid.org/0000-0001-9045-6017

Introduction

Stroke is one of the leading causes of death worldwide [1, 2]. Global stroke epidemiology shows a steady trend toward an increase in incidence, reaching 9.6 million new cases annually. This figure strongly correlates with the demographic aging of the population. According to studies, one in four people will suffer a stroke during their lifetime, with ischemic stroke being the predominant form of cerebrovascular disease [2].

The pathophysiological mechanisms of ischemic stroke involve a complex cascade of interrelated processes, among which disruption of the blood-brain barrier plays a key role. Secondary damage in stroke involves oxidative stress and neuroinflammation, which lead to dysfunction of the cerebral vascular endothelium. These changes destabilize the brain microenvironment, initiating vasogenic edema and hemorrhagic transformation of ischemic tissue, while the activation of microglia

and astrocytes closes a vicious cycle that exacerbates ischemic damage and contributes to the progression of neurological deficits [3].

Acute cerebral ischemia triggers structural intracellular changes. The fate of neurons is determined by the degree and duration of pore opening, which alters the permeability of the mitochondrial membrane (Mitochondrial Permeability Transition Pore, mPTP), along with the development of energy deficiency, excitotoxicity, and oxidative stress. A moderate and transient increase in membrane permeability may be accompanied by reversible changes followed by cellular regeneration, whereas prolonged pore opening inevitably leads to death of cerebral structures. The pathophysiological process associated with mPTP opening is characterized by the release of key proapoptotic factors into the cytoplasm, including apoptosis-inducing factor (AIF) and secondary mitochondrial activator of caspases (SMAC/Diablo) [4]. In addition, the enzyme glycogen synthase kinase 3β (GSK-3β), which is involved in regulation of cell death, inflammation, and oxidative stress, is considered one of the important pathogenetic targets [5].

The use of lithium-containing drugs as a therapeutic agent has undergone significant evolution over the past decades, particularly in the field of neuroprotection [6–8]. Initially known for their mood-stabilizing properties in the treatment of mental disorders, lithium-containing drugs have recently become the focus of intense research interest due to their neuroprotective effects in traumatic brain injury, Alzheimer's disease, and amyotrophic lateral sclerosis [9–14].

Lithium is capable of modulating multiple signaling pathways, influencing apoptosis, autophagy, cytoskeletal remodeling, gene expression, energy metabolism, oxidative stress, and the inflammatory response. Key targets of its action include the Wnt/β-catenin pathway, adenylate cyclase, inositol monophosphatase, and cyclooxygenase. The molecular effects of lithium are mediated by its interaction with GSK-3β, as well as GPCRs, IMPA, and IPP [15]. The pleiotropic effect of this cation on cellular functions occurs through the phosphorylation of GSK-3β and its effects on cAMP-dependent, inositol-3-phosphate, and calcium-mediated signaling cascades. In addition, lithium influences the activity of GABA and NMDA receptors, participating in the regulation of calcium homeostasis [16]. Lithium treatment reduces the production of proinflammatory factors, including IL-1β and TNF-α, as well as other neuroinflammatory biomarkers in experimental animal models [17, 18]. Lithium exerts a cytoprotective effect on neuronal cell cultures in the presence of β-amyloid and colchicine [19]. The use of lithium ascorbate improves stress adaptation in in vitro and in vivo models [20].

The aim of this study is to investigate the neuroprotective properties of lithium chloride in a model of photochemically induced stroke in rats.

Materials and Methods

Experimental studies involving laboratory animals were conducted in accordance with the Principles of Good Laboratory Practice (Russian Federation National Standard GOST R 53434-2009, March 2010) and protocols reviewed and approved by the Animal Ethics Committee of the A. N. Belozersky Research Institute of Physico-Chemical Biology (Minutes No. 2/20 dated February 12, 2020). The study was approved by the Ethics Committee of the V. A. Negovsky Research Institute of General Reanimatology, Federal Research Center for Intensive Care Medicine (meeting minutes No. 1/25/5 dated February 7, 2025).

The study was conducted on 32 outbred male Wistar white rats weighing 310±12.5 g and aged 14–18 weeks.

Modeling of photoinduced ischemic stroke. The model was induced following intraperitoneal administration of chloral hydrate (Sigma-Aldrich, USA) at a dose sufficient to induce anesthesia (400 mg/kg body weight), diluted in a 0.9% sodium chloride solution (Solopharm, Russia) at a rate of 10 mL/kg body weight. Focal ischemic stroke was modeled in the sensorimotor cortex of rats using photochemically induced thrombosis of cortical vessels. The photosensitive dye Bengal rose (3%, 40 mg/kg intravenously; Sigma-Aldrich, USA) was injected into the jugular vein. Afterward, the rat's head was secured in a stereotaxic frame (Bregma coordinates: 0.5 mm distal and 2.5 mm lateral), and the skull was exposed via a midline incision, with the periosteum removed. The cerebral hemisphere in the area of the sensorimotor cortex was irradiated with a green laser at $\lambda = 550$ nm for 15 min. After the skin was sutured, the rats were placed in a cage under an infrared heating lamp until they emerged from anesthesia. Body temperature was maintained at 37 ± 0.5°C throughout the experiment. Body temperature was measured using a rectal sensor, and thermoregulation was performed automatically by connecting the heating module to a thermostat and setting the threshold values.

Grouping of animals. After regaining consciousness and the ability to regulate body temperature independently, 120 minutes following induced ischemic stroke, the animals were administered intravenously a 0.9% sodium chloride solution, 1.5 mL/kg (control group, NaCl, $n = 16$) or a 4.2% lithium chloride solution, 63 mg/kg (comparison group, LiCl, $n = 16$).

After administration of the solutions, the animal's general condition (level of consciousness, mobility) was assessed, and analgesia was administered

(paracetamol 50 mg/kg subcutaneously). The animal was then transferred to a cage with free access to water and food. Throughout the experiment, the partial pressures of O_2 and CO_2 in the animal chamber were continuously monitored using an indoor atmosphere control unit («INSOVT» JSC, Russia).

Instrumental methods. The studies were performed using a magnetic resonance imaging (MRI) scanner with a magnetic field strength of 7 Tesla and a gradient system of 105 mT/m (BioSpec 70/30 USR, Bruker, Germany). The extent of brain damage was assessed using graphical analysis of MRI images, with calculation of the volume of the damaged brain area.

Immunohistochemical studies. The immunohistochemical analysis included NeuN, Cas-3, and Iba-1 markers. These markers were selected based on their biological functions.

The NeuN protein (Neuronal Nuclei, also known as Fox-3 or RBFOX3) is expressed in most mature neurons but is absent in glial cells, stem cells, and immature neuroblasts. Decreased NeuN expression is associated with loss of neuronal integrity [21].

Caspase-3 is an enzyme involved in the process of apoptosis.

The Iba-1 protein (Ionized calcium-binding adapter molecule 1) is a specific marker of microglia and macrophages involved in the immune response and inflammatory processes in nervous and other tissues [22].

The cells in which expression of these proteins was detected were designated as NeuN-positive, Cas-3-positive, and Iba-1-positive.

For immunohistochemical analysis on the 14th day after stroke, immediately following euthanasia (decapitation under anesthesia with 6% chloral hydrate), the rat brains were fixed in 4% formalin, embedded in paraffin, and sectioned to a thickness of 4 μm. The sections were deparaffinized in xylene and rehydrated in ethyl alcohol. High-temperature antigen retrieval was performed in citrate buffer, pH 6 (Target Retrieval Solution, DAKO, Glostrup, Denmark). The sections were cooled, washed three times in distilled water, and three times in phosphate-buffered saline (PBS IHC Wash Buffer + Tween, Cell Mark, Rocklin, USA) with a 5-minute exposure time. To suppress endogenous peroxidase, the sections were incubated in 3% hydrogen peroxide for 10 minutes. To prevent non-specific binding of primary or secondary antibodies to tissue proteins, Protein Block Serum-free (Abcam, UK) was used with a 30-minute exposure. The sections were incubated at 37°C for 1 hour with primary antibodies against Iba1 (ab5076, 1:500) and NeuN (ab177487, 1:200), Anti-Caspase-3 (ab13847, 1:100), and anti-Von Willebrand factor (ab9378, 1:200) diluted in Antibody Diluent (ab64211, Abcam, UK). The sections were then washed in PBS twice for 5 minutes each. After washing the sections in PBS, they were stained with hematoxylin, rinsed in running water, dehydrated, and mounted. Images were acquired using a Nikon Eclipse Ni-e microscope (Japan), and digital analysis was performed using NIS-Elements software (Nikon Europe B.V., Netherlands) and ImageJ, Fiji. Results were presented as signal intensity (Mean Intensity) in arbitrary units (AU).

Methods for assessing neurological disorders. The limb placement test (LPT) was conducted according to a protocol based on the method described by De Ryck et al. [23] and modified by Jolkkonen et al. [24]. The rats were habituated to human hands 3 days prior to testing. The test consisted of seven trials assessing the sensorimotor integration of the forelimbs and hindlimbs in response to tactile, proprioceptive, and visual stimulation.

Statistical analysis of the data was performed using Microsoft Excel (Microsoft Corporation, 2021), Statistica 12.0 (StatSoft, Inc., 2014), and MedCalc 23.1.2 (MedCalc Software Ltd, 2025). The data were tested for normality of distribution of variables in the samples using the Shapiro–Wilk test. Samples with a normal distribution were tested for equality of variances (F-test). Data were presented as mean and standard deviation ($M \pm SD$), as well as median with interquartile range (Me [$Q1$–$Q3$]). Samples with a normal distribution and equal variances were compared using Student's t-test. Parameters in groups with a non-normal distribution and samples with unequal variances were compared using the Mann–Whitney U-test. Results of LPT test across groups were compared using the area under the curve (AUC) for serial measurements. A two-sided significance level of $p < 0.05$ was used to assess intergroup differences.

Results

The animals in the NaCl and LiCl groups were comparable in terms of body weight ($p = 0.585$) and age (0.931) (Table).

The test results showed a statistically significant reduction in the severity of neurological deficits in the LiCl group compared with the NaCl group ($p < 0.0001$). (Fig. 1).

The average extent of brain damage resulting from induced ischemic stroke was statistically significantly lower by nearly 30% in the LiCl group ($p = 0.0236$) (Fig. 2).

NeuN-positive cells were present in the area of ischemic damage in both groups. At the same time, in the penumbra zone, the signal intensity of NeuN-positive cells was statistically significantly higher in the LiCl group than in the control group, amounting to 80 AU vs. 41 AU ($p = 0.0001$) (Table, Fig. 3).

In the area outside the ischemic lesion, there was no significant difference in the signal intensity of NeuN-positive cells between the groups. When determining the signal intensity of Cas-3-positive

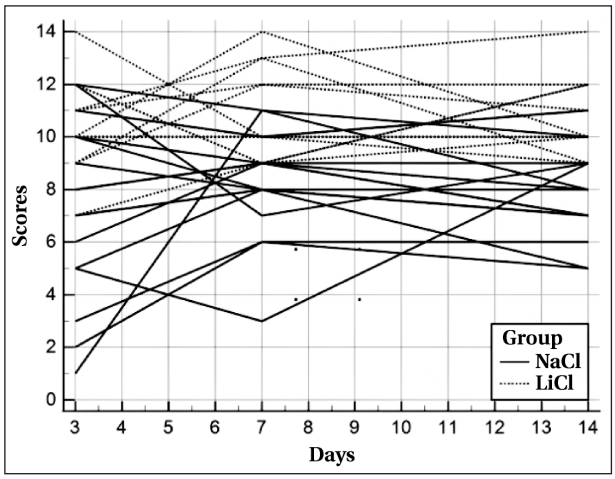

Fig. 1. Results of the «Limb placement test» test over time.
Note. Each line represents the individual trend in test results for a single animal in the study group.

and Iba-1-positive cells, a statistically significant decrease was observed in the LiCl group compared to the control group: by 25% and 58%, respectively (Table).

Discussion

The present study demonstrated significant neuroprotective effects of lithium chloride in a model of photochemically induced ischemic stroke in rats. The results showed that LiCl treatment reduced the volume of the ischemic lesion by 30% compared to the control group, as confirmed by MRI data. This is consistent with previously published studies in which lithium exhibited neuroprotective properties by modulating key pathogenic mechanisms of ischemia, such as oxidative stress, neuroinflammation, and apoptosis [25–27].

A key finding of the study was the significant increase in the signal intensity of NeuN-positive neurons in the penumbra zone observed in animals treated with lithium chloride. This indicates that neuronal viability is preserved and the extent of neuronal damage is reduced. At the same time, no intergroup differences in the signal intensity of NeuN-positive neurons were observed in the area outside the ischemic lesion, which underscores the selective action of lithium chloride on the ischemic zone. The data obtained support the hypothesis that lithium is capable of inhibiting apoptosis by

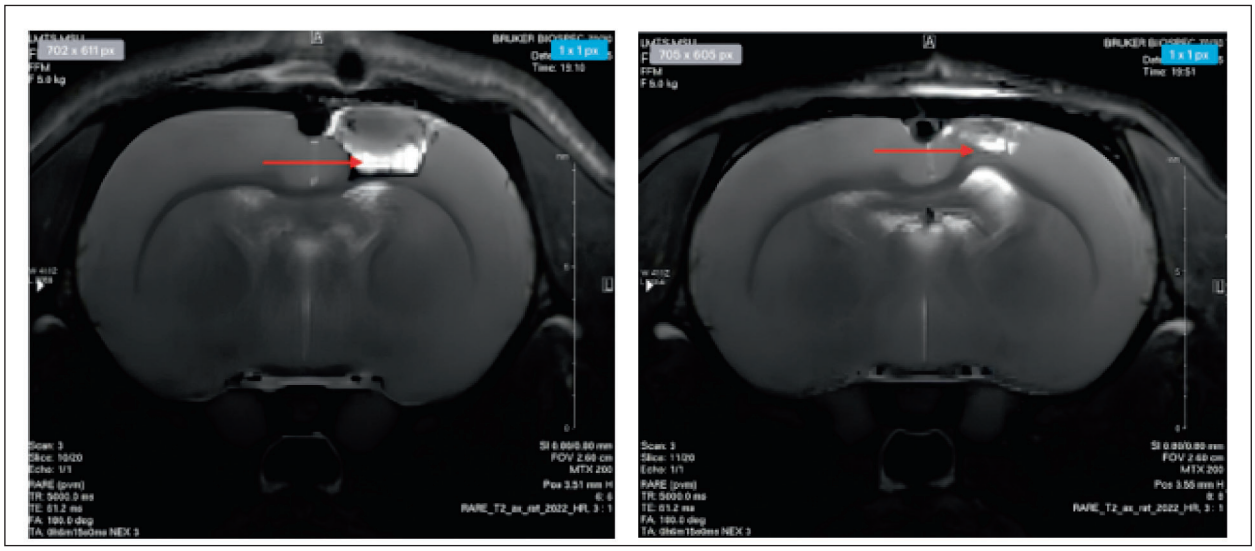

Fig. 2. T2-weighted MRI images in the axial plane, acquired on a 7-Tesla scanner (BioSpec 70/30 USR, Bruker).
Note. The hyperintense signal (white) corresponds to an area of vasogenic edema and ischemic injury. The red arrows indicate the boundaries of the ischemic lesion in the sensorimotor cortex of the brain. Left: NaCl group (control); right: LiCl group. A reduction in the area of ischemic damage was visually noted in the LiCl group.

Table. Comparison of groups by study parameters.

Parameters	Parameter values in the groups		*p*
	NaCl	LiCl	
Bode weight, g	350±36	350±31	0,585
Age, weeks	17 [14–17]	16,5 [14–17]	0,931
LPT, AUC	86±18	115±13	<0,0001
Lesion volume, mm³	12,9 [10–13,8]	10 [5–11,8]	0,0236
NeuN penumbra, AU	41 [25–50,2]	80 [40–83]	0,0001
NeuN outside lesion	350 [180–451,2]	362,5 [200–435]	0,920
Cas-3, AU	13856 [10448–18142,2]	10385 [9000–12681,2]	0,0008
Iba, AU	2836±486	1179±319	<0,0001

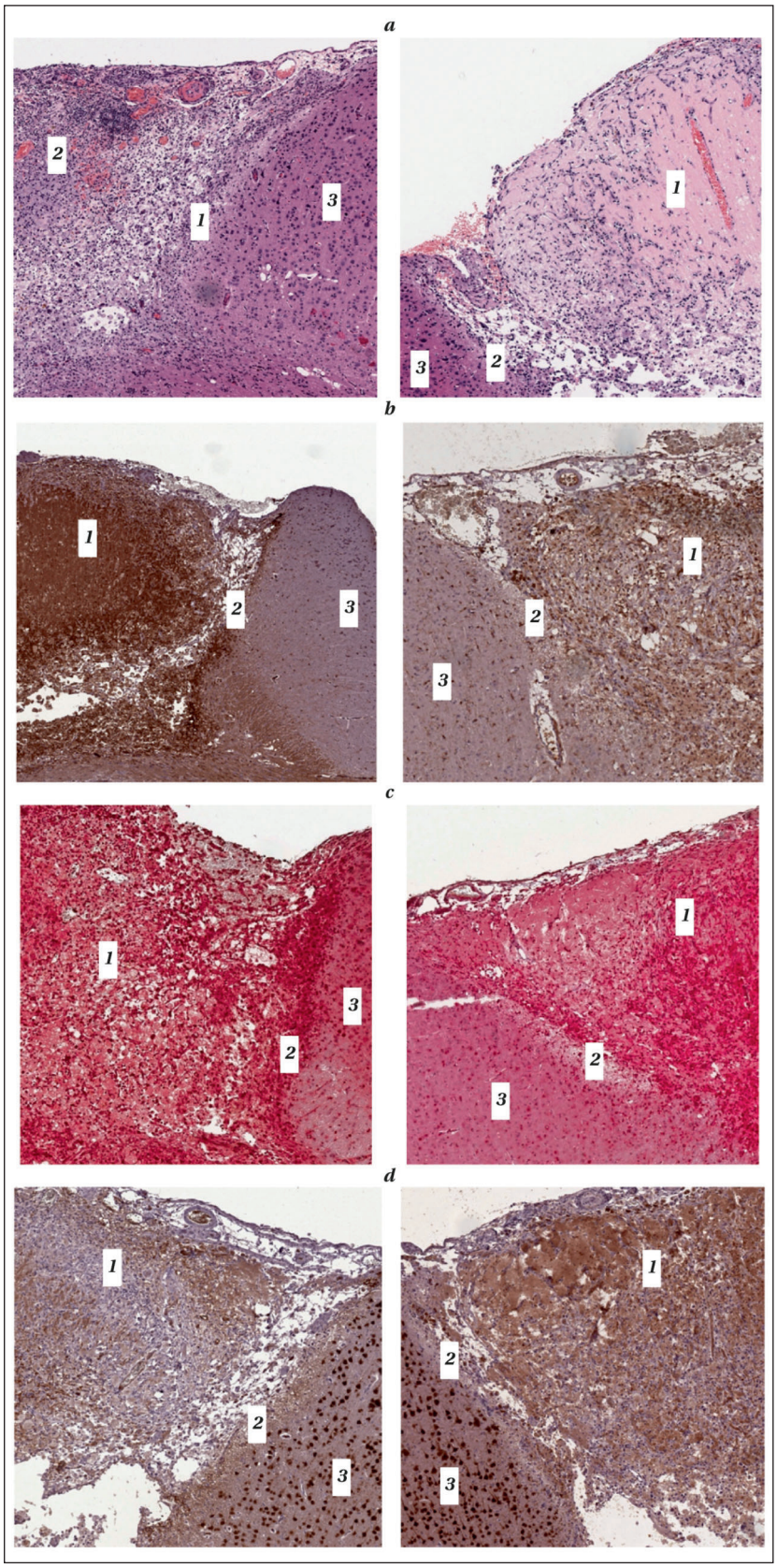

Fig. 3. Representative images of histological sections of rat brain.
Note. 20× objective. *a* — hematoxylin and eosin staining; *b* — sections with a lesion site stained for Iba-1; *c* — combined cell staining: von Willebrand factor (vWf) in red, caspase-3 (Cas-3) in brown; *d* — NeuN-positive cells. *1* — lesion; *2* — penumbra; *3* — intact tissue.

suppressing caspase-3 activity, which is consistent with the results of other studies [28, 29].

The decrease in the intensity of Iba-1-positive cells in the LiCl group indicates a reduction in microglial activation and, consequently, a weakening of the neuroinflammatory response. This confirms the role of lithium in modulating inflammatory processes, which has been previously described in a study focusing on its effects on pro-inflammatory cytokines [30].

Lithium mechanisms of action, such as inhibition of GSK-3β and regulation of calcium homeostasis, play a significant role in its neuroprotective properties [31, 32]. The results obtained complement existing data, confirming that lithium medications may be a promising means for the therapy of ischemic stroke, especially in combination with other neuroprotective agents.

Conclusion

Lithium chloride demonstrated marked neuroprotective properties in a model of photochemically induced ischemic stroke in rats, which were manifested by:

— a 30% reduction in the volume of the ischemic lesion;

— an increase in the intensity of NeuN-positive neuron signals in the penumbra area;

— a 25% and 58% decrease in the expression levels of caspase-3 and Iba-1, respectively.

The improvement in neurological functions in rats treated with lithium chloride confirms the clinical significance of its neuroprotective effect.

Notably, the favorable safety profile of lithium at the doses used in this experiment, combined with the obtained data on its positive effects, suggests a promising outlook for preclinical studies of its neuroprotective properties.

References

1. *Толпыгина С.Н., Загребельный А.В., Чернышева М.И., Воронина В.П., Кутишенко Н.П., Дмитриева Н.А., Лерман О.В., с соавт.* Отдаленная выживаемость больных, перенесших острое нарушение мозгового кровообращения, в различных возрастных группах в регистре РЕГИОН-М. *Российский кардиологический журнал*. 2023; 28 (2): 5250. *Tolpygina S.N., Zagrebelny A.V., Chernysheva M.I., Voronina V.P., Kutishenko N.P., Dmitrieva N.A., Lerman O.V., et al.* Long-term survival of patients with acute cerebrovascular accidents in different age groups in the REGION-M registry. *Russian Journal of Cardiology=Rossiyskiy Kardiologichesky Zhurnal*. 2023; 28 (2): 5250. (In Russ.).
DOI: 10.15829/1560-4071-2023-5250.
2. *GBD* 2016 *Stroke Collaborators.* Global, regional, and national burden of stroke, 1990–2016: a systematic analysis for the Global Burden of Disease Study 2016. *Lancet Neurol.* 2019; 18 (5): 439–458.
DOI: 10.1016/S1474-4422(19)30034-1.
PMID: 30871944.
3. *Cheng J., Zheng Y., Cheng F., Wang C., Han J., Zhang H., Lan X., et al.* Different roles of astrocytes in the blood-brain barrier during the acute and recovery phases of stroke. *Neural Regen Res.* 2026; 21(4): 1359–1372.
DOI: 10.4103/NRR.NRR-D-24-01417.
PMID: 40537147.
4. *Yang J., Wu S., He M.* Extracellular vesicle-mediated delivery of mitochondrial circRNA MTCO2 protects against cerebral ischemia by modulating mPTP-dependent ferroptosis. *Redox Biol.* 2025; 86: 103806.
DOI: 10.1016/j.redox.2025.103806.
PMID: 40768899.
5. *Лихванцев В.В., Мороз В.В., Гребенчиков О.А.* Механизмы фармакологического прекондиционирования мозга и сравнительная эффективность препаратов-ингибиторов гликоген-синтетазы-киназы-3 прямого и непрямого действия. *Общая реаниматология.* 2012; 8 (6): 37–42. *Likhvantsev V.V., Moroz V.V., Grebencchikov O.A.* The mechanisms of pharmacological preconditioning of the brain and the comparative efficacy of the drugs — direct-and indirect-acting glycogen synthase kinase-3 inhibitors: experimental study. *General Reanimatology = Obshchaya Reanimatologiya.* 2012; 8 (6): 37–42. (in Russ.&Eng.).
DOI: 10.15360/1813-9779-2012-6-37.
6. *Karati D., Meur S., Roy S., Mukherjee S., Debnath B., Jha S.K., Sarkar B.K., Naskar S., et al.* Glycogen synthase kinase 3 (GSK3) inhibition: a potential therapeutic strategy for Alzheimer's disease. *Naunyn Schmiedebergs Arch Pharmacol.* 2025; 398 (3): 2319–2342.
DOI: 10.1007/s00210-024-03500-1.
PMID: 39432068.
7. *Allam E., Abdel Ghafar S.K., Hussein M., Al-Emam A., Radad K.* Lithium chloride rescues dopaminergic neurons in a Parkinson's disease rat model challenged with rotenone. *CNS Neurol Disord Drug Targets.* 2025; 24 (8): 636–647.
DOI: 10.2174/0118715273365449250224090655.
PMID: 40114566.
8. *Godoy J.A., Mira R.G., Inestrosa N.C.* Intracellular effects of lithium in aging neurons. *Ageing Res Rev.* 2024; 99: 102396.
DOI: 10.1016/j.arr.2024.102396. PMID: 38942199.
9. *Шарикадзе Д.Т., Габитов М.В., Редкин И.В., Кузовлев А.Н., Мороз В.В.* Нейропротекторный потенциал хлорида лития при моделировании черепно-мозговой травмы. *Общая реаниматология.* 2025; 21 (5): 44–50. *Sharikadze D.T., Gabitov M.V., Redkin I.V., Kuzovlev A.N., Moroz V.V.* Neuroprotective potential of lithium chloride in a model of traumatic brain injury. *General Reanimatology = Obshchaya Reanimatologiya.* 2025; 21 (5): 44–50.
DOI: 10.15360/1813-9779-2025-5-2528.
10. *Черпаков Р.А., Гребенчиков О.А.* Влияние концентрации хлорида лития на его нейропротекторные свойства при ишемическом инсульте у крыс. *Общая реаниматология*. 2021; 17 (5): 101–110. *Cherpakov R.A., Grebencchikov O.A.* Effect of lithium chloride concentration on its neuroprotective properties in ischemic stroke in rats. *General Reanimatology = Obshchaya Reanimatologiya.* 2021; 17 (5): 101–110. (in Russ.&Eng.).
DOI: 10.15360/1813-9779-2021-5-101-110.
11. *Шарикадзе Д.Т., Габитов М.В., Лобанов А.В., Гребенчиков О.А., Кузовлев А.Н.* Изучение влияния хлорида лития на уровень провоспалительных цитокинов после черепно-мозговой травмы. *Патологическая физиология и экспериментальная терапия*. 2025; 69 (1): 58–64. *Sharikadze D.T., Gabitov M.V., Lobanov A.V., Grebenshchikov O.A., Kuzovlev A.N.* The effect of lithium chloride on the level of pro-inflammatory cytokines after traumatic brain injury. *Pathological Physiology and Experimental Therapy = Patologicheskaya Fiziologiya i Exsperimentalnaya Terapiya.* 2025; 69 (1): 58–64. (in Russ.).
DOI: 10.25557/0031-2991.2025.01.
12. *De-Paula V.J.R., Radanovic M., Forlenza O.V.* Lithium and neuroprotection: a review of molecular targets and biological effects at subtherapeutic concentrations in preclinical models of Alzheimer's disease. *Int J Bipolar Disord.* 2025; 13 (1): 16.
DOI: 10.1186/s40345-025-00386-7.
PMID: 40348943.
13. *Gildengers A.G., Ibrahim T.S., Zeng X., Aizenstein H.J., Alkhateeb S.K., Anderson S.J., Chu C., et al.* The LATTICE Study: Design of a pilot feasibility randomized controlled trial of lithium to delay cognitive decline in mild cognitive impairment. *Alzheimers Dement (NY).* 2025; 11 (2): e70112.
DOI: 10.1002/trc2.70112. PMID: 40501510.
14. *Boll M.C., Alcaraz-Zubeldia M., Rios C., González-Esquivel D., Montes S.* A phase 2, double-blind, placebo-controlled trial of a valproate/lithium combination in ALS patients. *Neurologia.*2025; 40 (1): 32–40.
DOI: 10.1016/j.nrleng.2022.07.003. PMID: 36049647.
15. *Puglisi-Allegra S., Ruggieri S., Fornai F.* Translational evidence for lithium-induced brain plasticity and neuroprotection in the treatment of neuropsychiatric disorders. *Transl Psychiatry.* 2021; 11: 1–10.
DOI: 10.1038/s41398-021-01492-7.
PMID: 34226487.
16. *Gogoleva I.V., Gromova O.A., Torshin I.Y., Grishina T.R., Pronin A.V.* The neurobiological role of lithium salts. *Neurosci Behav Physi.* 2023; 53: 939–945.
DOI: 10.1007/s11055-023-01485-7.

17. *Singulani M.P., Ferreira A.F.F., Figueroa P.S., Cuyul-Vásquez I., Talib L.L., Britto L.R., Forlenza O.V.* Lithium and disease modification: a systematic review and meta-analysis in Alzheimer's and Parkinson's disease. *Ageing Res Rev.* 2024; 95: 102231. DOI: 10.1016/j.arr.2024.102231. PMID: 38364914.
18. *Almeida O.P., Singulani M.P., Ford A.H., Hackett M.L., Etherton-Beer C., Flicker L., Hankey G.J., et al.* Lithium and stroke recovery: a systematic review and meta-analysis of stroke models in rodents and human data. *Stroke.* 2022; 53: 2935–2944. DOI: 10.1161/STROKEAHA.122.039203. PMID: 35968702.
19. *Fan M., Song C., Wang T., Li L., Dong Y., Jin W., Lu P.* Protective effects of lithium chloride treatment on repeated cerebral ischemia-reperfusion injury in mice. *Neurological Sciences.* 2015; 36 (2): 315–321. DOI: 10.1007/s10072-014-1943-x. PMID: 25192664.
20. *Pronin A.V., Gromova O.A., Sardaryan I.S., Torshin I., Stelmashuk E.V., Ostrenko K.S, Aleksandrova O.P., et al.* The adaptogenic and neuroprotective properties of lithium ascorbate. *Neuroscience and Behavioral Physiology.* 2018; 48 (4): 409–415. DOI: 10.1007/s11055-018-0579-3.
21. *Yuan X., Li W., Yan Q., Ou Y., Long Q., Zhang P.* Biomarkers of mature neuronal differentiation and related diseases. *Future Sci OA.* 2024; 10 (1): 2410146. DOI: 10.1080/20565623.2024.2410146. PMID: 39429212.
22. *Green T.R.F., Rowe R.K.* Quantifying microglial morphology: an insight into function. *Clin Exp Immunol.* 2024; 216 (3): 221–229. DOI: 10.1093/cei/uxae02. PMID: 38456795.
23. *De Ryck M., Van Reempts J., Borgers M., Wauquier A., Janssen P.A.* Photochemical stroke model: flunarizine prevents sensorimotor deficits after neocortical infarcts in rats. *Stroke.*1989; 20 (10): 1383–90. DOI: 10.1161/01.str.20.10.1383. PMID: 2799870.
24. *Jolkkonen J., Puurunen K., Rantakömi S., Härkönen A., Haapalinna A., Sivenius J.* Behavioral effects of the alpha(2)-adrenoceptor antagonist, atipamezole, after focal cerebral ischemia in rats. *Eur J Pharmacol.* 2000; 400 (2–3): 211–219. DOI: 10.1016/s0014-2999(00)00409-x. PMID: 10988336.
25. *Ghanaatfar F., Ghanaatfar A., Isapour P., Farokhi N., Bozorgniahosseini S., Javadi M., Gholami M., et al.* Is lithium neuroprotective? An updated mechanistic illustrated review. *Fundam Clin Pharmacol.* 2023; 37 (1): 4–30. DOI: 10.1111/fcp.12826. PMID: 35996185.
26. *Ates N., Caglayan A., Balcikanli Z., Sertel E., Beker M.C., Dilsiz P., Caglayan A.B., et al.* Phosphorylation of PI3K/Akt at Thr308, but not phosphorylation of MAPK kinase, mediates lithium-induced neuroprotection against cerebral ischemia in mice. *Exp Neurol.* 2022; 351: 113996. DOI: 10.1016/j.expneurol.2022.113996. PMID: 35122865.
27. *Wang W., Lu D., Shi Y., Wang Y.* Exploring the neuroprotective effects of lithium in ischemic stroke: a literature review. *Med Sci.* 2024; 21 (2): 284–298. DOI: 10.7150/ijms.88195. PMID: 38169754.
28. *Ghribi O., Herman M., Spaulding N.K., Savory J.* Lithium inhibits aluminum-induced apoptosis in rabbit hippocampus, by preventing cytochrome c translocation, Bcl-2 decrease, Bax elevation and caspase-3 activation. *Journal of Neurochemistry.* 2002; 82 (1): 137–145. DOI: 10.1046/j.1471-4159.2002.00957.x. PMID: 12091474.
29. *King T.D., Bijur G.N., Jope R.S.* Caspase-3 activation induced by inhibition of mitochondrial complex I is facilitated by glycogen synthase kinase-3β and attenuated by lithium. *Brain Research.* 2001; 919 (1): 106–114. DOI: 10.1016/S0006-8993(01)03041-2.
30. *Habib M.Z., Ebeid M.A., Faramawy Y., Saad S.S., Magdoub H.M., Attia A.A., Aboul-Fotouh S., et al.* Effects of lithium on cytokine neuro-inflammatory mediators, Wnt/β-catenin signaling and microglial activation in the hippocampus of chronic mild stress-exposed rats. *Toxicol Appl Pharmacol.* 2020; 399: 115073. DOI: 10.1016/j.taap.2020.115073. PMID: 32454056.
31. *Sakrajda K., Rybakowski J.K.* The mechanisms of lithium action: the old and new findings. *Pharmaceuticals (Basel).* 2025; 18 (4): 467. DOI: 10.3390/ph18040467.
32. *Bortolozzi A., Fico G., Berk M., Solmi M., Formaro M., Quevedo J., Zarate C.A., et al.* New advances in the pharmacology and toxicology of lithium: a neurobiologically oriented overview. *Pharmacol Rev.* 2024; 76 (3): 323–357. DOI: 10.1124/pharmrev.120.000007.

Received 15.08.2025
Accepted 13.05.2026
Online First 02.06.2026

https://doi.org/10.15360/1813-9779-2026-3-2682

Post-Ischemic Long-Term Neuronal Changes in the Sensorimotor Cortex in the Experimental Setting

Viktor A. Akulinin[1]*, Sergei S. Stepanov[1], Kirill S. Tagakov[1], Vladislav I. Sergeev[1], Dmitry B. Avdeev[1], Galina U. Zhanaidarova[2], Dmitry V. Akulinin[3], Anastasia Yu. Shoronova[1], Irina G. Tsuskman[1]

[1] Omsk State Medical University, Ministry of Health of Russia, 12 Lenin Str., 644099 Omsk, Russia
[2] Karaganda Medical University, 40 Gogolya Str.,100008 Karaganda, Republic of Kazakhstan
[3] Plekhanov Russian University of Economics, 36 Stremyanny Lane, 109992 Moscow, Russia

For citation: *Viktor A. Akulinin, Sergei S. Stepanov, Kirill S. Tagakov, Vladislav I. Sergeev, Dmitry B. Avdeev, Galina U. Zhanaidarova, Dmitry V. Akulinin, Anastasia Yu. Shoronova, Irina G. Tsuskman.* Post-Ischemic Long-Term Neuronal Changes in the Sensorimotor Cortex in the Experimental Setting. *Obshchaya Reanimatologiya = General Reanimatology.* 2026; 22 (3): 28–40. https://doi.org/10.15360/1813-9779-2026-3-2682 [In Russ. and Engl.]

***Correspondence to:** Victor A. Akulinin, v_akulinin@outlook.com

Summary

The aim of the study was to identify the characteristics of dynamic reactive neuronal changes in sensorimotor cortex (SMC) layers III and V of the rat brain in the remote period (up to 270 days) following bilateral common carotid arteries ligation (CCAL).

Methods. The experiment was conducted on 66 male Wistar rats (a prospective cohort study with sequential terminal outcomes): intact control ($n=6$) and groups with survival at 30, 90, 150, 210, and 270 days post-bilateral CCAL ($n=6$ in each group after adjusting for mortality). Histological methods (Nissl and hematoxylin-eosin staining) were used to assess the total neuronal numerical density (NND), the density of four types of reactive altered cells (hyperchromatic shriveled cells — HCSC; hyperchromatic non-shriveled cells — HCNSC; hypochromatic cells — HCC; shadow cells — SC) and the neuroglial index (NGI). Paired and multiple comparison methods, linear mixed models (LMM) with random intercept for the animal (to account for the paired data structure), Jonckheere–Terpstra test, quadratic trend test, correlation analysis, and △-analysis were applied.

Results. A biphasic reduction in NND was observed in layer III of the SMC (maximum of -44.6% at 30 days, $p<0.001$) with a wave-like dynamics (quadratic trend: $F=16.4$, $p<0.001$). HCNSC peak at 30 days (+683%) followed by a decrease, while HCC showed a delayed peak at 150 days (+500%); both parameters showed a mixed pattern (steadily increasing trend: $Z=1.88$, p=0.030 for HCNSC; $Z=2.45$, $p=0.007$ for HCC; quadratic component: $F=8.2$ and 7.4, $p<0.01$). SCs demonstrated non-monotonous dynamics (quadratic trend: $F=19.2$, $p<0.001$) with a delayed peak at 210 days. NGI peaked at 30 days (transient gliosis, +95.5%, steadily decreasing trend, $Z=-4.92$, $p<0.001$). The decrease in NND was less pronounced in layer V of the SMC, (–11.6% at 150 days, $p=0.048$), but there was an extreme increase in HCSC at 30 days (+945% from control, with a continuously decreasing trend, $Z=-2.94$, $p=0.002$), a monotonous depletion of HCC (linear increasing trend, $Z=4.82$, $p<0.001$), and a prolonged building up gliosis (NGI +42% by 270 days, mixed pattern: steadily increasing trend $Z=4.15$, $p<0.001$; quadratic component $F=5.1$, $p=0.028$). LMM confirmed a significant «Layer × Time» interaction for all parameters ($F=24.1$–71.2; $p<0.001$). A correlational analysis revealed moderate positive correlations between the layers (for SCs: $r=0.58$; $r\_partial=0.52$; $p=0.004$; for HCSC: $r=0.52$; $p=0.008$; for NGI: $r=0.44$; $p=0.016$). The △-analysis showed consistency in changes for SC, HCSC, and NGI. The extremum moments for SC (210 days) and HCSC (30 days) were synchronous in both layers. Temporal precedence of layer III was found for NGI (early peak of gliosis at 30 days compared to 270 days in layer V), as well as for HCSC and HCC (30–150 days compared to 90 days in layer V). Temporal precedence of layer V was identified for the first peak of SC (90 days compared to 210 days in layer III).

Conclusion. Chronic ischemia induces various damage scenarios: layer III is characterized by a biphasic reduction in NND, asynchronous peaks of HCSC (30 days) and HCC (150 days), a delayed SC peak (210 days), and transient gliosis (a model of damage with delayed degeneration); layer V exhibits an extreme early increase in HCSC (30 days), early peak of SC (90 days), and prolonged gliosis (a model of progressive degeneration). Correlation and △-analysis indicate moderate synchrony in the degeneration processes; no convincing evidence of cascading damage propagation from superficial layers to deeper ones was obtained.

Keywords: chronic cerebral ischemia; sensorimotor cortex; cortical layers; hyperchromatic neurons; shadow cells; neuroglial index; white rats

Conflict of interest. The authors declare no conflict of interest.

Information about the authors:
Viktor A. Akulinin: https://orcid.org/0000-0001-6097-7970
Sergei S. Stepanov: https://orcid.org/0000-0003-0741-3337
Kirill S. Tagakov: https://orcid.org/0000-0002-8310-896X

Vladislav I. Sergeev: https://orcid.org/0000-0002-5878-7403
Dmitry B. Avdeev: https://orcid.org/0000-0003-4976-7539
Galina U. Zhanaidarova: https://orcid.org/0000-0003-1143-4843
Dmitry V. Akulinin: https://orcid.org/0009-0002-4208-2748
Anastasia Y. Shoronova: https://orcid.org/0000-0002-6362-3796
Irina G.Tsuskman: https://orcid.org/0000-0003-3667-7905

Introduction

Chronic cerebral ischemia (CCI) is a key pathophysiological factor in cerebral insufficiency and underlies discirculatory encephalopathy and vascular cognitive impairment, which represent one of the most significant medical and social challenges in neurology [1, 2]. The pathophysiology of CCI is based on prolonged hypoperfusion, leading to a complex of metabolic disruptions, oxidative stress, neuroinflammation, and, ultimately, neuronal death and glial activation [3, 4]. Despite significant progress in understanding the general mechanisms of ischemic injury, layer-specific vulnerability of various cortical regions during prolonged hypoperfusion remains insufficiently studied.

The sensorimotor cortex, as an integrative region, plays a critical role in the organization of voluntary movements and processing of somatosensory information, therefore level of its dysfunction directly correlates with the clinical presentation of motor and sensory disorders in cerebrovascular disease [5]. Cortical architecture is organized in layers with unique cyto- and chemoarchitectonics, neuronal composition, and connection patterns in each layer, which determine their functional specialization and, likely, differences in resistance to damaging factors [6]. Thus, the large pyramidal neurons of layer V, which give rise to the corticospinal tract, are characterized by a high level of metabolic activity and may be highly sensitive to energy deficiency [7]. At the same time, neurons in layer III, which form corticocortical associative connections, may be secondarily affected due to disruptions in neural networks and trophic support [8]. Data from experimental studies on models of acute focal ischemia (middle cerebral artery occlusion) do indeed indicate the heterogeneity of damage to cortical layers involving both neurons and glial cells [9]. However, the dynamics of reactive and degenerative changes in specific cortical layers in the long term following the onset of chronic hypoperfusion, which mimics progressive vascular pathology in humans, have been described only fragmentarily.

One of the widely used experimental models for studying CCI is the bilateral common carotid artery ligation (2-vessel, 2VO — 2 vessels occlusion) model in rodents, which leads to a sustained reduction in cerebral blood flow and the development of delayed neurodegenerative changes [10]. Analysis of specific pathomorphological markers resulting from reactive neuronal changes (hyperchromia, shrinkage, chromatolysis), and emergence of shadow cells allows for the assessment not only of the extent of damage but also of the adaptive potential of neural tissue, as well as the dynamics of the neurodegenerative process [11]. The accompanying glial reaction, quantitatively assessed via the neuroglial index, is an integral component of pathomorphosis, it can be either protective or destructive in nature, depending on the timing and context [12].

It has been hypothesized that different cortical layers exhibit not only quantitative but also qualitative differences in the pathomorphological responses to chronic ischemia, which may reflect distinct mechanisms of vulnerability and adaptation.

The aim of this study was to identify the characteristics of the dynamics of neuronal responses in layers III and V of the sensorimotor cortex (SMC) of the rat brain at long-term intervals (up to 270 days) following bilateral common carotid arteries ligation (CCAL).

Materials and Methods

The study was conducted on 66 sexually mature male Wistar rats (weighing 250–300 g). The experiment was designed as a prospective cohort study with sequential terminal removal of animals. The animals were divided into 6 groups: an intact control group (n=6, not subjected to surgery) and 5 experimental groups with survival times of 30, 90, 150, 210, and 270 days (study time points) following bilateral CCAL.

To ensure 6 viable animals for analysis at each time point, the initial cohort size was calculated (n=11) taking into account the projected perioperative mortality (≈25%) and long-term mortality (≈20%). The experiment included 66 animals (11 in each of the 5 experimental groups + 6 intact controls). Perioperative mortality (first 7 days) was 23.6% (13 of 55 operated rats), primarily due to cerebral edema and ischemic respiratory failure. In the long-term period (8–270 days), another 17 animals (30.9% of those surviving the surgery) died due to progressive cachexia and infectious complications. The analyzed groups (n=6 for each time point) were formed from animals that reached the planned time point and were suitable for histological examination. The experiment was approved by the Local Ethics Committee at Omsk State Medical University (Protocol No. 11 dated September 16, 2022).

Under general anesthesia (Zoletil 100, 10 mg/kg, intramuscularly), a model of incomplete global ischemia was induced by irreversibly ligating both common carotid arteries. The neurovascular

bundles were dissected sequentially, both common carotid arteries were exposed, and two ligatures were applied to each artery at a distance of 2–3 mm from one another. Control animals were not subjected to surgery.

Animals were euthanized by perfusion of 30 mL of a 4% paraformaldehyde solution in phosphate buffer (pH 7.2–7.4) through the aorta at a pressure of 90–100 mm Hg. The brain was embedded in paraffin. The sensorimotor cortex was isolated using stereotaxic atlases. Sections 7 μm thick were stained with Nissl's thionin and hematoxylin-eosin. The following were assessed: total numerical neuronal density (NND, cells/mm²); the density of four types of reactively altered neurons: (hyperchromatic shriveled cells — HCSC; hyperchromatic non-shriveled cells — HCNSC; hypochromatic cells — HCC; shadow cells — SC and the neuroglial index (NGI) — the ratio of the number of glial cells to the number of neurons. Histological sections were examined under a Leica DM 1000 microscope (Leica Microsystems, Germany). For each animal in layers III and V of the SMC, 5 fields of view were analyzed (×40 objective, 0.2 mm²). For each parameter, the arithmetic mean across the 5 fields was calculated for each animal, yielding an individual value (animal-level). Next, for each experimental group (n=6), a variation series was formed from the individual values. Total sample size: for intra-layer analysis — 6 animals per group; for inter-layer comparisons — 6 pairs per time point; for correlation analysis — 36 animals (all time points); for △-analysis — 80 pairs of changes.

Statistical analysis was performed in *R* (version 4.3.2) using the tidyverse, lme4, lmerTest, emmeans, rstatix, and ARTool packages. For each parameter, the mean and standard error ($M \pm SEM$), median, and interquartile range (Me [$Q1$; $Q3$]) were calculated. Normality was tested using the Shapiro–Wilk test. Since layers III and V were measured in the same animal (paired data), linear mixed models (LMMs) with a random intercept for the «Animal» factor were used for the two-factor analysis. Effective degrees of freedom were estimated using the Satterthwaite method. When the residuals were non-normal, the Oshima–Algina rank transformation (ART, related to aligned ranks transformation 0 ART anova) was applied, followed by an LMM on the ranks. Analysis of temporal trends (monotonic trend): Jonckheere–Terpstra test. Non-monotonic (quadratic) trend: test for a quadratic component in Kruskal–Wallis rank-order ANOVA with orthogonal polynomials. A correlation analysis was performed. Correlations were calculated at the level of individual animals (n=36) using Pearson's coefficient and partial correlations (with the control of «Time» factor). To assess the consistency of the direction of parameter changes between adjacent time points, △-analysis was applied, and a comparison of the moments of parameter extrema in layers III and V of the rat brain's SMC was also performed. △-analysis was based on pseudo-individual trajectories formed by randomly pairing individual animals from independent terminal cohorts (30→90, 90→150, 150→210, 210→270 days). For this reason, this approach was considered exploratory and was not classified as a full-fledged equivalent of lag modeling.

The effective sample size was 80 unique pairs (4 transitions × 20 random pairings without repetition in a single iteration). A significance level of $\alpha = 0.05$ was adopted. Correction for multiple comparisons was performed using the Bonferroni method.

Results

In the control group, typical normochromatic pyramidal neurons predominated in layers III and V of the rat brain SMC. When stained with hematoxylin-eosin, they appeared as pyramidal or pear-shaped cells with a perikaryon diameter ranging from 15–25 μm (in layer III of the SMC) to 20–35 μm (in layer V of the SMC), with a central bright, rounded nucleus (8–12 μm) and a distinct dark-purple nucleolus; the pink eosinophilic cytoplasm had a granular structure due to uniformly distributed basophilic clumps of Nissl bodies. A distinct apical dendrite extended from the cell apex toward the surface of the cortex. Among the normochromatic cells, isolated, non- shriveled hyperchromatic neurons were noted (Fig. 1).

Throughout the entire observation period (30–270 days) following bilateral CCAL, various types of reactively altered neurons were detected in the SMC. Hematoxylin-eosin staining revealed polymorphism in the reactive changes of SMC neurons, reflecting prolonged hypoperfusion and compensatory-adaptive processes. However, the proportion of reactively altered neurons was significantly lower than in acute ischemia. The following types of altered neuronal cells were identified: 1) hyperchromatic non-shrunken cells (HCNSC), 2) hyperchromatic shriveled cells (HCSC), 3) hypochromic (HCC), 4) vacuolated, 5) shadow cells (SC), 6) phagocytosed, 7) atrophic (simplified), 8) hypertrophied (complex) (Fig. 2).

Long-term follow-up after permanent occlusion of both common carotid arteries revealed polymorphism in the reactive changes of neurons in the sensorimotor cortex, as detected by hematoxylin-eosin staining. Atrophically altered neurons were identified, characterized by reduced perikaryon size, a flattened pyramidal shape, a thinned apical dendrite, moderately basophilic cytoplasm, and a compact but structurally intact nucleus. Concurrently, hypertrophied neurons were recorded, characterized by an increase in perikaryon size, intense cytoplasmic basophilia, and a hypertrophied nucleolus.

Hyperchromatic, abnormally shrunken, shriveled (pyknomorphic) neurons represented cells at

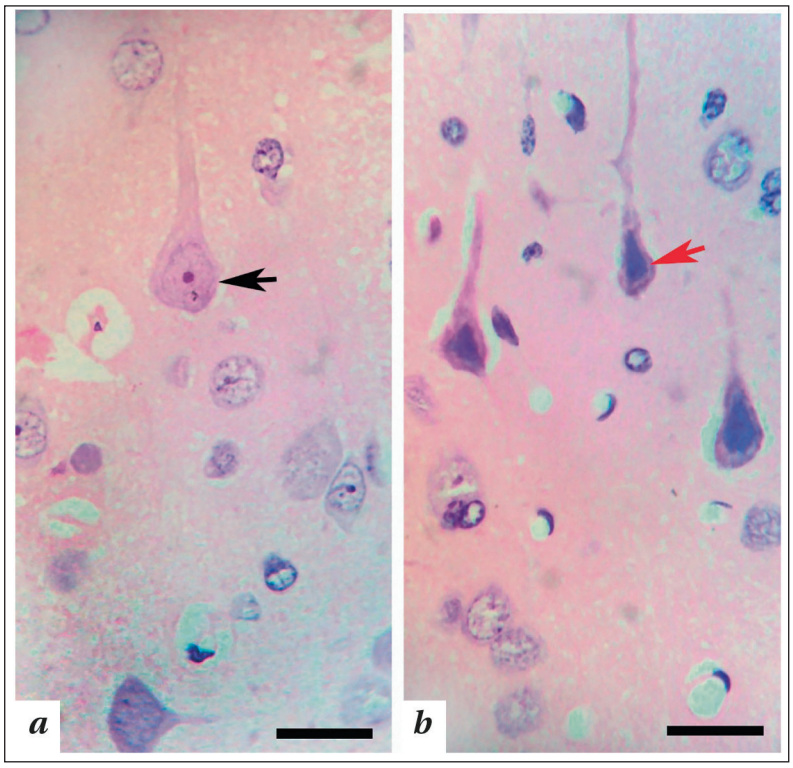

Fig. 1. Pyramidal neurons in layer V of the sensorimotor cortex of rats in the control group.
Note. Black arrow — normochromatic; red arrow — hyperchromatic, non- shriveled neurons. Hematoxylin-eosin staining (*a*, *b*). 100× objective, scale bar — 20 μm.

various stages of coagulative necrosis: with markedly reduced, angular perikarya and homogeneous, intense basophilia of the cytoplasm and nuclei, which was a consequence of critical hypoxia episodes. A sign of severe hydropic dystrophy under conditions of persistent metabolic stress was vacuolated neurons, whose cytoplasm contained multiple optically empty vacuoles, indicating edema and swelling of organelles (mitochondria, endoplasmic reticulum). «Shadow cells» with nearly complete lysis of the perikaryon indicated the complete loss of neurons in areas of maximum damage.

The presence of neurons with ischemic changes («red neurons»), characterized by eosinophilic cytoplasm and pyknotic nuclei, indicated the occurrence of acute episodes of hypoxia in a scenario of chronic hypoperfusion. Neurons with signs of chromatolysis were also noted, reflecting reactive changes associated with ribonucleoproteins degeneration.

The background changes consisted of diffuse and focal gliosis (with a predominance of activated microglia) and spongiosis (exhaustion and vacuolization of the neuropil). Against this altered background, reactively transformed neurons were arranged chaotically, forming areas of thinning and patterns of neuronophagy.

Morphometric analysis showed biphasic change in the NND in layer III of the SMC: a 44.6% decrease from the control level by day 30 ($p<0.001$), followed by an increase by days 150–210 and a subsequent decrease by day 270 (28.0% below control, $p<0.001$) (Tables 1, 2; Fig. 3). In layer V of the SMC, the decrease in NND was less obvious: the maximum drop of 11.6% was observed at day 150 ($p=0.048$) (Table 3). The accumulation of hyperchromic shrunken neurons was more pronounced in layer V. For the remaining parameters (HCNSC, HCC, SC, NGI), layer III demonstrated greater vulnerability (Table 3).

Table 3 presents the maximum deviation of each morphometric parameter from the reference values, expressed as a percentage, as well as the vulnerability ratio (the maximum change in layer V divided by the maximum change in layer III). A ratio greater than 1 indicates greater sensitivity in

Table 1. Results of a multiple intergroup comparison of morphometric parameters within each layer (intact control and time points 30, 90, 150, 210, and 270 days after ligation of the common carotid arteries).

Layer	Parameter	Criterion	Statistics	df	*p*
III	NND	Kruskal–Wallis	$H=29.2$	5	<0.001
	HCSC	ANOVA	$F=52.4$	5.30	<0.001
	HCNSC	Kruskal–Wallis	$H=28.8$	5	<0.001
	HCC	Kruskal–Wallis	$H=29.5$	5	<0.001
	SC	Kruskal–Wallis	$H=27.1$	5	<0.001
	NGI	ANOVA	$F=98.2$	5.30	<0.001
V	NND	Kruskal–Wallis	$H=17.6$	5	0.003
	HCSC	ANOVA	$F=360.5$	5.30	<0.001
	HCNSC	ANOVA	$F=127.4$	5.30	<0.001
	HCC	ANOVA	$F=84.1$	5.30	<0.001
	SC	ANOVA	$F=287.9$	5.30	<0.001
	NGI	Kruskal–Wallis	$H=28.6$	5	<0.001

Note. NND — total numerical neuronal density; HCSC — hyperchromatic shriveled cells (neurons); HCNSC — hyperchromatic non-shriveled cells; HCC — hypochromic cells; SC — shadow cells; NGI — neuroglial index; df — degrees of freedom. For the Kruskal–Wallis test, the *H*-statistic is given; for ANOVA, the *F*-statistic is given.

layer V, while a ratio less than 1 indicates greater sensitivity in layer III.

In layer III of the SMC, the Jonkheere-Terpstra test revealed statistically significant monotonic trends for HCSC (Z=–2.98, p=0.001 — decreasing), HCNSC (Z=1.88, p=0.030 — increasing), HCC (Z=2.45, p=0.007 — increasing), and NGI (Z=–4.92, p>0.001 — decreasing). No significant monotonic trends were detected for NND and SC (p>0.05). However, the test for the quadratic component showed high significance for NND (F=16.4, p<0.001), HCNSC (F=8.2, p=0.006), HCC (F=7.4, p=0.009), and SC (F=19.2, p<0.001), confirming the non-monotonic (wave-like) nature of their dynamics. For HCNSC and HCC, a mixed pattern was identified (both components are significant) (Table 4).

In Layer V of the SMC, the Jonkheere-Terpstra test revealed significant monotonic trends for all parameters except NND: HCSC (Z=–2.94, p=0.002 — decreasing), HCNSC (Z=2.30, p=0.011 — increasing), HCC (Z=4.82, p<0.001 — increasing), SC (Z=–3.85, p<0.001 — decreasing), NGI (Z=4.15, p<0.001 — increasing). The quadratic component test was not significant for most parameters (p>0.05), with the exception of HCNSC (p=0.048) and NGI (p=0.028), where a mixed pattern was observed (Table 4).

Strong intralayer correlations were identified in the SMC for layer III: total NND was negatively correlated with all parameters (r ranging from –0.88 to –0.45), SC correlated negatively with NGI (r=–0.70), whereas HCSC, HCNSC, and HCC formed a cluster of positive correlations (r ranging from 0.46 to 0.95) (Table 5.1).

For layers III and V, there was no interlayer correlation for total NND (r=0.08), a moderate positive correlation for HCSC (r=0.52), moderate negative correlations for HCNSC (r=–0.38), HCC (r=–0.39) and SC (r=–0.54), as well as a weak positive correlation with NGI (r=0.35) (Table 5.2).

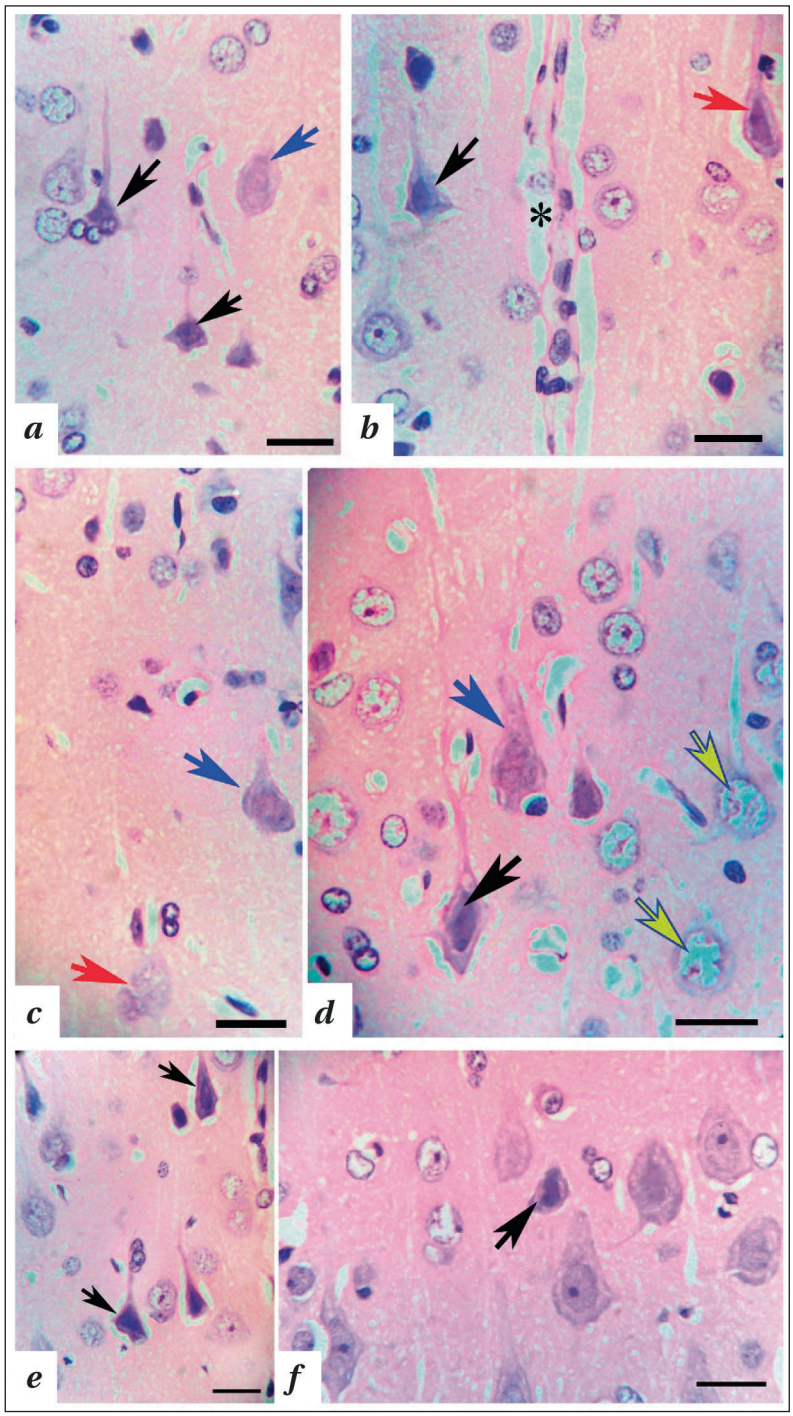

Fig. 2. PReactively altered pyramidal neurons in layer V of the rat sensorimotor cortex following BCCAL.

Note. Hematoxylin-eosin staining. 100× objective, scale bar = 20 µm. *a*, *b* — 30 days after bilateral CCAL. Black arrows — hyperchromatic shreveled neurons. Blue arrow — hypochromatic neurons. Red arrow — vacuolated («red») neurons. * — microvessel with signs of perivascular edema. *c*, *d* — 90 days after bilateral CCAL. Black arrow — hyperchromatic neurons. Blue arrows — hypochromatic neurons. Red arrow — shadow cells. Yellow arrows — signs of edema and swelling of neuropil cell bodies. *e* — 150 days; *f* — 210 days after bilateral CCAL. Black arrows — hyperchromatic neurons.

To assess differences in the dynamics of pathological processes between layers III and V, linear mixed models (LMMs) with a random intercept for the animal were used (Table 6). The «Layer × Time» interaction effect was statistically significant for all six morphometric parameters (p<0.001). The foremost interaction was observed for HCSC (F=71.2), indicating fundamentally different dynamics of irreversible ischemic damage in

Table 2. Reactive neurons at the time points of the study: comparison with controls (2.1) and percentage distribution in layers III and V of the rat sensorimotor cortex (2.2).

2.1. Comparison with control

Layer	Parameter	Time point, day	Difference	95% CI	*p-corr*	η^2_p
III	NND	30	–31.9	[–39.5; –24.3]	< 0.001	0.89
		270	–20.0	[–27.6; –12.4]	< 0.001	
	HCSC	90	+10.4	[8.0; 12.8]	< 0.001	0.91
	HCNSC	30	+8.2	[6.5; 9.9]	< 0.001	0.88
		210	+9.3	[7.6; 11.0]	< 0.001	
	HCC	150	+8.0	[6.6; 9.4]	< 0.001	0.90
	SC	210	+27.0	[24.0; 30.0]	< 0.001	0.94
	NGI	30	+0.84	[0.78; 0.90]	< 0.001	0.95
V	HCSC	30	+10.4	[9.6; 11.2]	< 0.001	0.97
	NGI	270	+0.45	[0.38; 0.52]	< 0.001	0.89

2.2. Interlayer comparison

Time point, day	Parameter	Neurons proportion in layers (% , *Me* [*IQR*])		*p*	*p-corr*
		III	V		
30	HCSC	18.7 [16.5–21.0]	27.4 [25.3–29.6]	0.004	0.016
	HCNSC	23.7 [21.0–25.5]	13.0 [11.5–14.5]	< 0.001	< 0.001
	HCC	4.5 [3.2–5.8]	9.2 [8.0–10.5]	< 0.001	< 0.001
	SC	20.7 [18.0–23.0]	8.8 [7.2–10.9]	< 0.001	< 0.001
90	HCSC	27.2 [24.5–29.0]	19.5 [18.8–20.0]	0.016	0.064
	HCNSC	13.6 [11.5–15.8]	18.7 [16.8–20.0]	0.031	0.124
	HCC	13.2 [11.0–15.0]	13.6 [12.1–14.6]	0.720	> 0.05
	SC	25.9 [20.5–30.0]	15.5 [15.3–15.8]	0.016	0.064
150	HCSC	18.8 [17.0–20.5]	21.9 [20.7–23.1]	0.016	0.064
	HCNSC	13.9 [12.0–15.5]	18.8 [17.8–19.7]	0.004	0.016
	HCC	17.1 [15.0–18.8]	12.8 [10.2–14.6]	0.016	0.064
	SC	26.7 [22.0–31.0]	14.1 [13.1–16.0]	0.004	0.016
210	HCSC	14.9 [13.0–16.5]	21.2 [20.0–21.6]	< 0.001	< 0.001
	HCNSC	18.9 [16.5–21.0]	12.9 [11.1–13.7]	0.004	0.016
	HCC	10.6 [8.5–12.8]	5.9 [5.0–7.2]	0.004	0.016
	SC	30.5 [26.3–32.0]	16.9 [16.0–17.9]	0.004	0.016
270	HCSC	20.6 [18.0–23.0]	22.8 [21.8–23.3]	0.031	0.124
	HCNSC	17.7 [15.5–19.8]	10.4 [9.9–11.5]	< 0.001	< 0.001
	HCC	10.5 [8.8–12.2]	5.7 [5.1–7.1]	0.004	0.016
	SC	37.3 [33.0–41.0]	16.8 [14.0–19.4]	0.004	0.016

Note. NNND — total numerical neuronal density; HCSC— hyperchromatic shriveled cells (neurons); HCNSC — hyperchromatic non-shriveled cells; HCC — hypochromic cells; SC — shadow cells; CI — confidence interval; η^2_p — partial eta-squared (measure of effect size); Me — median; IQR — interquartile range. Percentages were calculated using the formula: (density of a given cell type / NND) × 100%. In Table 2.1, for NND, HCSC (layers III and V), and HCC (layer V), we used Tukey's post-hoc test (ANOVA); for the others, we used Dunn's method with Bonferroni correction (Kruskal–Wallis). In Table 2.2, the Wilcoxon signed-rank test for dependent samples with Bonferroni correction was used for inter-layer comparisons (adjusted significance level $p < 0.005$ for 10 comparisons).

Table 3. Comparative analysis of the vulnerability of layers III and V of the rat sensorimotor cortex at study time points.

Parameters	Layers, % max. changes vs control		Ratio V/III
	III	V	
NND	–44.6 (30 day)	–11.6 (150 day)	0.26
HCSC	+473 (90 day)	+945 (30 day)	2.00
HCNSC	+683 (30 day)	+527 (90 day)	0.77
HCC	+500 (150 day)	+364 (90 day)	0.73
SC	+1800 (210 day)	+455 (90 day)	0.25
NGI	+95.5 (30 day)	+42 (270 day)	0.44

Note. NND — total numerical neuronal density; HCSC — hyperchromatic shriveled cells (neurons); HCNSC — hyperchromatic non-shriveled cells; HCC — hypochromatic cells; SC — shadow cells; NGI — neuroglial index. The maximum percentage change was calculated using the formula: [(maximum parameter value after CCAL — control value) / control value] × 100% (for indicators showing an increase, «+») or [(minimum value after CCAL — control value) / control value] × 100% (for indicators showing a decrease, «–»). A vulnerability ratio > 1 indicates higher sensitivity of layer V, < 1 indicates higher sensitivity of layer III. The time period during which the maximum change was recorded is indicated in parentheses.

the examined layers. △-analysis (consistency of the direction of changes between adjacent time points) showed that for SC, HCSC, and NGI, changes in layers III and V were co-directional significantly more often than by chance (68%, 66%, and 64%, respectively; $p < 0.05$ for all). The highest consistency was observed for SC — a marker of complete neuronal death.

To assess whether one layer might be leading the other, we compared the timing of extreme pa-

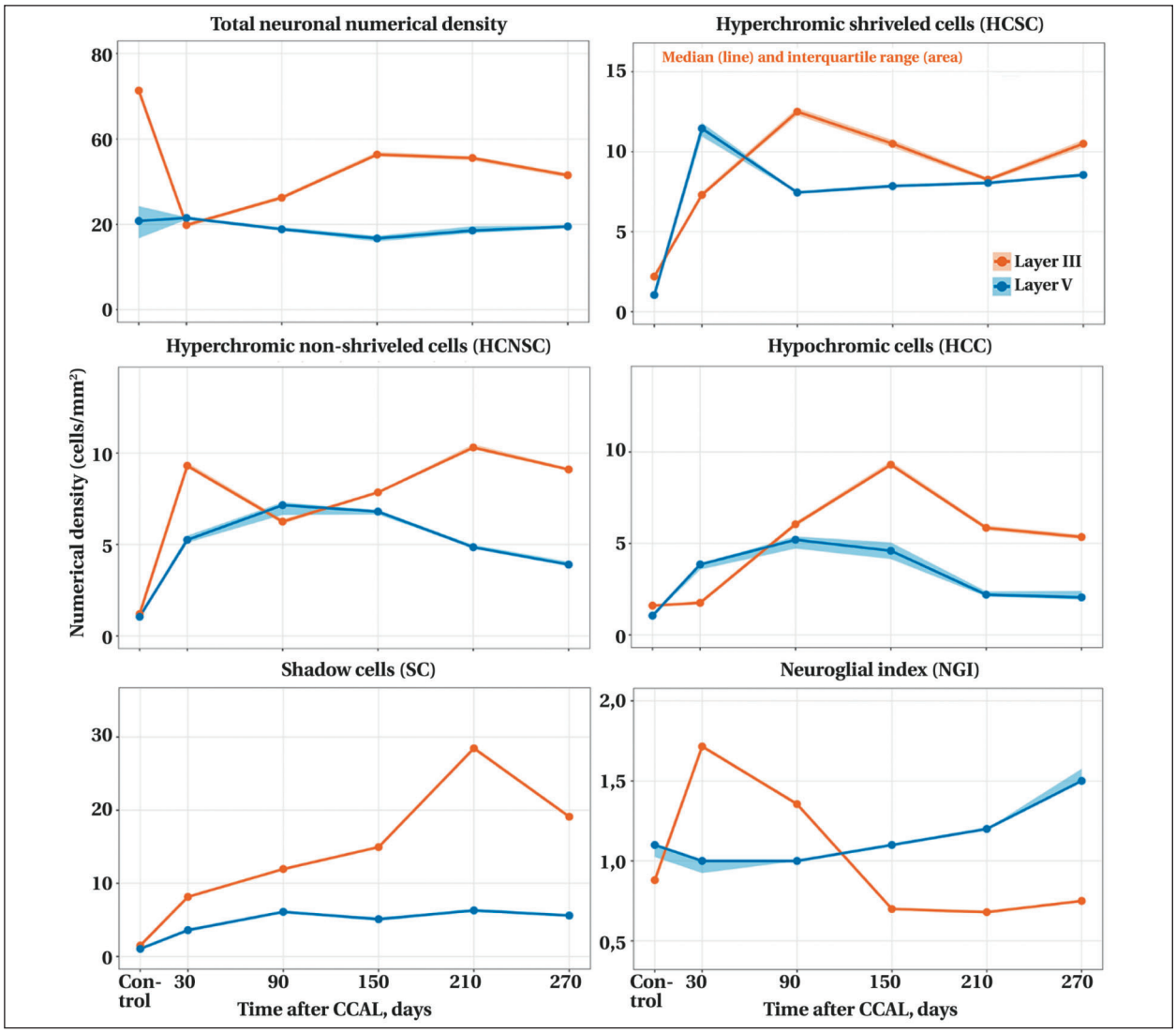

Fig. 3. Comparison of the dynamics of the density of reactive and pathologically altered neurons in layers III and V of the rat sensorimotor cortex at the long-term following ligation of the common carotid arteries.
Note. On the graphs: median — line; interquartile range — box (not shown for minimal values).

rameter values (maxima and minima) in layers III and V of the SMC based on group averages. Synchronization of the extrema — that is, the occurrence of a maximum or minimum at the same time — was observed for the HCSC and for the secondary SC peak. The HCSC peak was recorded in both layers at 30 days; however, in layer V, the damage intensity was +945%, whereas in layer III, the HCSC peak was delayed and less pronounced (90 days, +473%). The secondary SC peak was also synchronous in both layers and recorded at 210 days (layer III: +1800%, layer V: +455%). A temporal priority of layer III, i.e., the onset of the extreme values occurring earlier than in layer V, was identified for total NND, HCNSC and HCC, and NGI. The first minimum of total NND was recorded at 30 days in layer III and at 150 days in layer V. The maximum of HCNSC was reached at 30 days in layer III (+683%) and at 90 days in layer V (+527%). The maximum for HCC was recorded at 150 days in layer III (+500%) and at 90 days in layer V (+364%); meanwhile, in layer III, HCC began to increase as early as 30 days, reaching a plateau by 150 days

The maximum NGI was observed at 30 days in layer III (+95.5%) and at 270 days in layer V (+42%), with the most pronounced lead being 240 days. A temporal priority of layer V was identified only for the first SC peak: 90 days in layer V (+455%) versus 210 days in layer III (+1800%). Analysis of the dynamics of HCNSC and HCC showed that in layer III, HCNSC reaches its maximum early (30 days) followed by a decline, whereas HCC has a delayed peak (150 days). In layer V, both parameters peaked synchronously at 90 days.

Discussion

This study is the first to conduct a comparative analysis of the long-term (up to 270 days) dynamics of reactively altered neurons in layers III and V of the sensorimotor cortex in a model of chronic cere-

Table 4. Results of the Jonckheere-Terpstra test and the quadratic trend test.

Layer	Parameter	*Z*	*p* (Jonckheere)	Trend	*F* (quad.)	*p* (quad.)	pattern
III	NND	3.12	0.999	нет	16.4	< 0.001	non-monotonic
	HCSC	–2.98	0.001	МУ	1.8	0.185	linear
	HCNSC	1.88	0.030	МВ	8.2	0.006	mixed
	HCC	2.45	0.007	МВ	7.4	0.009	mixed
	SC	–1.35	0.088	нет	19.2	< 0.001	non-monotonic
	NGI	–4.92	< 0.001	МУ	2.1	0.152	linear
V	NND	–1.02	0.154	нет	0.8	0.382	no trend
	HCSC	–2.94	0.002	МУ	3.2	0.079	linear
	HCNSC	2.30	0.011	МВ	4.1	0.048	mixed
	HCC	4.82	< 0.001	МВ	0.9	0.347	linear
	SC	–3.85	< 0.001	МУ	2.9	0.094	linear
	NGI	4.15	< 0.001	МВ	5.1	0.028	mixed

Note. NND — total numerical neuronal density; HCSC — hyperchromatic shriveled cells (neurons); HCNSC — hyperchromatic non-shriveled cells; HCC — hypochromatic cells; SC — shadow cells; NGI — neuroglial index. The Jonkheere–Terpstra test checks for the presence of a monotonic (constantly increasing or constantly decreasing) trend. A positive *Z*-value indicates an increasing trend, while a negative value indicates a decreasing trend. The quadratic trend test was performed using Kruskal–Wallis rank-sum analysis with orthogonal polynomials. MD — monotonically decreasing; MI — monotonically increasing.

Table 5. Pearson correlation matrices (r) between the intra- (5.1) and inter-layer (5.2) parameters of the rat sensorimotor cortex following ligation of the common carotid arteries.

5.1. Correlations between parameters in layer III ($p < 0.05$)

Parameters	*R* values for the compared parameters				
	HCSC	**HCNSC**	**HCC**	**SC**	**NGI**
NND	**–0.84**	**–0.82**	**–0.85**	**–0.45**	**–0.88**
HCSC		**0.78**	**0.76**	**0.52**	**0.68**
HCNSC			**0.95**	**0.48**	**0.75**
HCC				**0.46**	**0.74**
SC					**–0.70**

5.2. Correlations between the same parameters in layers III and V

Parameters	*r* (III and V)	*p*
NND	0.08	0.64
HCSC	**0.52**	**0.001**
HCNSC	**–0.38**	**0.02**
HCC	**–0.39**	**0.02**
SC	**–0.54**	**< 0.001**
NGI	**0.35**	**0.04**

Note. Statistically significant correlations ($p < 0.05$) are shown in bold, ($n = 36$ paired observations).

Table 6. Analysis of the connections between layers III and V of the rat sensorimotor cortex.

6.1. Two-factor LMM with a random intercept for the Animal (the «Layer × Time» interaction effect)

Parameters	*F*	df1	df2	*p*
NND	38.4	5	29.1	< 0.001
HCSC	71.2	5	28.9	< 0.001
HCNSC	36.8	5	29.0	< 0.001
HCC	30.5	5	29.2	< 0.001
SC	24.1	5	28.8	< 0.001
NGI	28.6	5	29.0	< 0.001

6.2. Correlation and △-analysis

Parameters	Correlation *r* (95% CI)	Partial *r*	Consistency, %	*p*
SC	0.58 [0.31; 0.76]	0.52	68	0.004
HCSC	0.52 [0.23; 0.73]	0.48	66	0.008
NGI	0.44 [0.14; 0.67]	0.37	64	0.016

Note. NND — total numerical neuronal density; HCSC — hyperchromatic shriveled cells (neurons); HCNSC — hyperchromatic non-shriveled cells; HCC — hypochromatic cells; SC — shadow cells; NGI — neuroglial index; LMM (Linear Mixed Model) — a linear mixed model with a random intercept for the «Animal» factor: Parameter ~ Layer × Time + (1 | Animal); df — degrees of freedom (according to Satterwhite); partial correlation — controlling for the «Time» factor; △-analysis was performed on 80 pairs of changes (4 time points × 20 animals); binomial test vs. null hypothesis of 50% agreement.

bral ischemia (bilateral CCAL) using appropriate statistical methods that account for pairwise dependence (linear mixed models with random intercepts for the animal) and the limitations of a small number of time points—in favor of △-analysis and analysis of extrema. Chronic ischemia, unlike acute infarction, more often causes progressive dysfunction and dystrophy rather than massive coagulative necrosis [1, 3, 11]. Therefore, the prioritized classification and grading of altered neurons, taking into account the specifics of the bilateral CCAL model, had their own distinctive features.

The morphological picture following bilateral CCAL revealed a spectrum of changes — ranging

from potentially reversible dystrophic changes (atrophy, vacuolization) to irreversible necrobiotic changes (coagulative necrosis, lysis) — which supported the model of progressive neurodegeneration under conditions of chronic cerebral hypoperfusion. The detection of «red neurons» in the long-term indicated a dynamic, progressive nature of the damage, in which acute ischemic episodes superimposed on the chronic process. Meanwhile detection of hypertrophied neurons indicated concomitant compensatory-plastic processes. This morphological mosaic reflected the competition between two pathogenetic trends: destructive (neurodegeneration) and adaptive (neuroplasticity). Preservation of the pool of hypertrophied neurons may have represented a structural reserve of the cortex and a morphological substrate for partial functional recovery, which explained the clinical variability of neurological deficits in chronic cerebral ischemia.

According to our data, layer III proved to be more sensitive to neuronal loss, the accumulation of reversible dystrophic forms (HCNSC, HCC), and delayed death (SC), whereas layer V was characterized by a selectively high vulnerability to irreversible ischemic damage leading to emergence of the hyperchromatic shriveled (HCSC) neuron type. A biphasic decrease in NND in layer III with wave-like dynamics (quadratic trend, $F=16.4$, $p<0.001$) indicated damage with partial recovery and delayed secondary degeneration, which is consistent with the concept of dissociative neurodegeneration in chronic ischemia [8]. The first phase of the decrease (by 44.6% at 30 days, $p<0.001$) reflected the direct consequences of acute hypoperfusion and an energy crisis.

The subsequent partial recovery (150–210 days, NND 55.6–56.3 cells/ mm²) may have been associated with adaptation and compensatory mechanisms, including the plasticity of surviving neurons and temporary functional-spatial reorganization of neural networks. The final decrease in NND by 270 days (to 51.5 cells/ mm², –28.0% of control) indicated the exhaustion of compensatory potential and development of delayed secondary degeneration. NND decrease was less evident in layer V (maximum –11.6% at 150 days, $p=0.048$) and did not show a statistically significant trend (Jonkheere–Terpstra test, $p=0.154$; quadratic component, $p=0.382$). This corresponds to a model of slowly progressive atrophy without pronounced recovery waves.

Thus, layer III was characterized by non-monotonic (wave-like) dynamics of NND, HCNSC, HCC, and SC, reflecting processes of partial recovery and delayed degeneration. In contrast, layer V was characterized by linear (monotonic) dynamics of most parameters, which corresponded to a model of slowly progressive atrophy without marked compensation waves. The most obvious difference between the layers was observed for SC: in layer III — a non-monotonic pattern with a delayed peak (210 days); in layer V — a monotonic decline following an early peak (90 days).

The extreme increase in HCSC in layer V at 30 days (945% higher than the control) confirmed high metabolic vulnerability of the large pyramidal neurons of the corticospinal tract [7]. The V/III layers vulnerability ratio based on HCSC was 2.00, indicating a significantly higher sensitivity of layer V to irreversible ischemic damage. The «dark neuron» phenomenon is traditionally regarded as a marker of severe, often irreversible ischemic damage [11, 13]. A monotonically HCSC decreasing trend in layer V ($Z=-2.94$, $p=0.002$) indicated gradual elimination of these cells following acute injury. In layer III, by contrast, the peak of HCSC was delayed until 90 days and was less pronounced (+473%), which may indicate a slower development of coagulative necrosis in the superficial layers.

HCNSC and HCC dominated in layer III, but their dynamics differed fundamentally. HCNSC peaked at 30 days (+683%), reflecting an acute response to ischemic stress characterized by protein overexpression and preservation of cellular architecture [14–16]. HCC, in contrast, had a delayed peak at 150 days (+500%), indicating increasing suppression of protein synthesis and chromatolysis as compensatory mechanisms were exhausted. The temporal disparity between HCNSC and HCC peaks is a novel, not described previously phenomenon, indicating that hyperchromic and hypochromic responses represent not merely different stages of a single process, but qualitatively distinct mechanisms of response to chronic ischemia. The wave-like dynamics of HCNSC (quadratic trend, $F=8.2$, $p=0.006$) and HCC mixed pattern (monotonically increasing trend, $Z=2.45$, $p=0.007$; quadratic component, $F=7.4$, $p=0.009$) indicated a recurrent nature of functional disruptions with periods of compensation and decompensation. In layer V, both parameters peaked synchronously at 90 days (HCNSC: +527%, HCC: +364%), which may indicate a more rapid depletion of metabolic reserves in the deep layers.

The dynamics of shadow cells — a marker of complete neuronal death — deserve special attention. In layer III, SC exhibited a non-monotonic pattern with a delayed peak at 210 days (quadratic trend, $F=19.2$, $p<0.001$; maximum increase of +1800% compared to control). In layer V, the SC peak was recorded earlier (90 days, +455% compared to control), followed by a monotonically decreasing trend ($Z=-3.85$, $p<0.001$). This difference may indicate different mechanisms of neuronal death: in layer III — delayed secondary degeneration occurring after the exhaustion of compensatory mechanisms; in layer V — earlier elimination of dead cells, directly associated with the extreme accumulation of HCNSC at 30 days.

The results indicate that neuronal loss in different layers occurred independently, whereas the accumulation of HCNSC was moderately synchronous. Negative interlayer correlations for HCNSC (r=–0.38), HCC (r=–0.39), and SC (r=–0.54) may indicate a redistribution of functional load between layers or an alternative pattern of complete degeneration (predominant damage to either layer III or layer V in different animals). Neuronal death in layer V occurred earlier, which may be a direct consequence of the extreme accumulation of HCNSC at 30 days. In layer III, neuronal death (SC) was delayed until day 210, which corresponds to the model of secondary degeneration following the exhaustion of compensatory mechanisms [8, 17, 18].

The diverse nature of the injury was confirmed by the dynamics of NGIs. Early transient gliosis in layer III (peaking at 30 days, +95.5% compared to control, followed by a steady decline, Z=–4.92, $p<0.001$) corresponded to the classical model of an acute astroglial reaction with possible involvement of astrocytes in neuroprotection and recovery of homeostasis [19, 20]. In contrast, a sustained increase in NGI in layer V over 270 days (maximum +42% by day 270, mixed pattern: monotonically increasing trend Z=4.15, $p<0.001$; quadratic component F=5.1, p=0.028) indicated a chronic neuroinflammatory process and prolonged glial activation, which over time may contribute to the progression of degeneration [19–21]. A statistically significant «Layer × Time» interaction for NGI (F=28.6, $p<0.001$) confirmed fundamentally different temporal dynamics of gliosis in analyzed layers.

Contrary to the initial hypothesis of a cascade-like spread of degeneration from superficial layers to deeper ones, the data from the analysis of reactively altered neurons did not confirm a directional (lag-like) influence between the layers of the SMC. Correlation analysis at the individual animal level (n=36) revealed statistically significant positive correlations between layers for the SC (r=0.58; 95% CI [0.31; 0.76]; $r\_partial$=0.52; p=0.004), HCSC (r=0.52; [0.23; 0.73]; $r\_partial$=0.48; p=0.008), and NGI (r=0.44; [0.14; 0.67]; $r\_partial$=0.37; p=0.016). High values of partial correlations (with the control of «Time» factor) indicated intragroup consistency — in the same animals, degenerative processes in different layers proceed synchronously.

△-analysis (consistency of the direction of changes between adjacent time points) showed that for SC, HCSC, and NGI, changes in layers III and V were in the same direction significantly more often than would be expected by chance: for SC — 68% (55 out of 80, p=0.004), for HCSC — 66% (53 out of 80, p=0.008), for NGI — 64% (51 out of 80, p=0.016). The highest consistency was observed for SC — a marker of complete neuronal death. Thus, according to the analysis of the numerical density of reactively altered neurons, pathological processes in layers III and V developed in parallel and moderately synchronously, rather than sequentially. This did not rule out the presence of complex network interactions between layers, but did not confirm the simple cascade model of «first layer III, then layer V».

A comparison of the times of the extrema revealed different patterns of temporal dynamics in layers III and V. Synchrony was observed for the HCSC (peak at 30 days in both layers) and for the secondary SC peak (210 days in both layers). For HCSC, this confirmed the simultaneous development of acute ischemic injury; however, the intensity of this damage was significantly higher in layer V (+945% versus +473% in layer III, where the peak occurred at 90 days), which is consistent with the high metabolic vulnerability of large pyramidal neurons of the corticospinal tract [7].

A temporal priority of layer III was identified for most parameters reflecting neuronal functional state (NND, HCNSC) and glial response (NGI). The first minimum of NND was recorded at 30 days in layer III and at 150 days in layer V. The maximum of HCNSC was reached at 30 days in layer III and at 90 days in layer V. The most pronounced advance (at 240 days) was observed for NGI: an early transient peak in layer III (30 days, +95.5%) and a late prolonged peak in layer V (270 days, +42%). According to the literature, this likely indicates different mechanisms of the glial response: neuroprotective astroglial activation in the superficial layers and chronic neuroinflammation in the deep layers [22–24]. For HCC, a predominance of layer V was identified (peak at 90 days versus 150 days in layer III), which may reflect a more rapid depletion of metabolic reserves in the deep layers.

A temporal priority of layer V was also observed for the first SC peak (90 days vs. 210 days). This implies that complete neuronal death in the deep layers occurred earlier, which may be a direct consequence of the extreme accumulation of HCSC in layer V at 30 days. In layer III, neuronal death was delayed until 210 days, which is consistent with a model of secondary degeneration following the exhaustion of compensatory mechanisms [8, 17, 18].

Thus, the analysis of extrema confirmed that pathological processes in layers III and V did not develop completely synchronously: functional disruptions (HCNSC) and the glial response occurred earlier in layer III, whereas complete neuronal death (SC) and the depletion of metabolic reserves (HCC) occurred earlier in layer V. However, for the key marker of irreversible damage (HCSC), synchrony was observed in terms of timing, but with varying intensity and a delayed peak in layer III.

The results obtained are consistent with studies demonstrating the heterogeneity of damage to cor-

tical layers during ischemia [10, 22–26], but for the first time they demonstrate long-term dynamics (up to 270 days) in a model of chronic hypoperfusion using appropriate statistical methods that account for individual variability. In contrast to data obtained in the acute ischemia model [11, 18, 27–29], massive coagulative necrosis was not observed; instead, progressive dystrophy with polymorphism of reactive changes dominated, which corresponded to the chronic nature of the injury and the model's characteristics — the presence of a well-developed collateral network in rodents. In addition, the small number of time points (6) limited the ability to identify complex nonlinear relationships, although the use of quadratic trends partially compensated for this limitation.

Conclusion

Chronic cerebral ischemia induced by bilateral ligation of the common carotid arteries led to statistically significant and qualitatively distinct changes in neuronal populations in layers III and V of the rat cerebral cortex during the long-term follow-up period (up to 270 days).

Layer III of the SMC was characterized by a biphasic decrease in total neuronal density (peaking at 30 days), asynchronous dynamics of hyperchromatic non-shriveled (peaking at 30 days) and hypochromatic neurons (peaking at 150 days) (quadratic trends), a delayed peak in shadow cells (210 days), and transient gliosis (peaking at 30 days, followed by a decline). This reflected a damage model featuring components of partial recovery and delayed secondary degeneration.

Layer V of the SMC was characterized by a less pronounced but sustained decrease in the overall neuronal density (peaking at 150 days, with no significant trend), an extreme early increase in hyperchromic shrunken neurons (day 30, which was twice the increase in layer III), a synchronous peak of hyperchromatic non-shriveled and hypochromatic neurons (day 90), monotonous depletion of hypochromatic neurons (linear increasing trend), an early peak of shadow cells (90 days), and prolonged progressive gliosis (by 270 days). This corresponded to a model of progressive degeneration with primary metabolic damage to large pyramidal neurons.

Linear mixed models with random intercepts for each animal confirmed the presence of a statistically significant interaction between the «Layer» and «Time» factors for all key morphometric parameters, demonstrating different temporal dynamics of pathological processes in the layers under study.

Correlation analysis at the individual animal level revealed moderate positive correlations between layers. △-analysis showed consistency in changes for shadow cells, hyperchromatic shriveled neurons, and the neuroglial index. The time points of the peaks for hyperchromatic shriveled neurons (30 days) and the secondary peak of shadow cells (210 days) were synchronous in both layers. A temporal priority of layer III of the SMC was detected for the total neuronal density, hyperchromatic non-shriveled neurons, and the neuroglial index (early time points). A temporal priority of layer V was identified for the first peak of shadow cells and hypochromatic neurons. No conclusive evidence of a cascade-like spread of damage from superficial to deep layers was obtained, with the exception of a possible lead in the glial reaction in layer III of the SMC.

The data obtained support the need for further comparative studies of layers III and V of the SMC in a larger sample of animals and for the development of therapeutic strategies aimed at both protecting metabolically vulnerable pyramidal neurons and modulating the glial response during chronic hypoperfusion.

References

1. *Iadecola C.* The pathobiology of vascular dementia. *Neuron.* 2013; 80 (4): 844–866. DOI: 10.1016/j.neuron.2013.10.008. PMID: 24267647.
2. *Morgan A. E., Mc Auley M. T.* Vascular dementia: from pathobiology to emerging perspectives. *Ageing Res Rev.* 2024; 96: 102278. DOI: 10.1016/j.arr.2024.102278. PMID: 38513772.
3. *Kalaria R.N.* The pathology and pathophysiology of vascular dementia. *Neuropharmacol.* 2018; 134 (Pt B): 226–239. DOI: 10.1016/j.neuropharm.2017.12.030. PMID: 29273521.
4. *Zhang X., Chang S., Liu J., Wang D.* Combined metabolomics and proteomics analysis of vascular cognitive impairment in hypertensive rats induced by endothelial injury. *PLoS One.* 2025; 20 (10): e0332827. DOI: 10.1371/journal.pone.0332827. PMID: 41066429.
5. *Schaechter J.D., Perdue K.L.* Enhanced corticospinal tract fiber integrity and motor recovery following stroke evidenced by diffusion tensor imaging. *Neurorehabil Neural Repair.* 2008; 22 (6): 758–772. DOI: 10.1177/1545968308317530.
6. *DeFelipe J.* The anatomical problem posed by brain complexity and size: a potential solution. *Front Neuroanat.* 2015; 9: 104. DOI: 10.3389/fnana.2015.00104. PMID: 26347617.
7. *Zhang S., Murphy T.H.* Imaging the impact of cortical microcirculation on synaptic structure and sensory-evoked hemodynamic responses *in vivo. PLoS Biol.* 2007; 5 (5): e119. DOI: 10.1371/journal.pbio.0050119. PMID: 17456007.
8. *Carmichael S.T.* Brain excitability in stroke: the yin and yang of stroke progression. *Arch Neurol.* 2012; 69 (2): 161–167. DOI: 10.1001/archneurol.2011.1175. PMID: 21987395.
9. *Kalinichenko S.G., Korobtsov A.V., Matveeva N.Yu., Pushchin I.I.* Structural and chemical changes in glial cells in the rat neocortex induced by constant occlusion of the middle cerebral artery. *Acta Histochem.* 2020; 122 (5): 151573. DOI: 10.1016/j.acthis.2020.151573. PMID: 32622419.
10. *Zhang X., Wei M., Fan J., Yan W., Zha X., Song H., Wan R., Yin Y., Wang W.* Ischemia-induced upregulation of autophagy preludes dysfunctional lysosomal storage and associated synaptic impairments in neurons. *Autophagy.* 2021; 17 (6): 1519–1542. DOI: 10.1080/15548627.2020.1840796. PMID: 33111641.
11. *Авдеев Д.Б., Степанов С.С., Горбунова А.В., Шоронова А.Ю., Макарьева Л.М., Акулинин В.А., Коржук М.С. с соавт.* Темные нейроны сенсомоторной коры белых крыс после острой неполной ишемии в аспекте артефактов фиксации и нейроглиальных взаимоотношений. *Журнал анатомии и гистопатологии.* 2021; 10 (2): 9–22. *Avdeev D.B., Stepanov S.S., Gorbunova A.V., Shoronova A.Yu., Makaryeva L.M., Akulinin V.A., Korzhuk M.S., et al.* Dark neurons of the sensorimotor cortex of white rats after acute incomplete ischemia in terms of fixation artifacts and neuroglial relationships. *Journal of Anatomy and Histopathology = Zhurnal Anatomiya i Gistopatologiya.* 2021; 10 (2): 9–22. (in Russ.). DOI: 10.18499/2225-7357-2021-10-2-9-22.
12. *Pekny M., Pekna M.* Astrocyte reactivity and reactive astrogliosis: costs and benefits. *Physiol Rev.* 2014; 94 (4): 1077–1098. DOI: 10.1152/physrev.00041.2013. PMID: 25287860.
13. *Зиматкин С.М., Бонь Е.И.* Темные нейроны мозга. *Морфология.* 2017; 152 (6): 81–86. *Zimatkin S. M., Bon E. I.* Dark neurons of the brain. *Morphollogy = Morfologiya.* 2017; 152 (6): 81–86. (in Russ.). DOI: 10.17816/morph.398200.
14. *Brown G.C.* Neuronal loss after stroke due to microglial phagocytosis of stressed neurons. *Int J Mol Sci.* 2021; 22 (24): 13442. DOI: 10.3390/ijms222413442. PMID: 34948237.
15. *Chen S., Shao L., Ma L.* Cerebral edema formation after stroke: emphasis on blood–brain barrier and the lymphatic drainage system of the brain. *Front Cell Neurosci.* 2021; 15: 716825. DOI: 10.3389/fncel.2021.716825. PMID: 34483842.
16. *Kalinichenko S.G., Pushchin I.I., Matveeva N.Yu.* Neurotoxic and cytoprotective mechanisms in the ischemic neocortex. *J Chem Neuroanat.* 2023; 128: 102230. DOI: 10.1016/j.jchemneu.2022.102230. PMID: 36603664.
17. *Hu C., Chen X., Wang M., Zhang L., Gao D., Zang L.* Analgecine protects against cerebral ischemia-reperfusion through apoptosis inhibition and anti-neuroinflammation in rats. *Neuropeptides.* 2022; 93: 102230. DOI: 10.1016/j.npep.2022.102230. PMID: 35378359.
18. *Behrouzifar S., Esmaily H.* The biological efficacy of Apelin against focal transient cerebral ischemia-reperfusion injury. A systematic review and meta-analysis of animal studies. *Brain Res.* 2024; 15: 1833: 148887. DOI: 10.1016/j.brainres.2024.148887. PMID: 38552935.

19. *Sofroniew M.V.* Astrocyte barriers to neurotoxic inflammation. *Nat Rev Neurosci*. 2015; 16 (5): 249–263.
DOI: 10.1038/nrn3898. PMID: 25891508.
20. *Wilson D.M., Cookson M.R., Van Den Bosch L., Zetterberg H., Holtzman D.M., Dewachter I.* Hallmarks of neurodegenerative diseases. *Cell*. 2023; 186: 693–714.
DOI: 10.1016/j.cell.2022.12.032. PMID: 36803602.
21. *Delgado-Martín S., Martínez-Ruiz A.* The role of ferroptosis as a regulator of oxidative stress in the pathogenesis of ischemic stroke. *FEBS Lett*. 2024; 598 (17): 2160–2173.
DOI: 10.1002/18733468.14894. PMID: 38676284.
22. *Wang X., Zhang X.Y., Liao N. Q., He Z.H., Chen Q.F.* Identification of ribosome biogenesis genes and subgroups in ischaemic stroke. *Front Immunol*. 2024; 15: 1449158.
DOI: 10.3389/fimmu.2024.1449158.
PMID: 39290696.
23. *Голубев А. М.* Морфологическая классификация повреждений нейронов. *Общая реаниматология*. 2025; 21 (5): 4–14. *Golubev A.M.* Morphological classification of neuronal damage. *General Reanimatology = Obshchaya Reanimatologiya*. 2025; 21 (5): 4–14. (in Russ. & Eng.). DOI: 10.15360/1813-9779-2025-5-2580.
24. *Sheikh A., Meng X., Kao J.P.Y, Kanold P.O.* Neonatal hypoxia-ischemia causes persistent intracortical circuit changes in layer 4 of rat auditory cortex. *Cereb Cortex*. 2022; 32 (12): 2575–2589.
DOI: 10.1093/cercor/bhab365.
PMID: 34729599.
25. *Chen J.-M., Shi G., Yu Lu-Lu., Shan W., Sun J.-Yu, Guo A.-C., Wu J.-P., Tang T.-S., Zhang X.-J., Wang Q.* 3-HKA promotes vascular remodeling after stroke by modulating the activation of A1/A2 reactive astrocytes. *Adv Sci (Weinh)*. 2025; 12 (11): e2412667.
DOI: 10.1002/advs.202412667.
PMID: 39854137.
26. *Yanumula A., Cusick J. K.* Biochemistry, extrinsic pathway of apoptosis. In: StatPearls [Internet]. Treasure Island (FL): StatPearls Publishing; 2025. PMID: 32809646 Free Books & Documents.
27. *Бонь Е.И., Максимович Н.Е., Карнюшко О.А., Зиматкин С.М., Новак А.А.* Изменения содержания bcl-2 в теменной коре и гиппокампе крыс при ишемии головного мозга различной степени тяжести. *Новости медико-биологических наук*. 2025; 25 (2): 42–47. *Bon E.I., Maksimovich N.E., Karnyushko O.A., Zimatkin S.M., Novak A.A.* Changes in content of bcl-2 in the parietal cortex and hippocampus of rats with cerebral ischemia of varying severity *News of Biomedical Sciences=Novosti Mediko-biologicheskih Nauk*. 2025; 25 (2): 42–47. (in Russ.).
28. *Боева Е.А., Калабушев С.Н., Варнакова Л.А., Любомудров М.А., Цоколаева З.И., Кузовлев А.Н., Мороз В.В. с соавт.* Аргон-кислородная смесь как мультисистемная терапия после остановки кровообращения: экспериментальное исследование. *Общая реаниматология*. 2026; 22 (1): 26–40. *Boeva E.A., Kalabushev S.N., Varnakova L.A., Lyubomudrov M.A., Tsokolayeva Z.I., Kuzovlev A.N., Moroz V.V., et al.* Argon-oxygen mixture as a multisystem therapy after circulatory arrest: an experimental study. *General Reanimatology = Obshchaya reanimatologiya*. 2026; 22 (1): 26–40. (in Russ. & Eng.). DOI: 10.15360/1813-9779-2026-1-2618.
29. *Song W., Teng L., Wang H., Pang R., Liang R., Zhu Z.* Exercise preconditioning increases circulating exosome miR-124 expression and alleviates apoptosis in rats with cerebral ischemia-reperfusion injury. *Brain Res*. 2025; 15: 1851: 149457.
DOI: 10.1016/j.brainres.2025.149457.
PMID: 39824375.

Received 18.02.2026
Accepted 13.05.2026
Online First 04.06.2026

https://doi.org/10.15360/1813-9779-2026-3-2729

Minimally Invasive Management of Superior Mesenteric Artery Syndrome with Concurrent Nutcracker Phenomenon: Case Report

Miloslav Mišánik[1], Marek Smolár[1]*, Martin Grajciar[1], Diana Musová[1], Lukáš Spevák[1], Ján Janík[1], Beata Drobná Sániová[2], Juraj Miklušica[1]

[1] Clinic of General, Visceral and Transplant Surgery, Jessenius Faculty of Medicine, Martin, Comenius University Bratislava, 2 Kollárova Str., 03601 Martin, Slovak Republic
[2] Clinic of Anaesthesiology and Intensive Care Medicine, Jessenius Faculty of Medicine, Martin, Comenius University Bratislava, 2 Kollárova Str., 03601 Martin, Slovak Republic

For citation: *Miloslav Mišánik, Marek Smolár, Martin Grajciar, Diana Musová, Lukáš Spevák, Ján Janík, Beata Drobná Sániová, Juraj Miklušica.* Minimally Invasive Management of Superior Mesenteric Artery Syndrome with Concurrent Nutcracker Phenomenon: Case Report. *Obshchaya Reanimatologiya = General Reanimatology.* 2026; 22 (3): 41–47. https://doi.org/10.15360/1813-9779-2026-3-2729 [In Engl.]

***Correspondence to:** Marek Smolár, marino.smolar@gmail.com

Summary

Superior mesenteric artery (SMA) syndrome is a rare cause of high duodenal obstruction.

We report a case of an asthenic male (BMI 17.9 kg/m²) presenting with acute bowel obstruction.

Methods. Multiphase CT demonstrated marked pre-stenotic dilation of the D2 of the duodenum (max 8.8 cm) and compression of the D3 between the aorta and SMA, with an aortomesenteric angle of 11–12° and distance of 7 mm. A morphological, asymptomatic nutcracker phenomenon was present without hematuria. CT-suggested colitis was ruled out endoscopically and histologically. After consultation with vascular surgeon and shared decision-making, the patient opted for enteral bypass. The patient's preoperative anaesthesiology assessment revealed no contraindications to general anaesthesia for the planned laparoscopic procedure. A laparoscopic laterolateral, anisoperistaltic duodenojejunostomy was performed using a linear stapler (minimal blood loss; operative time 76 minutes) with a perianastomotic drain.

Results. Postoperatively, the nasogastric tube was removed on POD2, oral intake resumed from POD3, and the drain removed on POD4. Transient rise in CRP/leukocytosis on POD2 (negative presepsin) was managed empirically with ampicillin/sulbactam (Clavien–Dindo II). Patient was discharged on POD6 (7-day stay). At three months follow-up he remained symptom-free with objective nutritional gain (BMI + 2.3 kg/m²).

Conclusion. This case supports laparoscopic duodenojejunostomy as a safe and effective definitive option in hemodynamically stable patients with CT-quantified SMA obstruction. A concomitant asymptomatic nutcracker phenomenon does not require vascular intervention nor alter operative strategy.

Keywords: superior mesenteric artery syndrome; SMA; Wilkie's; duodenal obstruction, aortomesenteric angle, nutcracker phenomenon, laparoscopic duodenojejunostomy

Conflict of interest. The authors declare no conflict of interest.

Acknowledgments. The authors of the case report would like to thank the patient for his willingness to cooperate and for his consent to share medical information for the purposes of the educational process and for the writing of publications.

Information about the authors:
Miloslav Mišánik: https://orcid.org/0009-0000-8924-6645
Marek Smolár: https://orcid.org/0000-0002-7381-5513
Martin Grajciar: https://orcid.org/ — no ORCID
Diana Musová: https://orcid.org/0009-0004-7008-4323
Lukáš Spevák: https: /orcid.org/ — no ORCID
Ján Janík: https://orcid.org/ — no ORCID
Beata Drobná Saniova: https://orcid.org/0009-0009-4453-4446
Juraj Miklušica: https://orcid.org/0009-0003-6442-4064

Introduction

Superior mesenteric artery (SMA) syndrome (Wilkie's syndrome) is a rare cause of high duodenal obstruction resulting from compression of the third (D3) portion of the duodenum between the aorta and the overlying SMA [1, 2].

Its estimated population incidence is low, most commonly reported at approximately 0.013–0.3%. Diagnosis relies on the clinical findings and contrast-enhanced CT with assessment of the aortomesenteric angle and the aortomesenteric distance [1, 2].

The nutcracker entity denotes compression of the left renal vein between the aorta and the SMA. The nutcracker phenomenon is a morphological, often incidental finding without symptoms, whereas the nutcracker syndrome represents the symptomatic form with hematuria and/or venous congestion [3, 4].

Coexistence of SMA syndrome with a nutcracker entity is rare and has been reported mainly in single case reports [5–7].

Here, we present SMA syndrome with a con-

current asymptomatic nutcracker phenomenon managed by laparoscopic duodenojejunostomy. The case report was prepared in accordance with the SCARE criteria [8].

Patient consent

The authors of the case study obtained a written consent from the patient to publish this case study and to use the medical information and visual aids.

Ethics Commission

The approval of the ethics committee was not necessary as the article is a completely anonymized case study and no experiments were performed. A clear written consent was obtained from the patient regarding the photographs and information being published.

Case report

An asthenic man (BMI 17.9 kg/m²) was evaluated in the Emergency Department for acute ileus presenting with sudden epigastric pain, recurrent vomiting, and cessation of flatus. His history included hospitalization in 2013 for abdominal pain, then assessed as duodenoparesis with esophageal dysmotility. From that time until the current episode he tolerated solid food and maintained a stable weight without significant loss. On admission, abdominal distension was present with maximal tenderness in the epigastrium and absent bowel sounds. Laboratory tests showed leukocytes 19.6×10^9/L and CRP 11 mg/L, with mild hyponatremia. Initial X-ray/ultrasound confirmed a sub-ileus/ileus pattern. A subsequent multiphase abdominal CT demonstrated marked prestenotic dilatation of the D2 duodenum (up to 8.8 cm) and compression of the D3 segment between the aorta and the superior mesenteric artery (SMA), with an aortomesenteric angle of 11–12° and an aortomesenteric distance of 7 mm (Fig. 1). Segmental colitic changes of the colon described on CT (suspected IBD) were later excluded by pancolonoscopy during differential work-up. Incidentally, the CT also revealed the morphological picture of an asymptomatic nutcracker phenomenon (compression of the left renal vein

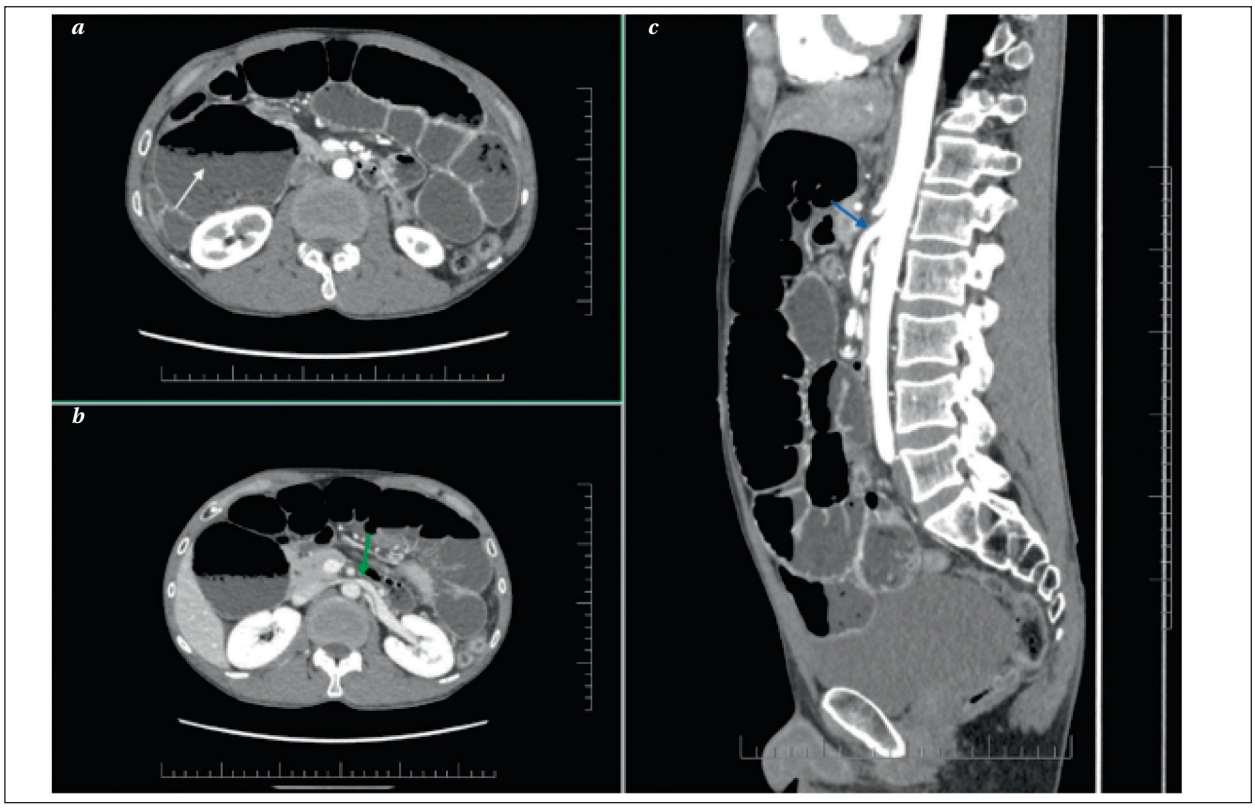

Fig. 1. CT findings in SMA syndrome with concurrent nutcracker phenomenon.
a — axial image — marked pre-stenotic dilation of D2 of the duodenum (max 8.8 cm, arrow); *b* — axial image — pre-stenotic dilation of the left renal vein with tapering at the aortomesenteric space (asymptomatic nutcracker phenomenon, arrow); *c* — sagittal image — narrow aortomesenteric angle ~11–12° with the transition point in D3 (arrow). Source: author.

Table. Objective parameters, reference thresholds and clinical interpretation. Patient data: present case; reference thresholds per [1, 2]; nutcracker definition per [3]; BMI per WHO [9].

Parameter	Patient value	Reference values / thresholds	Interpretation
Aortomesenteric angle (CT)	11–12°	Physiologic ~28–65°; suspicious for SMA ⩽ 22° [1, 2]	Strongly supportive of SMA
Aortomesenteric distance (CT)	7 mm	Physiologic ~10–28 mm; suspicious for SMA ⩽ 8 mm [1, 2]	Strongly supportive of SMA
D2 (second portion) dilation, max diameter	8.8 cm	In SMA typically marked proximal duodenal dilation (often >3–4 cm) [1,2]	High-grade obstruction proximal to D3
BMI	17.9 kg/m²	< 18.5 kg/m² = underweight (predisposing factor for SMA) [9]	Asthenic habitus — predisposition for AMS
Nutcracker phenomenon (left renal vein)	present; no hematuria	Phenomenon = morphologic LRV compression without symptoms; Syndrome = with hematuria/ venous congestion [3]	Asymptomatic finding; does not change acute management
Endoscopy/histology for IBD	not confirmed	—	CT 'colitic' changes without endoscopic/histologic correlation

Note. Published «normal» ranges for aortomesenteric angle/distance vary slightly; the thresholds ⩽ 22° and ⩽ 8 mm are among the most commonly cited and clinically used [1, 2].

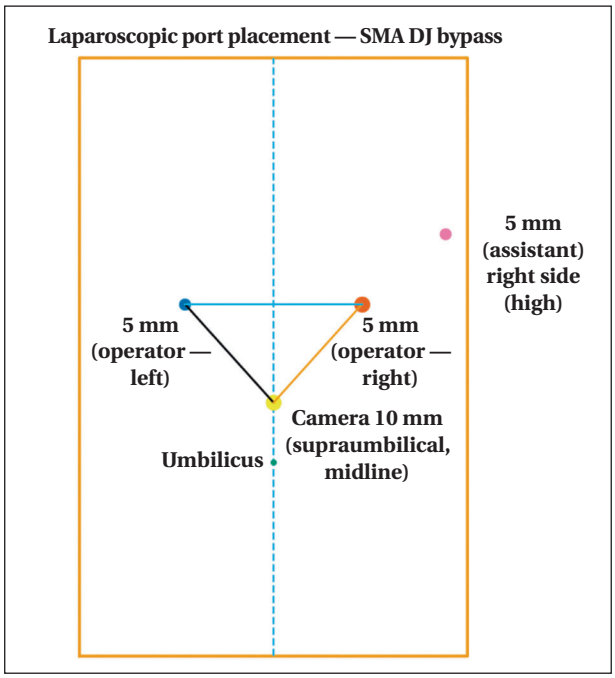

Fig. 2. Port Placement for laparoscopic DJ bypass.
Source: author.

between the aorta and SMA) without clinical manifestations. The relevant measurements and threshold values are summarized in Table.

After consultation with vascular surgery, the diagnosis of Wilkie's syndrome was confirmed, operative options and risks were explained. SMA transposition was proposed, but the patient preferred an intestinal bypass. Following preoperative optimization (hydration, proton-pump inhibitor, LMWH prophylaxis, nutritional support; internal medicine/anaesthesiology assessment: ASA II), we performed a laparoscopic latero-lateral, anisoperistaltic, stapled duodenojejunostomy. General anaesthesia was administered in accordance with the requirements for a laparoscopic procedure (patient intubation, inhalational anaesthesia, and analgesia with opioids plus sedatives). Port configuration: a 10 mm camera port supraumbilically on the midline, above it, for triangulation, a 5 mm (left, operator) and a 10 mm (right, operator) port and a separate 5 mm assistant port to the right above the triangulation (Fig. 2). A drain was left near the anastomosis. The procedure was completed without intraoperative complications with minimal blood loss, an operative time 76 minutes and no need for conversion.

POD1: CRP 113 mg/L, leukocytes 16×10^9/L. POD2: leukocytes rose to ~20×10^9/L and CRP to 306 mg/L; presepsin was negative, therefore empiric antibiotic therapy with ampicillin/sulbactam (Unasyn) was initiated, with subsequent improvement and decline of inflammatory markers (Clavien–Dindo II). The nasogastric tube was removed on POD2. Oral refeeding began on POD3 with stepwise advancement (liquids to soft diet) and emphasis on small, frequent, high-energy/high-protein meals, complemented by oral nutritional supplements. Estimated requirements were calculated using a pragmatic weight-based method (ideally from ideal body weight): ~25–30 kcal/kg/day (≈105–126 kJ/kg/day; 1 kcal = 4.184 kJ) with ~1.2–1.5 g protein/kg/day [10]. Electrolytes (phosphate, potassium, magnesium) were monitored during refeeding according to local protocol. If oral intake remained insufficient (e. g., < 60% of the target), escalation to enteral feeding distal to the anastomosis (or short-term parenteral nutrition) was considered. The drain was removed on POD4. The patient was discharged on POD6 (total hospital stay of 7 days) with a structured nutritional plan for home focused on ongoing weight gain (small frequent energy-

dense meals) including a prescription for high-energy, high-protein oral nutritional supplements (e. g., 2–3 servings daily) in addition to meet the calculated targets. At 3-month outpatient follow-up he reported good dietary tolerance without dyspeptic symptoms and weight gain, with BMI increased by 2.3 kg/m².

Discussion

Superior mesenteric artery (SMA) syndrome (Wilkie's syndrome) is a rare vascular variant in which a narrowed aortomesenteric angle and reduced aortomesenteric distance lead to compression of the D3 portion of the duodenum between the aorta and the SMA. It typically occurs in asthenic patients with low BMI, after rapid weight loss, or in the presence of anatomic predispositions [1, 2, 11–13].

In our case, the clinical picture of high-grade obstruction correlated with the CT findings (aortomesenteric angle 11–12°, distance 7 mm) and marked prestenotic dilation of D2, meeting the most commonly reported diagnostic criteria for SMA syndrome [1, 2, 11, 13].

Diagnosis relies on contrast-enhanced CT with multiplanar reformations (MPR). The aortomesenteric angle is measured on a sagittal plane aligned to the SMA axis, the aortomesenteric distance on a coronal plane at the D3 level, with additional assessment of the extent of oral duodenal dilatation. Although published ranges vary slightly, thresholds of ⩽ 22° and ⩽ 8 mm are among the most frequently cited and clinically used [1, 2, 11–13]. Because the aortomesenteric angle and distance vary with posture and respiration, standardizing measurement conditions (phase, MPR alignment) is important. In our case we used portal-venous phase with MPR aligned to the SMA axis and at the D3 level [11, 12]. Our diagnostic measurements and visual correlates (angle 11–12°, distance 7 mm, D2 dilatation) are shown in Fig. 1 and summarized against reference thresholds in Table [1, 2, 9, 11–13].

As complementary tests in selected cases, an upper GI contrast study (barium transit) or EGD may be considered to document the transition zone and exclude an intraluminal obstruction [11, 12, 14].

The differential diagnosis of high duodenal obstruction includes annular pancreas, congenital membranes/webs, malrotation, Crohn's disease, and neoplasms, which can mimic SMA syndrome [11–13].

A concomitant nutcracker entity (compression of the left renal vein between the aorta and the SMA) represents a separate spectrum of vascular anomalies. The phenomenon denotes an isolated morphologic finding without clinical manifestations, whereas the syndrome is a symptomatic condition with hematuria, lumbar pain, or signs of venous congestion [3, 4]. Coexistence of SMA syndrome and a nutcracker entity has been reported in single case reports, and the two diagnoses are linked by a narrowed aortomesenteric angle [5–7]. In our case, this was an asymptomatic nutcracker phenomenon without hematuria that did not affect therapeutic decision-making focused on relieving the duodenal obstruction (Fig. 1, *b*).

Diagnostic ambiguity at the initial evaluation of our patient is also noteworthy. The index CT described segmental colitic changes (suspected IBD), which were ruled out by pancolonoscopy and histology. The dynamics of ileus, bowel distension, and reactive mucosal changes can mimic inflammatory bowel disease. Endoscopic verification with biopsy is therefore essential to avoid inappropriate treatment.

Management of SMA syndrome is stepwise. In selected patients, conservative therapy may be initiated (nutritional intervention aimed at restoring the fat pad within the aortomesenteric angle, postprandial positioning, prokinetics, and, if needed, enteral feeding distal to the obstruction). Conservative management works best with shorter symptom duration and lesser dilatation. In practice, a time-limited trial is undertaken with clear nutritional targets (weight/angle increase) and lifestyle measures [1, 2, 11–13]. Persistent symptoms, marked dilatation, or recurrences indicate surgery [1, 2, 11–13]. Because conservative management had failed to provide sustained symptom relief, surgical bypass was considered appropriate in our patient.

Nutritional rehabilitation is central in SMA syndrome because it targets the underlying mechanism: low BMI and loss of retroperitoneal/mesenteric fat reduce the aortomesenteric angle and distance, thereby aggravating duodenal compression, while weight restoration may rebuild the protective «fat cushion» and contribute to symptom improvement. Accordingly, conservative management when feasible is typically built around nutritional therapy (together with postural measures, prokinetics and decompression) and should be guided by explicit, objectively monitored goals focused on weight restoration [1, 2, 11–13].

From a practical standpoint, energy and protein targets can be set pragmatically at approximately 25–30 kcal/kg/day (≈ 105–126 kJ/kg/day) and 1.2–1.5 g protein/kg/day (preferably using ideal body weight in underweight patients), with early re-establishment of oral intake supported by high-energy/high-protein oral nutritional supplements [10, 15]. If oral intake remains inadequate, enteral feeding distal to the obstruction (e. g., nasojejunal/jejunal feeding) should be considered, while parenteral nutrition is reserved for intolerance or failure of enteral strategies [10, 15]. In markedly underweight patients or after prolonged poor intake, cautious caloric escalation with monitoring and correction of phosphate, potassium and magnesium (and con-

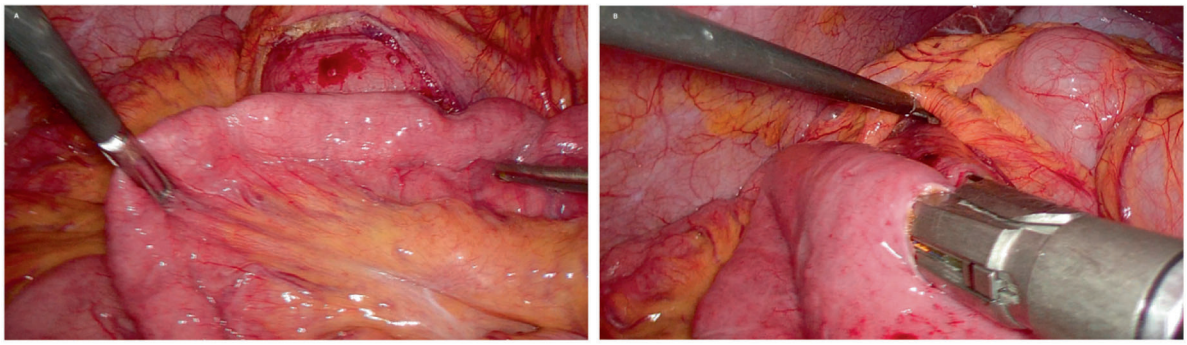

a *b*

Fig. 3. Intraoperative views — duodenojejunostomy.
Note. *a* — jejunum aligned and approximated to the third part of the duodenum at the intended laterolateral anisoperistaltic anastomosis site; *b* — linear stapler positioned intraluminally across the duodenum and jejunum immediately before firing. After construction the enterotomies were oversewn in two layers. Source: author.

sideration of thiamine supplementation according to protocol) is recommended to mitigate refeeding syndrome risk [16]. Even after definitive surgical bypass, continuation of a structured nutritional plan after discharge (energy-dense small frequent meals, oral supplements, and dietitian follow-up) helps secure sustained weight restoration, which was also observed at follow-up in our patient.

Among operative options, duodenojejunostomy (DJ), preferably laparoscopic, is considered the first-line method, as it reliably bypasses the site of compression, provides rapid relief of obstruction, and has a favorable postoperative profile compared with open surgery. The surgical principle of the DJ bypass is illustrated in Fig. 3 [1, 2, 11–13, 17].

Alternatives to the intestinal bypass include Strong's procedure (division of the ligament of Treitz with derotation of the duodenum), which may fail when the duodenum is firmly fixed, and gastrojejunostomy, which does not address the obstruction at D3 and carries risks of bile reflux and blind-loop syndrome. Therefore, it is used only exceptionally [1, 2, 11–13].

Laparoscopic DJ shows high success rates and low morbidity in published series. Long-term outcomes confirm sustained improvement in symptoms and BMI, although patients with concomitant motility disorders may have a poorer prognosis [11, 12, 17]. In our case, given the marked D2 dilatation, unequivocal CT quantification, and patient preference, laparoscopic DJ was chosen. The procedure was performed with minimal blood loss, an operative time of 76 minutes, and no need for conversion. The postoperative course corresponded to a Clavien–Dindo II stage, consistent with common, pharmacologically manageable complications after minimally invasive visceral procedures. Published data support the safety profile of the laparoscopic approach in this indication as well [1, 2, 17].

Transposition of the superior mesenteric artery is a less frequently used alternative in which caudal reimplantation of the SMA increases the aortomesenteric angle and relieves D3 compression. This technically demanding vascular procedure requires appropriate expertise and is considered on a case-by-case basis (e. g., after failure/contraindication of DJ/Strong's, specific anatomy, or concomitant planned vascular reconstruction). In available reviews, SMA transposition is described in small series and case reports and is not regarded as first-line because of its greater complexity compared with DJ [11–13].

When nutcracker syndrome is clinically manifest (hematuria, lumbar pain, venous congestion), options include open transposition of the left renal vein or endovascular stenting of the LRV. The choice depends on age, severity, anatomy, and institutional experience. LRV stenting is a less invasive solution with good short-term outcomes, but it requires antithrombotic therapy and surveillance for thrombosis or stent migration; long-term data are limited [3, 14, 18].

In overlap with SMA syndrome, when duodenal obstruction is treated by DJ bypass (and the patient declines vascular SMA transposition), LRV stenting can be considered for symptomatic nutcracker syndrome as a standalone or staged procedure. Rarely, regression of duodenal compression after LRV stenting has been reported due to altered anatomic relationships [5].

Limitations and strengths of our case. This is a single-case report with a 3-month follow-up and without postoperative re-measurement of aortomesenteric parameters; generalizability is therefore limited. Strengths include quantified diagnostics (angle/distance, Table 1, Fig. 2), a detailed

surgical description with a minimally invasive approach (Fig. 3), and an objective nutritional benefit (BMI + 2.3 kg/m²).

Conclusion

Minimally invasive duodenojejunostomy is a safe and effective definitive option in hemodynamically stable patients with superior mesenteric artery syndrome and clearly confirmed obstruction. Compared to alternatives (Strong's procedure, gastrojejunostomy), it reliably bypasses the site of compression and provides rapid recovery with low morbidity. Concurrent asymptomatic nutcracker phenomenon does not require vascular intervention and does not change the surgical strategy. Based on our case, we support a laparoscopic-first strategy within multidisciplinary decision-making in appropriately selected patients.

References

1. *Van Horne N., Jackson J.P.* Superior mesenteric artery syndrome. *StatPearls*. Treasure Island (FL): StatPearls Publishing; 2023.
2. *Welsch T., Büchler M.W., Kienle P.* Recalling superior mesenteric artery syndrome. *Dig Surg*. 2007; 24 (3): 149–156. DOI: 10.1159/000102097. PMID: 17476104.
3. *Kurklinsky A.K., Rooke T.W.* Nutcracker phenomenon and nutcracker syndrome. *Mayo Clin Proc*. 2010; 85 (6): 552–559. DOI: 10.4065/mcp.2009.0586. PMID: 20511485.
4. *Yoon T., Kim S.H., Kang E., Kim S.* Nutcracker phenomenon and syndrome may be more prevalent than previously thought. *Korean J Radiol*. 2022; 23 (11): 1112–1114. DOI: 10.3348/kjr.2022.0617. PMID: 36305049.
5. *Farina R., Iannace F.A., Foti P.V., Conti A., Ini F., Libra F., Fanzone L., et al.* A case of nutcracker syndrome combined with Wilkie syndrome with unusual clinical presentation. *Am J Case Rep*. 2020; 21: e922715. DOI: 10.12659/AJCR.922715. PMID: 32317620.
6. *Shi Y., Shi G., Li Z., Chen Y., Tang S., Huang W.* Superior mesenteric artery syndrome coexists with Nutcracker syndrome in a female: a case report. *BMC Gastroenterol*. 2019; 19 (1): 15. DOI: 10.1186/s12876-019-0932-1. PMID: 30674275.
7. *Khan H., Al-Jabbari E., Shroff N., Barghash M., Shestopalov A., Bhargava P.* Coexistence of superior mesenteric artery syndrome and nutcracker phenomenon. *Radiol Case Rep*. 2022; 17 (6): 1927–1930. DOI: 10.1016/j.radcr.2022.03.063. PMID: 35401899.
8. *Agha R.A., Franchi T., Sohrabi C., Mathew G., Kerwan A.; SCARE Group.* The SCARE 2020 guideline: updating Consensus Surgical Case Report (SCARE) guidelines. *Int J Surg*. 2020; 84: 226–230. DOI: 10.1016/j.ijsu.2020.10.034. PMID: 33181358.
9. World Health Organization. Body mass index (BMI).https://www.who.int/data/gho/data/theemes/topics/topic-details/GHO/body-mass-index?ysclid=mpmidu791c13.
10. *Weimann A., Braga M., Carli F., Higashiguchi T., Hübner M., Klek S., Laviano A., et al. ESPEN guideline: clinical nutrition in surgery. Clin Nutr*. 2017; 36 (3): 623–650. DOI: 10.1016/j.clnu.2017.02.013. PMID: 28385477.
11. *England R.J., Li N.* Superior mesenteric artery syndrome: a review of the literature. *J Am Coll Emerg Physician Open*. 2021; 2 (3): e12454. DOI: 10.1002/emp2.12454. PMID: 34179879.
12. *Oka A., Awoniyi M., Hasegawa N., Yoshida Y., Tobita H., Ishimura N., Ishihara S.* Superior mesenteric artery syndrome: diagnosis and management. *World J Clin Cases*. 2023; 11 (15): 3691–3384. DOI: 10.12998/wjcc.v11.i15.3369. PMID: 37383896.
13. *Lee T.H., Lee J.S., Jo Y., Park K.S., Cheon J.H., Kim Y.S. Jang J.Y., et al.* Superior mesenteric artery syndrome: where do we stand today? *J Gastrointest Surg*. 2012; 16 (12): 2203–2211. DOI: 10.1007/s11605-012-2049-5. PMID: 23076975.
14. *Avgerinos E.D., Saadeddin Z., Humar R., Salem K., Singh M., Hager E., Makaroun M., et al.* Outcomes of left renal vein stenting in patients with nutcracker syndrome. *J Vasc Surg Venous Lymphat Disord*. 2019; 7 (6): 853–859. DOI: 10.1016/j.jvsv.2019.06.016. PMID: 31471277.
15. *Weimann A., Braga M., Carli F., Higashiguchi T., Hübner M., Klek S., Laviano A. et al.* ESPEN practical guideline: clinical nutrition in surgery. *Clin Nutr*. 2021; 40 (7): 4745–4761. DOI: 10.1016/j.clnu.2021.03.031. PMID: 34242915.
16. *da Silva J.S.V., Seres D.S., Sabino K., Adams S.C., Berdahl G.J., Citty S.W., Cober M.P., et al.* ASPEN Consensus recommendations for refeeding syndrome. *Nutr Clin Pract*. 2020; 35 (2): 178–195. DOI: 10.1002/ncp.10474. PMID: 32115791.
17. *Wills M.V., Barajas-Gamboa J.S., Mocanu V., Conner A., Brown J., Restrepo-Rodas G., Lee S., et al.* Long-term outcomes of laparoscopic duodenojejunostomy for superior mesenteric artery syndrome. *Surg Endosc*. 2025; 39 (8): 5235–5243. DOI: 10.1007/s00464-025-11774-6. PMID: 40576774.
18. *Reed N.R., Kalra M., Bower T.C., Vrtiska T.J., Ricotta 2nd J.J., Gloviczki P.* Left renal vein transposition for nutcracker syndrome. *J Vasc Surg*. 2009; 49 (2): 386–393. DOI: 10.1016/j.jvs.2008.09.051. PMID: 19216958.

Received 07.10.2025
Accepted 13.05.2026
Online First 08.06.2026

https://doi.org/10.15360/1813-9779-2026-3-2668

Use of VA-ECMO in the Prenatal Period in a Patient with Acute Myocardial Infarction Complicated by Cardiogenic Shock: Case Report

Evgeniy S. Dumanyan[1,2*], Yuri N. Markov[1], Marat F. Mukhamadeev[1], Radik R. Khafizov[1], Bulat I. Zagidullin[1], Ainagul Zh. Bayalieva[2,3], Veronica R. Davydova[2,3], Nigina A. Nigmatullina[3], Gulnara M. Khairutdinova[1], Liliya A. Shakirzyanova[1], Antonina A. Panina[1]

[1] R.S. Akchurin Emergency Hospital,
18 Naberezhnochelninsky Ave.,423803, Naberezhnye Chelny, Republic of Tatarstan, Russia
[2] Kazan State Medical University, Ministry of Health of Russia,
49 Butlerova Str., 420012 Kazan, Russia
[3] Republican Clinical Hospital, Ministry of Health of the Republic of Tatarstan,
138 Orenburgsky Trakt, 420064 Kazan, Russia

For citation: *Evgeniy S. Dumanyan, Yuri N. Markov, Marat F. Mukhamadeev, Radik R. Khafizov, Bulat I. Zagidullin, Ainagul Zh. Bayalieva, Veronica R. Davydova, Nigina A. Nigmatullina, Gulnara M. Khairutdinova, Liliya A. Shakirzyanova, Antonina A. Panina.* Use of VA-ECMO in the Prenatal Period in a Patient with Acute Myocardial Infarction Complicated by Cardiogenic Shock: Case Report. *Obshchaya Reanimatologiya = General Reanimatology.* 2026; 22 (3): 48–54. https://doi.org/10.15360/1813-9779-2026-3-2668 [In Russ. and Engl.]

***Correspondence to:** Evgeniy S. Dumanyan, pro_medol@mail.ru

Summary

The aim is to demonstrate the successful use of veno-arterial extracorporeal membrane oxygenation (VA-ECMO) in a patient developing acute myocardial infarction (AMI) and cardiogenic shock due to spontaneous coronary artery dissection in the third trimester of pregnancy.

Patient and investigative techniques. We analyzed laboratory and hemodynamic parameters, mechanical ventilation settings and ECMO circuit parameters in a 32-week pregnant woman with acute myocardial infarction and cardiogenic shock caused by spontaneous coronary artery dissection. We reviewed all stages of patient's management from hospital admission, including initiation of ECMO, performing of cesarean section under extracorporeal support, and patient's transportation to tertiary center for heart transplantation.

Results. The use of VA-ECMO in a patient with AMI at 32 weeks of gestation provided biventricular circulatory support, which allowed to stabilize severe cardiogenic shock and safely place coronary stents, providing sufficient placental blood flow to preserve the life of the fetus. A cesarean section (CS) was performed under VA-ECMO support resulting in delivery of a live baby-girl weighing 1.8 kg with an Apgar score of 5/6. The mother was transported after CS to the V. I. Shumakov National Medical Research Center for Transplantation and Artificial Organs, Ministry of Health of the Russian Federation, where emergency orthotopic heart transplantation (OHT) was performed.

Conclusion. We present a case report of spontaneous coronary artery dissection leading to AMI and cardiogenic shock and requiring life-saving circulatory support with VA-ECMO. The case demonstrates the urgent need of both treatment arms including established protocol of coronary angiography with percutaneous coronary intervention, and timely employed individual approach, that include VA-ECMO, intra-aortic balloon pump, and left ventricular decompression. The use of high-tech methods and a professionally employed multidisciplinary approach saved the lives of both the mother and the child.

Keywords: extracorporeal membrane oxygenation; pregnancy; acute myocardial infarction; cardiogenic shock; spontaneous coronary artery dissection; caesarean section

Conflict of interest. The authors declare no conflict of interest.

Information about the authors:
Evgeniy S. Dumanyan: https://orcid.org/0000-0003-0937-4060
Yuri N. Markov: https://orcid.org/0000-0002-8211-5981
Bulat I. Zagidullin: https://orcid.org/0000-0001-5294-7288
Marat F. Mukhamadeev: https://orcid.org/0000-0003-4371-7151
Radik R. Khafizov: https://orcid.org/0000-0003-4345-1234
Ainagul Zh. Bayalieva: https://orcid.org/0000-0001-7577-3284
Veronica R. Davydova: https://orcid.org/0000-0003-4718-5076
Nigina A. Nigmatullina: https://orcid.org/0000-0003-4441-8858
Gulnara M. Khairutdinova: https://orcid.org/0000-0002-8152-8514
Liliya A. Shakirzyanova: https://orcid.org/0009-0004-2696-0330
Antonina A. Panina: https://orcid.org/0000-0003-4399-8723

Introduction

According to the US Center for Disease Control and Prevention, in 2023, «other cardiovascular causes» accounted for 10.4% of all maternal deaths, with bleeding accounting for 18.1%. These statistics included all deaths during pregnancy and within 1 year after childbirth [1]. The incidence of acute coronary syndrome (ACS) during pregnancy ranges from 3 to 6 cases per 100,000 pregnancies. Maternal mortality from ACS ranges from 5 to 10% [2]. The common causes of ACS in pregnant women include atherosclerosis [3, 4] and spontaneous coronary artery dissection (SCAD) [5]. SCAD, which can develop before and after childbirth, is the cause of acute myocardial infarction (AMI) in pregnant women in 27–43% of cases. The mortality rate for AMI in pregnant women is currently 5–11% [6].

SCAD is a spontaneous, non-traumatic, and non-iatrogenic dissection of the coronary artery (CA) wall with the formation of a false lumen [7]. Only 43% of SCAD cases occur during the peripartum period. Two pathohistological theories of its development are described in a publication by Sharonne N. Hayes and colleagues [7]. It is hypothesized that hormonal shifts (changes in the sensitivity of estrogen and progesterone receptors) associated with pregnancy lead to alterations in arterial architecture. SCAD is rarely associated with inflammatory diseases.

According to a multicenter prospective study, cardiovascular diseases account for the majority of maternal morbidity and are responsible for more than 25% of maternal deaths in the United States [8]. There are several diseases that can lead to cardiovascular complications during pregnancy. They include arterial hypertension, arrhythmias and cardiomyopathies, congenital or acquired valve defects, coronary artery disease (a leading cause of SCAD), pulmonary hypertension, and venous thromboembolism or amniotic fluid embolism. Cardiomyopathy and/or heart failure account for more than 50% of cardiovascular disorders during pregnancy. Cardiogenic shock (CS) during pregnancy caused by severe myocardial damage leads to reduced cardiac output, hypoperfusion of target organs, and hypoxia in the mother and fetus. Cardiogenic shock carries a poor prognosis, with in-hospital mortality rates of 30–50% and long-term mortality of about 50%. Temporary or long-term mechanical circulatory support (MCS) is used in management of cardiogenic shock caused by cardiomyopathy or SCAD [8]. Veno-arterial extracorporeal membrane oxygenation (VA-ECMO) as one of MCS modalities addresses the problem of tissue hypoperfusion, but creates a risk of bleeding, along with the risk of placental abruption, which directly threatens fetal life [8].

In publications on the use of ECMO in obstetric patients, both veno-venous extracorporeal membrane oxygenation (VV-ECMO), used for indications such as pulmonary embolism, viral pneumonias, and sepsis, and VA-ECMO [9], [10] are reported. Reports of VA-ECMO use in the peripartum period are extremely rare and are usually limited to isolated case reports. Thus, in a literature review by A. M. Sarah et al. [10], 45 cases of ECMO use in the antenatal period were reviewed: 41 VV-ECMO cases and 4 VA-ECMO cases. Overall maternal survival was 77.8% and fetal survival was 65%. According to a systematic review by Emily E. Naoum et al. [11], among 358 women who received MCS in the peripartum period, ECMO was used antenatally in 22.6% of patients, VA-ECMO in 40.5% of cases, and overall maternal survival was 74.3%. Of the 358 pregnant women included in the study, only 3 patients had SCAD as the cause of the life-threatening condition.

In the Russian Federation, the use of ECMO has increased markedly over the past 15 years [12–15]. In obstetrics, ECMO is most often used in the postpartum period. The first reported experience of a cesarean delivery in a patient on VV-ECMO was described by a team of authors from Krasnodar [16].

The purpose of this case report was to demonstrate the successful use of VA-ECMO in a patient at 32 weeks of gestation with a confirmed diagnosis of spontaneous coronary artery dissection and ST-elevation myocardial infarction complicated by cardiogenic shock.

Case Report

On Day 1 (07/04/25) at 08:40, a 31-year-old female patient was brought by an ambulance crew to the emergency department of the R.S. Akchurin Emergency Hospital (R.S. Akchurin Emergency Hospital, Republic of Tatarstan, Naberezhnye Chelny) with a diagnosis of «ST-elevation acute myocardial infarction of anterolateral localization. Spontaneous coronary artery dissection (?). Cardiogenic shock, SCAI C [17]. Pregnancy, 31–32 weeks». According to the updated SCAI (Society for Cardiac Angiography and Interventions) classification of cardiogenic shock stages, the patient's CS on admission corresponded to stage C, progressing to stage D. Complaints upon admission include general weakness, occasional chest burning equal to 2–3 scores on a 10-score VAS for the past 5–6 days, and maximum pain intensity on the morning of hospitalization. Objectively, the patient was conscious, and her hemodynamic parameters were stable with vasopressor support (noradrenaline at a dose of 0.25 μg/kg/min). BP 105–110/75 mm Hg, HR 67–72/min, SpO_2 98%. ECG: sinus rhythm, HR 67/min, QS in V2–V3 leads, qR in V4 lead, ST-segment elevation in I, aVL, and V2–V6 leads. ST-segment depression in III and aVF leads. Blood troponin level: 367 pg/mL.

To determine the extent of coronary artery involvement, coronary angiography (CAG) was per-

formed. Particular attention was paid to positioning the patient on the operating table and protecting the fetus from X-ray radiation. CAG findings were as follows: coronary circulation type — right-dominant. Left main coronary artery — occlusion in the distal third (dissection of the LAD, LCx). LAD — occluded. TIMI 0 flow. LCx — occluded. TIMI 0 flow. RCA — no stenoses detected. TIMI 3 flow.

Left common femoral artery and vein cannulation was performed. VA-ECMO was initiated. Indirect stenting of the left main coronary artery and the LAD (segments 5 and 6) was performed using Calypso (R-Vascular) drug-eluting coronary stents, 3.0×33 mm and 3.5×33 mm, respectively. Balloon angioplasty of the circumflex artery. Intravascular ultrasonography (IVUS).

After percutaneous coronary intervention (PCI), the patient was transferred to the cardiac intensive care unit. BP 98/89–120/87 mm Hg, CVP 14–10 mm Hg, pulmonary artery pressure 42/15 mm Hg, PCWP 25–29 mm Hg, heart rate 104–112 beats/min. ECG showed sinus rhythm. Norepinephrine 0.05 μg/kg/min, dobutamine 3 μg/kg/min. Urine output was 0.8–1.2 mL/kg/h. Arterial blood lactate: 2.1–1.8 mmol/L. Echocardiography: LVEF 33%, LVOT VTI 8 cm. EDV 136 mL, LV ESV 91 mL. Continuous fetal heart rate monitoring showed fetal heart rate varying from 138 to 152 beats/min.

The ECMO lines and oxygenator were primed with 0.9% NaCl solution, and 5,000 units of heparin were added to the solution. Before cannulation and connection, the circuit was placed on circulation and warmed to 37.0°C, with FiO_2 of 100% and a fresh gas flow of 3 L/min. Ultrasound scanning of the inguinal vessels was performed beforehand to determine their diameter and identify any anatomical variants or anomalies. Vascular cannulation was performed using a percutaneous dilatational technique under X-ray guidance, with local infiltration anesthesia using 40 mL of 1% lidocaine solution, potentiated with fentanyl — 50 μg intravenously. The ECMO device used was the MEDOS DELTASTREAM III (Medos Medizintechnik AG, Germany); the arterial cannula was 15 Fr, 31 cm, and the venous cannula was 21 Fr, 60 cm, with multilevel fenestrations. The «door-to-VA-ECMO initiation» time was 80 minutes. Blood flow through the ECMO circuit was 3.5 L/min at 8,400 rpm, oxygen flow was 3.5 L/min, and FiO_2 was 100%. Heparin anticoagulation was administered at 10–17 U/kg/h with a target aPTT of 60–70 seconds, along with dual antiplatelet therapy: aspirin 125 mg and clopidogrel 75 mg.

After 14.5 hours, the patient reported recurrence of retrosternal pain and worsening shortness of breath. Subsequent angiography revealed a dissection of the LAD distal to the stented segment. Stenting of the dissection segment and coronary arteries IVUS were performed. An intra-aortic balloon pump catheter was inserted via the right common femoral artery into the aorta to unload the left ventricle in view of reduced LV contractility. The device was operating in 1:1 mode. Decreased LV myocardial contractility persisted, LVEF declined from 33% to 28%.

On Day 2 (07/05/25), further progression of heart failure manifested by a decrease in left ventricular myocardial contractility (LVEF 25–28%, LVOT VTI 6–7 cm, LVEDV 155 mL, LVESV 116 mL) (Fig.) and worsening respiratory failure due to recurrent pulmonary edema. Respiratory support was also provided, alternating high-flow nasal oxygen therapy (FiO_2 60–65%) with noninvasive mask ventilation (FiO_2 60–65%).

On Day 3 (07/06/25), due to a marked reduction in LVEF, worsening cardiovascular insufficiency, and decreased uteroplacental blood flow, a decision was made to proceed with delivery by cesarean section while on VA-ECMO. Given the high risk of postoperative uterine hemorrhage, a supply of packed red blood cells, platelet concentrate, cryoprecipitate, and fresh frozen plasma was prepared, and heparin infusion was discontinued 2 hours before surgery.

The procedure was performed in the catheterization lab. After induction of anesthesia (propofol 1.5 mg/kg, fentanyl 1.5 μg/kg, rocuronium 50 mg), the trachea was intubated using videolaryngoscope. At the time of intubation, ECMO circuit blood flow was increased by 0.7 L/min, and fresh gas flow by 0.5 L/min. The ventilator settings were: FiO_2 40–50%,

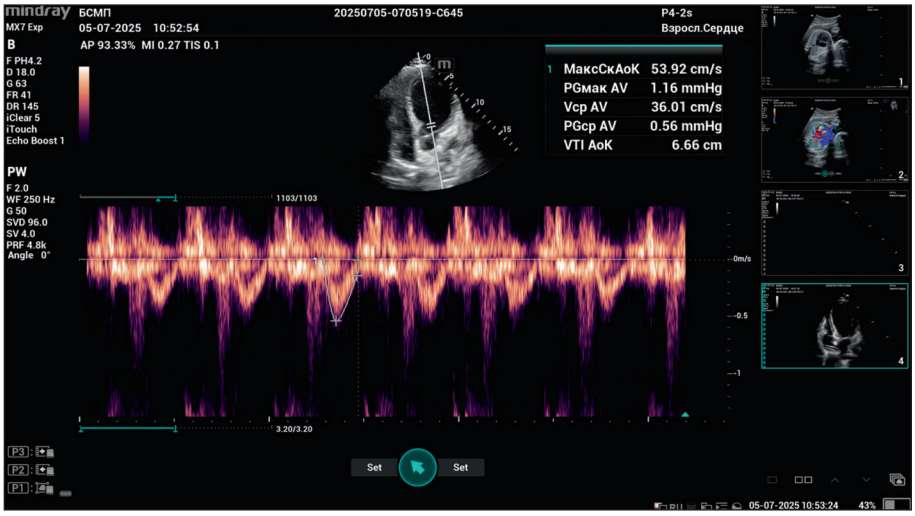

Fig. Parameters of cardiac contractile function (day 2).

respiratory rate (f) 10–12 breaths/min, tidal volume 5 mL/kg, PEEP 5–6 cm H_2O, and inspiratory pressure (Pinsp) 13 cm H_2O. After transition to mechanical ventilation, the VA-ECMO settings were: ECMO circuit blood flow 3.5–3.7 L/min, pump speed 8,400–8,700 rpm, oxygen flow 2.5–2.0 L/min, and FiO_2 70%. Before fetal extraction, guide catheters were advanced via the radial artery introducers to the ostia of the uterine arteries. The fetus was delivered. After delivery, balloon occlusion and embolization of the uterine arteries were performed. The uterus was sutured. A baby girl was born, weighing 1.8 kg, with an Apgar score of 8. The newborn was put on a ventilator and transported by ground ambulance to the Republican Pediatric Clinical Hospital in Kazan, Republic of Tatarstan.

Anesthesia was total intravenous: fentanyl at a dose of 2 μg/kg, propofol at a dose of 2 mg/kg/hour, and muscle relaxation with rocuronium bromide 50 mg. Intraoperative blood loss was 400 mL. The volume of postoperative blood loss over the following 24 hours was approximately 70–90 mL. Heparin infusion was resumed 8 hours after surgery at a rate of 8 U/kg/hour.

On Day 4 (07/07/25), echocardiography showed that the cardiac pumping function remained extremely poor (a spherical-shaped LV, spontaneous echo contrast, LVEF 10–15%), creating a risk of intracavitary thrombus formation. Atrial septal puncture was performed to decompress the LV. An additional 21 Fr cannula was advanced through the right common femoral vein into the left atrial cavity. The mechanical support setup was as follows: blood from the LA, RA, and IVC was drained into the ECMO circuit and returned via a cannula in the left common femoral artery, with an IABP catheter in the aorta.

The right common femoral vein was used as vascular access for cannulation of the left atrium. During catheterization, angiography revealed thrombosis of the common iliac vein. Thromboaspiration and balloon angioplasty of the right common iliac vein were performed. After that, it became possible to advance the cannula into the left atrium through the interatrial septum.

On Day 5 (07/08/25) ultrasonography revealed a 4×6 cm retroperitoneal hematoma in the area of the right iliac vein, which required relaparotomy. The source of the bleeding was not identified.

After relaparotomy, the patient was conscious. Mechanical ventilation was continued via an orotracheal tube in SIMV-PC mode: FiO_2 45%, rate 10/min, Vt 5 mL/kg, PEEP 6 cm H_2O, Pinsp 13–12 cm H_2O. Hemodynamic parameters: BP 128/68–121/72 mmHg, PAP 32/15 mmHg, HR 125–122/min, SpO_2 98–99%. ECMO parameters: 3.5–3.7 L/min, 8,400–8,700 rpm, oxygen flow 2.0 L/min, FiO_2 70%, heparin infusion 8 units/kg/hour, aPTT 55–85 sec.

On Day 6 (07/09/25), the patient was transported from Naberezhnye Chelny to Moscow by a combined mode of transport: 40 km from the

Table. Surgical procedures and associated complications.

Stages of treatment, date	Medical interventions		Complications, sequelae
	Procedure	Details	
Day 1, 04.07.2025	Cannulation of femoral vessels for VA-ECMO	The left common femoral artery and the left common femoral vein are cannulated	No
	LAD CAG/PCI, IVUS		No
	LAD CAG/PCI, IABP	PCI in the distal segments of LAD artery. Catheterization of the right common femoral artery for IABP	No
Day 2, 05.07.2026	Continuation of intensive therapy, consultations, and a medical council		
Day 3, 06.07.2025	Cesarean section, uterine arteries embolization		Blood-loss 400 mL
Day 4, 07.07.2025	CAG, interatrial septal puncture, insertion of additional cannula in the left atrium	Common iliac vein thrombosis, balloon angioplastya	Hemorrhagic shock retroperitoneal hematoma
Day 5, 08.07.2025	Re-laparotomy	Hematoma 4×6 cm in size, soft, 100–150 ml in volume in the projection of the right iliac vein.	No
Day 6, 09.07.2025	Medical evacuation by car + airplane	MV, VA-ECMO, IABP	No
	Transported to the V.I. Shumakov NMRC for Transplantation and Artificial Organs, MoH		No
Day 8, 11.07.2025	Re-laparotomy		No
	Orthotopic heart transplantation		No
Day 9, 07.12.2025	Weaning from VA-ECMO, IABP		No

R. S. Akchurin Emergency Hospital to Begishevo Airport (Nizhnekamsk), then about 900 km by plane to Zhukovsky Airport (Moscow), and then 60 km from Zhukovsky Airport to the Shumakov National Medical Research Center for Transplantology and Artificial Organs, Ministry of Health of the Russian Federation. The total medical evacuation time was approximately 5 hours.

All treatment stages and surgical procedures are presented in the table.

Discussion

Management of pregnant women with AMI during pregnancy and the postpartum period involves multiple objectives: treating cardiogenic shock and the myocardial infarction itself, preserving fetal viability, and preparing the patient for delivery, including an anticoagulation strategy required by the AMI treatment regimen and ECMO, as well as a hemostatic strategy for the delivery period. Administration of certain medications during pregnancy such as furosemide and sedatives (dexmedetomidine, propofol) poses an additional challenge, as they have strict restrictions for use during pregnancy, but still must be used when clinically indicated, e. g., for the treatment of pulmonary edema. These factors, along with many others, make effective management of cardiogenic shock during pregnancy really challenging.

This clinical case highlights the need to employ standard treatment protocols, and make rapid and timely decisions. The strong interest in SCAD in pregnant women is due, above all, to the limited amount of empirical data that would make it possible to develop a structured diagnostic and treatment protocol for the SCAD. As for the epidemiology, it is important to note that the overwhelming majority of SCAD patients are young women with low standard cardiovascular risk scores; however, it is difficult to assess the true prevalence of this condition because of under-diagnosis and the specific features of its clinical presentation [18].

The preparation of the patient and equipment required for ground and air transportation is not described, as this is a different topic worthy of a separate publication.

Conclusion

We presented a case report of SCAD in a pregnant woman, which resulted in AMI and CS, necessitating MCS with VA-ECMO. We showed that a combination of standard of care approaches, such as coronary angiography with percutaneous coronary intervention, and a timely individualized approach, including VA-ECMO, intra-aortic balloon pump, and left ventricular decompression, is required to manage such conditions. The use of advanced technologies and a professional multidisciplinary approach made it possible to save both the mother and the child.

References

1. The Centers for Disease Control and Prevention (CDC). Maternal Mortality Review Infor-mation Application («Maria»): The Centers for Disease Control and Prevention (CDC), 2023. https://www.cdc.gov/maternal-mortality/php/data-research/mmria-methods/index.html
2. Диагностика и лечение сердечно-сосудистых заболеваний при беременности 2018. Национальные рекомендации *Российский кардиологический журнал*. 2018 (3): 91–134. Diagnosis and treatment of cardiovascular diseases during pregnancy 2018. National guidelines *Russian Journal of Cardiology= Rossiyskiy Kardiologichesky Zhurnal*. 2018 (3): 91–134. (in Russ.). DOI: 10.15829/1560-4071-2018-3-91-134.
3. *Кочергин Н.А., Ганюков В.И., Тарасов Р.С., Барбараш О.Л.* Инфаркт миокарда с элевацией сегмента ST. *Эндоваскулярная хирургия*. 2015 (2): 95–98. *Kochergin N.A., Ganyukov V.I., Tarasov R.S., Barbarash O.L.* Myocardial infarction with ST segment elevation. *Russian Journal of Endovascular Surgery = Endovaskulyarnaya Khirurgiya*. 2015 (2): 95–98. (in Russ.).
4. *Шахова О.Б., Кузьмина И.И, Гвинджилия Т.Р., Дамиров М.М., Мурадян Н.А., Пархоменко М.В.* Инфаркт миокарда в послеродовом периоде. *Журнал им. Н.В. Склифосовского «Неотложная медицинская помощь»*. 2022; 11 (2): 368–373. *Shakhova O.B., Kuzmina I.I., Gvindzhiliya T.R., Damirov M.M., Muradyan N.A., Parkhomenko M.V.* Myocardial infarction in the postpartum period. *Russian Sklifosovsky Journal «Emergency Medical Care» = Zhurnal im. N.V. Sklifosovskogo «Neotlozhnaya Meditsinskaya Pomoshch»*. 2022; 11 (2): 368–373. (in Russ.). DOI: 10.23934/2223-9022-2022-11-2-368-373.
5. *Кузнецов А.А., Намитоков А.М., Сажнева А.В., Некрасов А.С., Космачёва Е.Д.* Клинический случай спонтанной диссекции левой коронарной артерии в послеродовом периоде. *Российский кардиологический журнал*. 2022: 46–56. *Kuznetsov A.A., Namitokov A.M., Sazhneva A.V., Nekrasov A.S., Kosmacheva E.D.* Spontaneous left coronary artery dissection in the postpartum period: a case report. *Russian Journal of Cardiology=Rossiyskiy Kardiologichesky Zhurnal*. 2022: 46–56. (in Russ.). DOI: 10.15829/1560-4071-2022-5059.
6. *Pierce T., Hovnanian M., Hedgire S., Ghoshhajra B.* Imaging of cardiovascular disease in pregnancy and the peripartum period. *Curr Treat Options Cardiovasc Med*. 2017; 19 (12): 94. DOI: 10.1007/s11936-017-0593-8. PMID: 29134367.
7. *Hayes S.N., Kim E.S.H., Saw J., Adlam D., Arsianian-Engoren S.,Economy K.E., Ganesh S.K., et al.* Spontaneous coronary artery dissection: current state of the science: s scientific statement from the American Heart Association. *Circulation*. 2018; 137 (19): e523-e557. DOI: 10.1161/CIR.0000000000000564. PMID: 29472380.
8. *Elad B., Karas M., Changhee L., Oren D., Fried J., Raikhelkar J., Clerkin K., et al.* Mechanical circulatory support for cardiogenic shock during the peripartum period. *Artif Organs*. 2025; 49 (2): 276–280. DOI: 10.1111/aor.14870. PMID:39345176.
9. *Webster C.M., Smith K.A., Manuck T.A.* Extracorporeal membrane oxygenation in pregnant and postpartum women: a ten-year case series. *Am J Obstet Gynecol MFM*. 2020; 2(2): 100108. DOI: 10.1016/j.ajogmf.2020.100108. PMID: 32835205.
10. *Moore S.A., Dietl C.A., Coleman D.M.* Extracorporeal life support during pregnancy. *J Thorac Cardiovasc Surg*. 2016; 151 (4): 1154–60. DOI: 10.1016/j.jtcvs.2015.12.027. PMID: 26825433.
11. *Naoum E.E., Chalupka A., Haft J., MacEachern M., Vandeven C.J.M., Easter S.R., Maile M., et al.* Extracorporeal life support in pregnancy: a systematic review. *J Am Heart Assoc*. 2020; 9 (13): e016072. DOI: 10.1161/JAHA.119.016072. PMID: 32578471.
12. *Скопец А.А.* Опыт применения экстракорпоральной мембранной оксигенации в акушерстве и гинекологии. *Инновационная медицина Кубани*. 2019; (4): 6–11. *Skopets A.A.* Experience of extracorporeal membrane oxygenation in obstetrics and gynecology. *Innovative Medicine of Kuban= Innovatsionnaya Meditsina Kubani*. 2019; (4): 6–11. (in Russ.). DOI: 10.35401/2500-0268-2019-16-4-6-11.
13. *Золотухин К.Н., Фаткуллина И.Б., Лазарева А.Ю., Поляков И.В., Быстрова Ю.Р., Мухаметкулова А.Р., Клявлин С.В.* Опыт применения экстракорпоральной мембранной оксигенации у родильницы с тяжелой преэклампсией. *Уральский медицинский журнал*. 2022; 21 (5): 88–93. *Zolotukhin K.N., Fatkullina I.B., Lazareva A.Yu., Polyakov I.V., Bystrova Yu.R., Mukhametkulova A.R., Klyavlin S.V.* Experience of extracorporeal membrane oxygenation in a woman with severe preeclampsia. *Ural Medical Journal = Uralskiy Meditsinskiy Zhurnal*. 2022; 21 (5): 88–93. (in Russ.). DOI: 10.52420/2071-5943-2022-21-5-88-93.
14. *Шелухин Д.А., Павлов А.И., Кузнецов С.В.* Первый в России успешный опыт применения продленной экстракорпоральной мембранной оксигенации у родильницы с синдромом Такоцубо. *Акушерство и гинекология*. 2019; 7: 131–136. *Shelukhin D.A., Pavlov A.I., Kuznetsov S.V.* The first successful

experience in Russia of using prolonged extracorporeal membrane oxygenation in a woman with Takotsubo syndrome. *Obstetrics and Gynecology = Akusherstvo i Ginecologiya*. 2019; 7: 131–136. (in Russ.).
DOI: 10.18565/aig.2019.7.131-136.

15. *Шилова А.С., Кецкало М.В., Площенков Е.В., Раимов М.Б., Вачнадзе Д.И., Троицкий Д.А., Самострол Н.Т. с соавт.* Тромбоэмболия высокого риска при беременности. *Акушерство и гинекология*. 2025; 1: 118–126. *Shilova A.S., Ketskalo M.V., Ploshchenkov E.V., Raimov M.B., Vachnadze D.I., Troitsky D.A., Samostrol N.T., et al.* High-risk thromboembolism in pregnancy. *Obstetrics and Gynecology = Akusherstvo i Ginecologiya*. 2025; 1: 118–126. (in Russ.). DOI: 10.18565/aig.2024.239.
16. *Скопец А.А., Жаров А.С., Потапов С.И., Афонин Е.С., Андреева М.Д., Галдина Т.В., Шульженко Л.В., с соавт.* Первый случай кесарева сечения у беременной во время экстракорпоральной мембранной оксигенации в Российской Федерации. *Вестник интенсивной терапии имени А.И. Салтанова*. 2019; (3): 90–97. *Skopets A.A., Zharov A.S., Potapov S.I., Afonin E.S., Andreeva M.D., Galdina T.V., Shulzhenko L.V., et al.* The first case of Cesarean section in a pregnant woman during extracorporeal membrane oxygenation (ECMO) in Russia. *Ann Crit Care = Vestnik Intensivnoy Terapii im A.I. Saltanova*. 2019; (3): 90–97. (in Russ.). DOI: 10.21320/1818-474X-2019-3-90-97.
17. *Kapur N.K., Kanwar M., Sinha S.S., Thayer K.L., Garan A.R., Hernandez-MontfortJ., Zhang Y., et al.* Criteria for defining stages of cardiogenic shock severity. *J Am Coll Cardiol*. 2022; 80 (3): 185–198.
DOI: 10.1016/j.jacc.2022.04.049.
PMID: 35835491.
18. *Ткачева О.Н., Шарашкина Н.В.* Инфаркт миокарда беременность. *Проблемы женского здоровья*. 2008; 3 (3): 25–30. *Tkacheva O.N., Sharashkina N.V.* Myocardial infarction and pregnancy. *Women's Health Issues = Problemy Zhenskogo Zdorovya*. 2008; 3 (3): 25–30. (in Russ.).

Received 27.01.2026
Accepted 13.05.2026
Online First 16.06.2026

https://doi.org/10.15360/1813-9779-2026-3-2678

Chronic Critical Illness: Definition, Epidemiology, Pathogenesis, and Clinical Manifestations (Brief Review)

Nikolay Yu. Dovbysh[1,2], Alexey I. Gritsan[1,2]*, Anna S. Cheverkova[1,2]

[1] Prof. V. F. Voino-Yasenetsky Krasnoyarsk State Medical University, Ministry of Health of Russia,
1 Partizana Zheleznyaka Str., 660022 Krasnoyarsk, Krasnoyarsk area, Russia
[2] Krasnoyarsk Regional Clinical Hospital,
3a Partizana Zheleznyaka Str., 660022 Krasnoyarsk, Krasnoyarsk area, Russia

For citation: *Nikolay Yu. Dovbysh, Alexey I. Gritsan, Anna S. Cheverkova.* Chronic Critical Illness: Definition, Epidemiology, Pathogenesis, and Clinical Manifestations (Brief Overview). *Obshchaya Reanimatologiya = General Reanimatology.* 2026; 22 (3): 55–66. https://doi.org/10.15360/1813-9779-2026-3-2678 [In Russ. and Engl.]

***Correspondence to:** Alexey I. Gritsan, gritsan67@mail.ru

Summary

The combination of syndromes and organ failure manifestations that develop after an acute critical illness (ACI) and demand the continuation of intensive care does not currently have a single definition. Meanwhile, the steadily increasing number of patients with such manifestations poses a challenge to the entire healthcare system. The complex pathogenesis and the differences in subtypes of chronic critical illness (CCI) necessitate a personalized approach to management of these patients.

Objective. To clarify the available data on the terminology of CCI, its prevalence, development timelines, clinical manifestations, pathogenesis, subtypes, and outcomes.

Materials and Methods. A literature review wasconducted using the PubMed, Google Scholar, and eLibrary databases. The review included 60 papers covering approaches to CCI definition, associated terminology, the investigation on of pathogenesis, clinical aspects, and CCI subtypes.

Results. Several case definitions were identified for CCI, reflecting the attitude toward this condition — either as one of the phases of acute critical illness or as a new disease. Additionally, two main approaches to diagnosing CCI were established: the first based on the duration of patient's stay in post-anesthesia care and intensive therapy (PACU/ICU) due to the need for intensive care, and the second based on the emergence of newly identified specific clinical and laboratory manifestations. The development of CCI is an unfavorable outcome of acute critical illness, leading to increased patient disability and a rise in mortality.

Conclusion. Further research is needed for deeper insights into development of CCI, establishing unified approaches to its definition, assessing risk factors, identifying its subtypes and associated organ dysfunctions.

Keywords: chronic critical illness; chronic critical condition; epidemiology; pathogenesis; subtypes

Conflict of interest. The authors declare no conflict of interest.

Information about the authors:
Nikolay Yu. Dovbysh: https://orcid.org/0000-0001-7222-9224
Alexey I. Gritsan: https://orcid.org/0000-0002-0500-2887
Anna S. Cheverkova: https://orcid.org/0009-0004-0691-6623

Introduction

Early publications on patients with prolonged stays in the ICU addressed issues related to prolonged mechanical ventilation (PMV). For example, the article by Cox JM [1] discusses the indications for initiating MV, approaches and methods for its implementation, i. e. via tracheotomy or nasotracheal intubation for prolonged ventilation. The author describes his experience with MV in one child via a nasotracheal tube for 30 days, and in four children with a tracheostomy in place for 4.5 years, and addresses the criteria for extubation and weaning procedures.

Alternatively, other emerging studies [2, 3] were discussing how the extent of administered therapy depends on the condition of critically ill patients, what were the indications for limiting or discontinuing intensive care in order to avoid sustaining life in those «whose biological existence continues, but who no longer have a human identity» [3].

In 1982, F. J. Indihar, D. P. Forsberg [4] noted that «chronic, long-term, protracted illnesses are attracting increasing attention as a major medical and social problem of our time.» In the same article, the authors describe a three-level dependency of patients on intensive care in the setting of a prolonged respiratory support unit. Level 1 includes patients requiring oxygen therapy, nebulizer therapy, rehabilitation, and educational interventions. Level 2 includes patients with minimal activity during the day who require mechanical ventilation, tracheostomy care, and physical therapy. At level 3 are patients with no activity at all, fully dependent on nursing care and respiratory therapy.

The distribution of conditions leading to hospitalization in this unit is noteworthy: the majority

of patients suffered from chronic obstructive pulmonary disease (72 patients), the sequelae of closed head injury (5 patients), and neuromuscular disorders (11 patients).

Thus, by the time the term «chronic critical ill» was proposed in 1985 by K. Girard and T. A. Raffin [2], the problem of chronic ventilator dependence and other intensive care measures among patients who had survived the acute phase of a critical illness had already been highlighted in a number of publications [1, 4].

Recently, there has also been a growing interest in the development of chronic critical illness (CCI) in patients who have survived acute critical illness (ACI), as evidenced by relevant domestic and international publications [5, 6]. This can be explained by the increasing number of such patients, significant medical, social and ethical challenges, and the economic costs associated with their care.

Study objective: to clarify existing data on the terminology of CCI, its prevalence, time to onset, clinical manifestations, pathogenesis, subtypes, and clinical outcomes.

Materials and Methods

A search for articles on patients' prolonged stays in the ICU was conducted in the PubMed, Google Scholar, and eLibrary databases using the following keywords in English: «chronic critical ill», «chronic critical illness», «persistent critical illness», and keywords in Russian «chronic critical condition» ,and «chronic critical illness». Relevance to the review's topic (pathogenesis, terminology, and outcomes of CCI) and availability of full-text access were established as inclusion criteria. Exclusion criteria included publications with limited information and those published more than 10 years ago, with the exception of fundamental works of foundational importance for the development of terminology and concepts related to the issue under consideration.

The study was conducted in accordance with the international guidelines for writing systematic reviews and meta-analyses, PRISMA (Preferred Reporting Items for Systematic Reviews and Meta-Analyses) [7]. The source selection flowchart is presented in Figure.

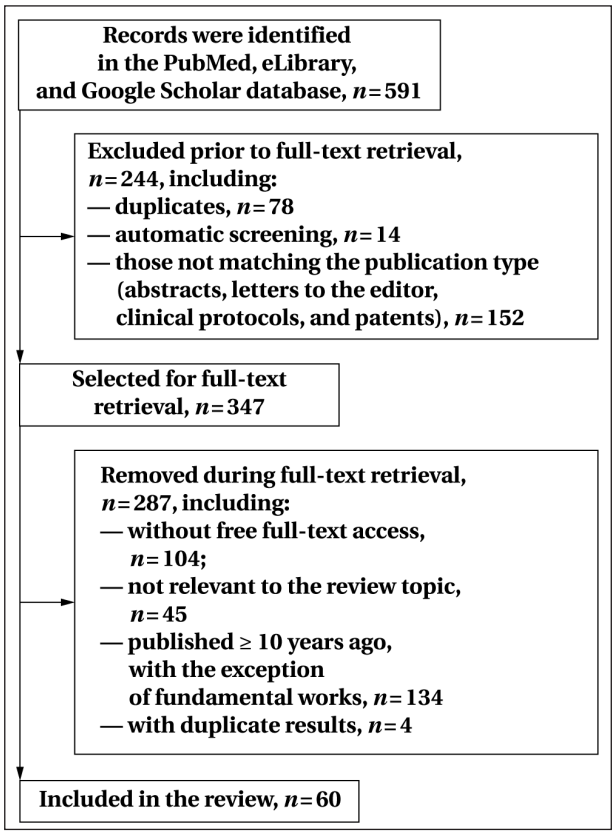

Figure. Source selection flowchart.

Results

Terminology of chronic critical illness. The term «chronic critical ill» was typically used in early studies, when forming cohorts of patients with prolonged stays in the ICU; however, since the late 2010s, the terms «chronic critical illness» and «persistent critical illness» have been used more frequently. All these terms have found widespread use in the English-language literature [2, 6, 8]. In French-language medical literature, it's «Patients Long Séjour» [9], which also refers to patients with prolonged stays in the ICU.

In Russian-language literature, both terms — «chronic critical illness» [5] and «chronic critical condition» (CCC) [10] are encountered.

At present, in addition to the lack of a single term to define this condition, there are also no uniform approaches regarding the circumstances under which a patient can be diagnosed with the development of CCI. The authors of the term CCI, K. Girard and T. A. Raffin, defined it as the patient's failure to survive despite extraordinary support over several weeks [2].

A number of authors consider the duration of stay in the ICU and the duration of mechanical ventilation to be the primary criteria for defining CCI.

In 1991, B. Daly et al. included the following factors as the criteria determining CCI: mechanical ventilation for at least 72 hours, provided that the patient survived and was discharged from the hospital [11].

In 1997, D. Scheinhorn et al. defined a patient with CCI as one with respiratory failure requiring PMV. Also in 1997, I. S. Douglas et al. categorize patients with CCI as those requiring PMV and intensive nursing care following intensive care for the primary illness, with a total ICU stay of at least 2 weeks.

In 2002, S. Carson et al. [12] defined a patient with CCI as one requiring prolonged therapy, including mechanical ventilation in an ICU setting,

and proposed a 21-day ICU stay as the simplest criterion.

In 2005, N. R. MacIntyre et al. [13] proposed the following criteria for CCI: a duration of continuous mechanical ventilation of 21 days or more, with for at least 6 hours per day. It's worth noting that mechanical ventilation lasting 21 days or more is considered PMV [10].

In 2008, M. D. Zilberberg et al. [14] published an article in which they attributed CCI development to the PMV for more than 96 hours after its initiation.

In 2019, G. Hermans et al. [15] proposed defining CCI as an ICU stay of 8 days or longer, based on their observations that once this time threshold was reached, patient mortality no longer depended on the initial severity of illness or the admission diagnosis.

All time-based criteria for establishing CCI in a patient have a drawback related to the fact that CCI is commonly associated with development of certain syndromes, which may be absent in a patient despite the predetermined duration of mechanical ventilation and ICU stay. It is believed that, depending on the characteristics of the underlying disease, CCI develops over varying timeframes — ranging from 7 to 22 days [16]. It has been proposed that CCI development begins at the point of time when the patient's ICU outcome is influenced not by the initial acute alteration of physiological parameters, but by their prior status [17]. It should be noted that in the study by T. Jeffcote et al., only 66% of patients with a confirmed diagnosis of CCI required mechanical ventilation by day 10 [18].

Other researchers, in turn, consider the emergence of new functional deficits and new syndromes in a patient to be indicative of CCI, which allows for a deviation from subjective criteria for establishing a CCI diagnosis — the duration of ICU stay and mechanical ventilation.

D. M. Nierman [19] in his paper published in 2002 categorizes patients with CCI as those who survived after ACI but developed severe functional impairments and remained dependent on intensive nursing care.

In 2010, J. E. Nelson et al. [20] defined CCI as a syndrome of significantly impaired metabolic, neuroendocrine, neuropsychiatric and immune functions in the presence of a tracheostomy and dependency on MV with persistent weaning failure. Emergence of such a robust criterion allows for objective recording the precise time of transition from acute to chronic critical illness.

In 2014, the Research Triangle Institute [21] developed and implemented a definition of CCI to standardize payment processes and patient location, incorporating the following criteria: the presence of a tracheostomy; sepsis or severe infections; severe injuries; multiple organ failure, ischemic stroke, intracerebral hemorrhage, or traumatic brain injury, combined with mechanical ventilation for at least 96 continuous hours and a stay in the ICU of at least 8 days. Including tracheostomy in CCI criteria has drawbacks as there are no universal standards regarding tracheostomy timing, which can vary significantly between different ICUs. (the decision is typically individualized rather than strictly protocol-driven).

Not all patients undergoing PMV can be classified as having CCI. For example, patients with irreversible neuromuscular diseases that necessitate PMV are not classified as having CCI due to the absence of systemic inflammation and multiple organ failure. The cohort of patients who are also not considered to have CCI includes those with end-stage cirrhosis and bronchopulmonary pathology, i. e., in cases where the disease itself has made it impossible to maintain the patient's homeostasis without intensive care [8].

The Methodological Recommendations «Rehabilitation in the Resuscitation and Intensive Care Unit (RehabIT)» [22] propose the following definition: «CCI is prolonged multi-organ failure with a shifting predominant syndrome of vital organ failure».

In 2024, H. Ohbe et al. proposed the following definition of chronic critical illness: CCI is a condition in which patients have survived a critical illness but require further prolonged stay in the ICU (typically 10 days or more); of these, the majority require prolonged mechanical ventilation (approximately 90%), approximately 50% of patients may require tracheostomy; these patients are characterized by prolonged reduced functional activity and the development of psychosocial problems [6]. The authors of this definition note that further research is needed to establish the characteristics of CCI and to standardize the definition itself.

An alternative perspective was presented by a group of Russian authors in a 2024 article [23]. When discussing the management of patients who have survived a critical condition, the authors move away from the definition of CCI, referring instead to the post-intensive care syndrome (PICS) and noting that the acute phase of this condition lasts from the 3rd to the 14th day of stay in the ICU.

In turn, the article by G. Voiriot et al. [24] defines CCI as the subacute stage of the disease requiring intensive care over an extended period, characterized by prolonged hospital stay, significant patient suffering, high mortality, and costly medical care. While PICS refers to associated with the ICU stay «residual health problems» to deal with after patient's discharge from the hospital.

CCI epidemiology, risk factors and outcomes. Data on the incidence of CCI vary depending on the country, year of assessment, level of the healthcare facility, organization of medical care, and criteria for CCI diagnosing [25].

An increase in the number of ICU patients who develop CCI has been reported in recent years, which is associated with improvements in intensive care and a reduction in early mortality. Based on data published in 2019, 88,000 patients were diagnosed with CCI in 1997, 380,000 patients — in 2009, and in 2020 the number of patients with CCI was expected to increase to 605,000 [15].

In a study by E. M. Viglianti et al., based on an analysis of 153,512 hospitalizations between 2015 and 2017 in the ICUs of 100 U.S. hospitals, it was shown that CCI developed in 4.9% of patients. In this study, patient's ICU stay exceeding 10 days was used by the authors as the CCI criterion [26]. A slightly earlier article by G. Van den Berghe [27] reported a significantly higher incidence of CCI in patients following ACI — 25%. The mortality rate for these patients in the ICU was 15–20%.

In a retrospective study conducted in Scotland [25] and including patients admitted to the ICU between 2005 and 2014, the reported CCI incidence was 33.8%. The authors diagnosed CCI in patients who had been in the ICU for more than 5 days and manifested signs of critical illness. It was noted that the total length of stay of these patients in the ICU accounted for 72.3% of the total number of bed-days. The 90-day survival rate in patients with CCI was the same as in patients without CCI, if CCI patients with CCI died within the first 30 days of their ICU stay were excluded from estimation.

Among the 2,500 patients admitted annually to ICU in Geneva, those with CCI accounted for 12% to 18%, with an average ICU stay of 13.8 days (the average stay for all ICU patients was 3.8 days). Approximately 52% of all ICU resources were spent on their treatment [9]. The authors note that the mean age of patients with CCI did not exceed that of the ICU patient population and was 60 ± 19 years. Mortality among patients with CCI was higher than among patients without this condition, reaching 15% compared to a mortality rate of 8–12% in the overall ICU patient population.

In the United Kingdom, the number of patients with PMV (21 days or more) was 4.4 per 100 ICU admissions; 6.3 per 100 patients who received mechanical ventilation upon admission to the ICU, and the total bed-days spent by these patients in the ICU accounted for one-third of all bed-days [28].

In a multicenter observational study by S. M. Bagshaw et al. [17], conducted between 2012 and 2014 in 12 ICUs in Alberta, Canada, with a total of 17,783 patients enrolled, CCI developed in 2,856 (16.1%) patients. In-hospital mortality in the group of patients with CCI was 23.9% compared to 15.5% in patients without CCI.

In the study by H. Ohbe [29], which included 2,395,016 ICU patients, 216,434 (9.0%) were diagnosed with CCI based on PMV following the development of sepsis, stroke, or tracheostomy. Mortality among patients with CCI was 28.6%. The authors note that in 2011, 47,729 cases of CCI were reported among ICU patients in Japan, and 46,494 cases — in 2017. During this period, while the mortality rate decreased from 30.6% to 28.2%, there was an increase in the number of patients who were completely dependent on care, and the proportion of patients discharged with impaired consciousness rose from 18.7% to 19.6%.

According to K. R. Chadda et al., 10% of ICU patients develop CCI, with a higher incidence among patients admitted with ACI, including sepsis (28%) and trauma (24%). The risk of developing CCI is higher in elderly patients with more severe course of the disease, and those with comorbidities [30]. Jeffcote et al. [18], in a study of CCI causes among 100 patients, found that patients admitted to the ICU due to respiratory failure, sepsis, or neurosurgical conditions are more likely to develop CCI.

In a study by Turkish authors, the incidence of CCI among patients treated in the ICU was 22%. A diagnosis of CCI was established when the patient's stay in the ICU lasted 21 days or more.

In a study by E. M. Viglianti et al. [31], which included patients from 6 ICUs at various university hospitals in the state of Michigan between 2014 and 2016, it was found that among 3,777 patients admitted to the ICU, 50 patients (13.2%) developed CCI (a ICU stay of more than 14 days was used as the criterion for CCI). In-hospital mortality of patients with CCI was 30%, while in patients without CCI, it was 8.2%. The researchers also found that the development of CCI is less likely in younger patients.

Baseline asthenia in a patient, which implies poor functional status, the presence of sarcopenia, muscle weakness, reduced physiological reserves, poor nutritional status, and decreased cognitive abilities, significantly increase the likelihood of adverse outcome [32], including higher mortality and longer ICU stay. It should be noted that asthenia occurs not only in elderly patients [33]. The CFS (Clinical Frailty Status) index, which characterizes age-related asthenia, was higher in patients with CCI. Thus, with a CFS score of 7–8, the risk of developing CCI reaches 4.8%, whereas with a CFS score of 1–2, the risk of developing CCI is only 2.8% [32]. The authors also noted that more severe asthenia, as assessed by the CFS scale, is associated with older age and a more severe condition as assessed by the APACHE III scale, was more common in women, and these patients were more likely to have sepsis at admission.

In published analysis of the medical records of 59,319 mechanically ventilated patients S. Okahara et al. [34] identified 8,331 (14%) patients with asthenia. The probability of weaning these patients

from MV was statistically significantly lower than in patients without asthenia. The authors also noted that the effect of asthenia on the failure to wean from MV was more evident in younger patients.

In a number of publications [35, 36], the authors indicate that neither the APACHE score nor other scales assessing the probability of death in patients with ACI demonstrated their predictive value in patients with CCI.

C. A. R. Feijó et al. express the same opinion based on the analysis of 86 medical records, including 13 (15%) CCI cases. The authors concluded that higher score on the APACHE II and SOFA scales were not predicting development of CCI, whereas the presence of chronic conditions such as chronic kidney disease and diabetes mellitus were predisposing to CCI development [37]. In this study, the CCI diagnosis was established in patients on mechanical ventilation for at least 6 hours per day for a minimum of 21 days.

The study by Loss et al. identified the following predictors of CCI development: high BMI, use of mechanical ventilation, development of sepsis, reduced level of consciousness as assessed by the Glasgow Coma Scale, and inadequate nutritional support by the 7th day from the onset of the disease [35].

In a prospective observational cohort study, J. C. Mira et al. [38] identified the following risk factors for CCI in 135 adult patients with severe trauma and hemorrhagic shock who did not die within the first 48 hours following injury: patient age $\geqslant$55 years; severe shock on admission (systolic blood pressure $\leqslant$70 mm Hg); transfusion of 5 or more units of packed RBCs within the first 24 hours; severe organ failure by Denver Multiple Organ Failure Scale; and presence of infectious complications. In this study, CCI diagnosis was established in patients with organ failure and ICU stay for $\geqslant$14 days. CCI developed in 25 (19%) patients with 16% mortality rate within first 4 months (vs 1.6% mortality in patients without CCI); 56% of these patients required post-discharge care in medical rehabilitation facilities.

In 2008, S. S. Carson et al. [39] assessed factors increasing the likelihood of death within 3 months or one year of disease onset in patients after PMV. They identified the need for vasopressors, hemodialysis, a platelet count of less than 150×10^9/L, and age 50 years or older as predictors of death. The ProVent (Prolonged Mechanical Ventilation Prognostic) score, developed by the authors based on these parameters, has been widely used to assess the probability of death in patients undergoing MV. At the same time, the authors note that different approaches to patient management may lead to biased results when using these indicators for assessment.

Subsequently, the ProVent score demonstrated high sensitivity and specificity in predicting one-year mortality. Thus, in an observational study of 150 therapeutic and surgical patients experiencing PMV for more than 21 days from the time of tracheal intubation, S. Jaiswal et al. [36] confirmed the predictive value of the scale's parameters for identifying the probability of death both within the first 3 months and during the first year.

C. I. Udeh et al. found that PMV experience in patients aged over 65 years is the strongest predictor of death within the first year in surgical and therapeutic settings [40].

The modified ProVent scale assigns one score for each of the following on day 21 of PMV: for patient's age of 50 years or older, presence of thrombocytopenia (less than 150×10^9/L), need for therapeutic dialysis, and administration of vasopressors; and 2 scores — for patient's age 65 years or older. According to a study by C. Dibiasi [41], one-year mortality in patients with CCI reaches 49%.

While the ProVent scale assesses the risk of 1 year mortality in critically ill patients who have been on mechanical ventilation for $\geqslant$21 days, the ProVent14 scale developed by Hough et al. assesses the risk in CCI patients on day 14 of mechanical ventilation [42]. This scale includes 5 parameters: age 50–64 years — 1 score, age $\geqslant$65 years — 2 score, thrombocytopenia (less than $100{,}000 \times 10^9$/L) — 1 score, use of vasopressors – 1 score, hemodialysis – 1 score, and patient's admission to the ICU unrelated to trauma — 1 score. In patients with a ProVent score of 0–1, the one-year mortality rate was 30%, whereas in patients with a score of 4 or more, the one-year mortality rate was 90%.

The probability of death in patients with CCI was assessed using the ProVent and ProVent14 scales/ The tracheostomy-ProVent scale developed by Jang et al. was employed in patients with a tracheostomy. The authors included six parameters in this scale: platelet count $< 150 \times 10^9$/L; $PaO_2/FiO_2 < 200$ mmHg, BMI < 23.0 kg/m^2, albumin concentration $<$ 28 g/L, presence of chronic cardiovascular disease, and immunosuppression. The first 4 parameters were assessed on the 14th day of mechanical ventilation; the last two were evaluated at admission.

H. Ohbe et al. found that 25% of patients who develop CCI die in the hospital; more than 50% of survivors require prolonged hospitalization or admission to specialized inpatient facilities with access to highly skilled nursing care, where the subsequent one-year mortality rate reaches 45%, and approximately 25% of patients with CCI are discharged home [6].

J. N. Darvall et al. found that the most common causes of death in patients with CCI were sepsis and multiple organ failure, which led to death of 16.7% of patients. In this study, CCI was diagnosed in patients who stayed in the ICU for more than

10 days, provided that the initial illness no longer determined the reason for their continued stay in the unit. Of notion, in one-third of these patients, MV had already been discontinued by the 10th day of their stay [43].

Patients who have survived CCI are characterized by a high rate of readmissions. According to M. Unroe et al., 67% of patients diagnosed with CCI were readmitted to hospitals within the first year after discharge [44].

In a study conducted at the respiratory center of the ICU at the University Hospital in Modena (Italy), A. Marchioni et al. found that ACI progressed to CCI in 33% of patients with acute respiratory failure [45]. Of these, 50% died within six months of discharge from the ICU, and only 10% were able to care for themselves at home. The researchers found that risk factors for development of CCI in patients with respiratory failure include a high APACHE II score — 17 scores or higher, the presence of septic shock on admission, the detection of multidrug-resistant flora, diaphragmatic dysfunction (as determined by ultrasonography), the development of a secondary infection during ICU stay, and an increase in C-reactive protein within 7 days of hospitalization. The diagnostic criteria for CCI in this study were: an ICU stay of more than 8 days, the presence of a tracheostomy, or mechanical ventilation for more than 21 days with a daily duration of at least 6 hours.

Publications by Russian researchers primarily address the issues of PMV in patients with acute cerebrovascular accidents. Thus, V. I. Ershov et al. [46], based on the study «Respiratory Therapy Registry in Patients with Acute Cerebrovascular Disease (RETAS)», conclude that development of ventilator-associated pneumonia determines mortality in patients with acute cerebrovascular disease after the acute phase of the stroke is over. In another article, the same authors note that the severity of neurological deficit in patients with acute ischemic stroke and a NIHSS score of >14 (moderate to severe stroke), combined with manifestations of malnutrition is an additional risk factor for an adverse outcome following PMV experience [47].

CCI pathogenesis. Disorders of the nervous, endocrine, and immune systems play a major role in CCI development. During the acute phase of illness, there is an increase in pituitary hormone levels, accompanied by fluctuations in «peripheral» hormones — concentrations of anabolic hormones and triiodothyronine decrease, while the concentration of the catabolic hormone cortisol increases. During transition to CCI, the entire hypothalamic-pituitary-adrenal (HPA) axis becomes hypo-reactive, yielding lower cortisol levels and increasing dopamine production. Meanwhile, impaired cortisol degradation and decreased rate of its systemic clearance results in gradual elevation of cortisol and suppression of ACTH secretion, disrupting normal feedback mechanisms. Dysregulated pulsatility in synchronized secretion of ACTH and cortisol results in breakdown of the normal dynamic correlation between the two hormones — so called ACTH-cortisol dissociation, leading eventually to the development of adrenal cortex atrophy [48]. Because of suppression of the gonadotropin-releasing hormone — follicle-stimulating/luteinizing hormones — gonads axis, there's a decrease of testosterone levels in men and progesterone levels in women with simultaneous paradoxical increase in estrogen concentrations, leading to increased aromatase enzyme activity. The circadian rhythm in critically ill is also disrupted, which is accompanied by impaired pulsatile function of the hypothalamic-pituitary system, pulsatile secretion of cortisol and thyroid-stimulating hormone, and fluctuations in melatonin levels. These changes lead to sleep disturbances in ICU patients, which negatively affect cognitive functions and adaptive immune response, leading to development of delirium. In addition to inflammation, artificial light, noise, and enteral nutrition also contribute in the development of circadian rhythm disturbances. Maladaptive processes buildup as CCI progresses, but unlike the adaptive processes observed during the acute phase, these processes promote excessive catabolism and suppress anabolic processes [49].

Disorders of the autonomic nervous system are associated with dysfunction of both the sympathetic and parasympathetic systems [50]. The hormones of the sympathetic nervous system — adrenaline and noradrenaline — activate leukocytes, increase cytokine synthesis, and stimulate the synthesis of acute-phase proteins in the liver. Acetylcholine, a hormone of the parasympathetic system, has an anti-inflammatory effect; when it interacts with acetylcholine receptors on leukocytes and lymphoid tissue, the synthesis of pro-inflammatory cytokines decreases. ACI is characterized by activation of the sympathetic nervous system and suppression of the parasympathetic nervous system. Transition to CCI in a bed-confined patient with inadequate protein-energy intake additionally augments parasympathetic system suppression.

Development of critical condition- associated polyneuromyopathy is an integral manifestation of CCI [51]. According to researchers, the development of polyneuromyopathy is associated with both microvascular insufficiency and impaired permeability of the blood-nerve barrier, as well as with processes of myosin molecule loss in the backdrop of lysosomal autophagy [52]. These processes are triggered by an inflammatory response, malnutrition, and muscle inactivity due to patient's immobility. Sedation, the use of muscle relaxants and corticosteroids, and

hyperglycemia are also risk factors for the development of critical condition polyneuromyopathy.

Involvement of cardiovascular system in CCI manifests as heart failure; disorders in the respiratory system are associated both with impaired ventilation (ventilator-induced weakness of the diaphragm and accessory respiratory muscles) and with development of infections — ventilator-associated and nosocomial pneumonia. Renal manifestations may include the development of acute kidney injury, oliguria, or anuria. In the endocrine system, CCI manifests as increased catabolism with loss of muscle mass, bone resorption due to immobility, vitamin D deficiency, development of adrenal insufficiency, and substitution of lean mass by adipose tissue. Involvement of hematopoietic and immune systems results in anemia, immunodeficiency and development of chronic inflammation. Infectious diseases manifest as recurrent infections caused by multidrug-resistant flora with poor wound healing. CCI — associated gastrointestinal tract disturbances manifest as malnutrition and malabsorption [20, 52, 53].

Two simple models of CCI development were discussed by C. E. Cox in his article published in 2012 [54]. According to the first model intensive care measures are still required after acute phase of critical illness is over. In this model, according to the author, it remains unclear which factors account for the continued need for such measures. The second model suggests the role of switchover to a prolonged inflammatory response and development of chronic post-shock syndrome with specific manifestations.

In their 2012 study, L. F. Gentile et al. [55] identified the following criteria characteristic of CCI: persistent inflammation, immunosuppression, and catabolic syndrome (PICS): chronicity of the condition (ICU stay of 10 days or more, or hospital stay exceeding 14 days); presence of inflammation (C-reactive protein concentration > 1.5 mg/L); immunosuppression (absolute lymphocyte count $< 0.80 \times 10^9$/L); manifestations of catabolism (albumin concentration < 30 g/L, creatinine-to-height ratio < 80%, weight loss > 10%, weight to height ratio < 18, retinol-binding protein concentration < 100 μg/L).

According to J. C. Mira et al., PICS occurs in 30–50% of patients with CCI [38]. The authors propose the following laboratory markers of PICS: CRP > 0.5 mg/L as a marker of persistent inflammation; an absolute lymphocyte count of $< 0{,}80 \times 10^9$/L—an indicator of persistent immunosuppression; and indicators of a catabolic state include: albumin concentration < 30 g/L, prealbumin < 100 mg/L, creatinine-height index < 80%, patient weight loss > 10% from baseline, or weight to height ratio < 18. The PICS concept, which implies the development of persistent inflammation, immunosuppression, and catabolic syndrome, was described based on observations of surgical ICU patients in whom the causes of primary severe inflammation were trauma or surgical sepsis and who experienced repeated damaging effects, primarily nosocomial infection. PICS represents a self-perpetuating cycle of organ failure, inflammation, and immunosuppression, leading to recurrent infections, metabolic disorders, and loss of muscle mass [56]. It should be noted that the presence of PICS is not a prerequisite for the development of CCI.

The study by Q. Zhou et al. [57] assessing potential concurrence of CCI and PICS among 168 patients with an ICU stay of 14 days or more, discovered discordant rates of the two conditions: 17 patients had isolated PICS without CCI; 70 patients developed CCI without manifestations of PICS; 50 patients were diagnosed with both CCI and PICS simultaneously; and 30 patients showed no signs of either CCI or PICS. These patients differed in terms of manifestations of organ failure, length of hospital stay, and mortality by the 28th day of hospital stay. In authors' opinion emergence of PICS in CCI worsens patient's prognosis. V. V. Likhvantsev et al. [58] make similar conclusions in their study: the presence of the triad of symptoms — inflammation, catabolism, and immunosuppression (the authors use the acronym ICIS in this context) — leads to a 2.5-fold mortality increase in patients with CCI.

L. Hesselink et al. [59] note in their study that there is no single definition for either CCI or PICS. The authors consider PICS to be present when ICU stay is 14 days or more, when patient experienced three or more infectious complications and manifests persistent catabolic state. Infectious complications were defined as presence of infection at hospital admission that required any intervention — administration of antibiotics and/or surgery. A catabolic state was defined as: weight loss of 10% or more, weight to height ratio < 18, or serum albumin concentration below 30 g/L. The authors considered this variant of PICS to be «clinical PICS» as opposed to «laboratory PICS,» in which a decrease in the absolute lymphocyte count $< 0{,}8 \times 10^9$/L for 2 or more days as a manifestation of immunosuppression, CRP > 50 mg/L for 2 or more days, and catabolic state meeting the criteria for «clinical PICS» during the first 30 days of hospital stay. Among 183 patients with polytrauma, 78 were diagnosed with CCI, of whom «clinical PICS» was diagnosed in 18 patients, «laboratory PICS» in 22 patients, and in 8 patients — a combination of both «clinical and laboratory PICS».

In the article discussing influence of persistent inflammation and immunosuppression on CCI development, R. B. Hawkins et al. [56] conclude that CCI has several phenotypes, including those associated not only with inflammation but also with the development of immunosuppression, or

a combination of inflammation and immunosuppression.

The differences identified by authors in a comparative study, including 29 patients with primary brain injuries (PBI) (traumatic brain injury (TBI), acute cerebrovascular accidents (ACVA)), and 121 patients without PBI allowed the authors to propose a neurometabolic type of CCI development characteristic of patients with brain injuries [60]. For this variant of CCI, on the first day of ICU admission patients with TBI/ACVA were characterized by higher levels of hemoglobin, hematocrit, lymphocyte count, total protein, and albumin, and lower levels of blood urea nitrogen, creatinine, and glucose compared to patients without PBI, while on the 20th day of hospital stay patients with brain injury had lower levels of blood calcium, creatinine, blood urea nitrogen, and glucose.

According to the study by E. M. Viglianti et al., patients with CCI are characterized by development of «new» organ failure in the long term [31]. The authors found that only 11 out of 50 patients with CCI did not develop new organ failure on days 4–14 of their stay in the ICU (ICU stay > 14 days was used as the criterion for CCI). A single organ system failure was documented in 15 (30%) patients with CCI, while in 24 (48%) patients organ failure involved more than one system. Cardiovascular failure was the most common — in 24 (61.5%) patients; respiratory failure — in 13 patients; renal failure — in 14 patients; liver failure — in 14 patients; and coagulopathy — in 5 patients. The causes of cardiovascular failure were sepsis in 19 of 27 cases, hypovolemia in 5 cases, cardiogenic causes in 2 cases, and tension pneumothorax in 1 case. 22 of the 50 patients were successfully extubated within 14 days of admission to the ICU (the median time to extubation was 5 days), and only 28 patients were on mechanical ventilation on the 15th day of their stay in the ICU. This allowed the authors to conclude that recurrent organ failure plays a greater role in CCI development than PMV, and focusing solely on the duration of ventilation may lead to an underestimation of CCI rate.

Similar findings were reported by T. Jeffcote et al. [18] — by the 10th day of ICU stay, more than 66% of patients with CCI were not on mechanical ventilation. At the same time, in patients with CCI, unlike in those without it, the authors observed treatment-resistant metabolic disorders significantly more often (in 12% and 3%, respectively), ventilator-associated pneumonia (in 21% and 1%, respectively), respiratory distress syndrome (in 10% vs 0%), liver failure (in 10% and 5%), systemic inflammatory response syndrome (in 57% and 14%), delirium (in 51% and 24%), and surgical complications (in 15% and 2%). Meanwhile, the incidence of critical illness myopathy was low in both groups — in patients with CCI (2 cases) and patients without CCI (1 case). The authors believe that CCI involves a cascade of interrelated pathophysiological processes affecting multiple systems and organs.

Conclusion

Improvements in intensive care practice have led to increasing the number of patients surviving ACI who develop a complex of new syndromes not related to CCI. Approaches to determining the time of CCI onset vary depending on the authors' views regarding the timing of the development of new functional deficits and the onset of new organ failure. Various subtypes of CCI may develop, characterized by a complex of indicators qualifying the states of protein and carbohydrate metabolism, immunosuppression, inflammation, and blood electrolyte composition, which influence the severity of its course.

Unified approaches are needed to define CCI, assess risk factors for its development, identify subtypes of progression, and detect characteristic organ dysfunction.

References

1. *Cox J.M.* Prolonged pediatric ventilatory assistance and related problems. *Crit Care Med.* 1973; 1 (3): 158–167. DOI: 10.1097/00003246-197305000-00011. PMID: 4585444.
2. *Girard K., Raffin T.A.* The chronically critically ill: to save or let die? *Respir Care.* 1985; 30 (5): 339–347. PMID: 10315661.
3. *Tagge G.F. Linacre Q.* 1975; 42 (2): 99–104. PMID: 11661177.
4. *Indihar F.J., Forsberg D.P.* Experience with a prolonged respiratory care unit. *Chest.* 1982; 81 (2): 189–192. DOI: 10.1378/chest.81.2.189. PMID: 6799254.
5. *Парфенов А. Л., Разживин В. П., Петрова М. В.* Хроническое критическое заболевание: современные аспекты проблемы (обзор). *Современные технологии в медицине.* 2022; 14 (3): 70–83. *Parfenov A. L., Razzhivin V. P., Petrova M. V.* Chronic critical illness: current aspects of the problem (review). *Modern Technologies in Medicine= Sovrem Tekhnologii Med.* 2022; 14 (3): 70–83. (in Russ.). DOI: 10.17691/stm2022.14.3.08.
6. *Ohbe H., Satoh K., Totoki T., Tanikawa A.,Shirasaki K., Kuribayashi Y., Tamura M., et al.; J-STAD (JAPAN Sepsis Treatment and Diagnosis) Study Group.* Definitions, epidemiology, and outcomes of persistent/chronic critical illness: a scoping review for translation to clinical practice. *Crit Care.* 2024; 28 (1): 435. DOI: 10.1186/s13054-024-05215-4. PMID: 39731183.
7. *Liberati A., Altman D.G., Tetzlaff J., Mulrow C., Gøtzsche P.C., Ioannidis J.P.A., Clarke M., et al.* The PRISMA statement for reporting systematic reviews and meta-analyses of studies that evaluate health care interventions: explanation and elaboration. *J Clin Epidemiol.* 2009; 62 (10): e1–34. DOI: 10.1016/j.jclinepi.2009.06.006. PMID: 19631507.
8. *Iwashyna T.J., Hodgson C.L., Pilcher D., Orford N., Santamaria J.D., Bailey M., Bellomo R.* Towards defining persistent critical illness and other varieties of chronic critical illness. *Crit Care Resusc.* 2015; 17 (3): 215–218. PMID: 26282262.
9. *Desarmenien M., Blanchard-Courtois A.L., Ricou B.* The chronic critical illness: a new disease in intensive care. *Swiss Med Wkly.* 2016: 146: w14336. DOI: 10.4414/smw.2016.14336. PMID: 27723899.
10. *Шестопалов А.Е., Яковлева А.В., Лукьянец О.Б., Петрова М.В.* Метаболические предикторы жизнеугрожающих состояний у больных в хроническом критическом состоянии. *Клиническое питание и метаболизм.* 2022; 3 (1): 38–49. *Shestopalov A.E., Yakovleva A.V., Lukyanets O.B., Petrova M.V.* Metabolic predictors of life-threatening conditions in patients in chronic critical illness. *Clinical Nutrition and Metabolism=Klinicheskoye Pitanie i Metabolizm.* 2022; 3 (1): 38–49. DOI: 10.17816/clinutr105625.
11. *Daly B., Phelps W., Rudy* E. A nurse-managed special care unit. *J Nur Adm.* 1991; (7–8): 31–38. PMID: 1870004.
12. *Carson S., Bach P.* The epidemiology and costs of chronic critical illness. *Crit Care Clin.* 2002; 18 (3): 461–476. DOI: 10.1016/s0749-0704 (02)00015-5. PMID: 12140908.
13. *MacIntyre N.R., Epstein S.K., Carson S., Scheinhorn D., Christopher K., Muldoon S.* Management of patients requiring prolonged mechanical ventilation: report of a NANDRC consensus conference. *Chest.* 2005; 128 (6): 3937–3954. DOI: 10.1378/chest.128.6.3937. PMID: 16354866.
14. *Zilberberg M.D., Luippold R.S., Sulsky S., Shorr A.F.* Prolonged acute mechanical ventilation, hospital resource utilization, and mortality in the United States. *Crit Care Med.* 2008; 36 (3): 724–30. DOI: 10.1097/CCM.0B013E31816536F7. PMID: 18209667.
15. *Hermans G., Van Aerde N., Meersseman P., Van Mechelen H., Debaveye Y., Wilmer A., Gunst J. et al.* Five-year mortality and morbidity impact of prolonged versus brief ICU stay: a propensity score matched cohort study. *Thorax.* 2019; 74 (11): 1037–1045. DOI: 10.1136/thoraxjnl-2018-213020. PMID: 31481633
16. *Iwashyna T.J., Hodgson C.L., Pilcher D., Bailey M., van Lint A., Chavan S., Bellomo R.* Timing of onset and burden of persistent critical illness in Australia and New Zealand: a retrospective, population-based, observational study. *Lancet Respir Med.* 2016; 4 (7): 566–573. DOI: 10.1016/S2213-2600(16)30098-4. PMID: 27155770.
17. *Bagshaw S.M., Stelfox H.T., Iwashyna T.J., Bellomo R., Zuege D., Wang X.* Timing of onset of persistent critical illness: a multi-centre retrospective cohort study Springer. *Intensive Care Med.* 2018; 44 (12): 2134–2144. DOI: 10.1007/s00134-018-5440-1. PMID: 30421256.
18. *Jeffcote T., Foong M., Gold G., Glassford N., Robbins R., Iwashyna T.J., Darvali J., et al.* Patient characteristics, ICU-specific supports, compli-

cations, and outcomes of persistent critical illness. *J Crit Care*. 2019; 54: 250–255. DOI: 10.1016/j.jcrc.2019.08.023. PMID: 31630075.
19. *Nierman D.M.* A structure of care for the chronically critically ill. *Crit Care Clin*. 2002; 18 (3): 477–491. DOI: 10.1016/s0749-0704 (02)00010-6. PMID: 12140909.
20. *Nelson J.E., Cox C.E., Hope A.A., Carson S.S.* Chronic critical illness. *Am J Respir Crit Care Med*. 2010; 182 (4): 446–454. DOI: 10.1164/rccm.201002-0210CI. PMID: 20448093.
21. *Kandilov A.M., Ingber M., Morley M., Coomer N., Dalton K.,Gage B., Superina C., et al.* Chronically Critically Ill Population Payment Recommendations (CCIP-PR). Final report. Research Triangle Park, NC: RTI International; 2014. 156 p. URL: https://www.cms.gov/priorities/innovation/Files/reports/ChronicallyCriticallyIllPopulation-Report.pdf. Accessed 05/06/2026.
22. «Реабилитация в отделении реанимации и интенсивной терапии (РеабИТ)» «Rehabilitation in the Department of Resuscitation and Intensive Care (ReabIT)» (in Russ.). (https://rehabrus.ru/ Docs/2021/MR-ReabIT_3.0.pdf.
23. *Белкин А.А., Рудник Е.Н., Белкин В.А., Нагаев Н.С., Пинчук Е.А., Рудник А.Е., Ткачук М.М.* Разработка и валидация ПИТС-индекса для оценки тяжести синдрома последствий интенсивной терапии: описательное проспективное не сравнительное когортное исследование. *Вестник интенсивной терапии имени А.И. Салтанова*. 2024; 4: 58–72. *Belkin A.A., Rudnik E.N., Belkin V.A., Nagaev N.S., Pinchuk E.A., Rudnik A.E., Tkachuk M.M.* Development and validation of the PICS index to assess the severity of the syndrome of consequences of intensive care: a descriptive prospective and unmatched cohort study. *AnnCritCare=Vestnik Intensivnoy Terapii imeni A.I. Saltanova*. 2024; 4: 58–72. (in Russ.).
24. *Voiriot G., Oualha M., Pierre A., Gandonnière C.S., Gaudet A., Jouan Y., Kallel H., et al.; la CRT de la SRLF.* Chronic critical illness and post-intensive care syndrome: from pathophysiology to clinical challenges. *Ann Intensive Care*. 2022; 12 (1): 58. DOI: 10.1186/s13613-022-01038-0. PMID: 35779142.
25. *Shaw M., Viglianti E.M., McPeake J., Bagshaw S.M., Pilcher D., Bellomo R., Iwashyna T.J., et al.* Timing of onset, burden, and postdischarge mortality of persistent critical illness in Scotland, 2005–2014: a retrospective, population-based, observational study. *Crit Care Explor*. 2020; 2 (4): e0102. DOI: 10.1097/CCE.0000000000000102. PMID: 32426744
26. *Viglianti E.M., Bagshaw S.M., Bellomo R., McPeake J.,Wang X.Q., Seelye S., Iwashna T.J.* Hospital-level variation in the development of persistent critical illness. *Intensive Care Med*. 2020; 46 (8): 1567–1575. DOI: 10.1007/s00134-020-06129-9. PMID: 32500182.
27. *Van den Berghe G.* On the neuroendocrinopathy of critical illness. Perspectives for feeding and novel treatments. *Am J Respir Crit Care Med*. 2016; 194 (11): 1337–1348. DOI:10.1164/rccm.201607-1516CI. PMID: 27611700.
28. *Lone N.I., Walsh T.S.* Prolonged mechanical ventilation in critically ill patients: epidemiology, outcomes and modelling the potential cost consequences of establishing a regional weaning unit. *Crit Care*. 2011; 15 (2): R102. DOI: 10.1186/cc10117. PMID: 21439086.
29. *Ohbe H., Matsui H., Fushimi K., Yasunaga H.* Epidemiology of chronic critical illness in Japan: a nationwide inpatient database study. *Crit Care Med*. 2021; 49 (1): 70–78. DOI: 10.1097/CCM.0000000000004723. PMID: 33177360.
30. *Chadda K.R., Puthucheary Z.* Persistent inflammation, immunosuppression, and catabolism syndrome (PICS): a review of definitions, potential therapies, and research priorities. *Br J Anaesth*. 2024; 132 (3): 507–18. DOI: 10.1016/j.bja.2023.11.052. PMID: 38177003.
31. *Viglianti E.M., Kramer R., Admon A.J., Sjoding M.W., Hodgson C.L., Bellomo R., Iwashyna T.J.* Late organ failures in patients with prolonged intensive care unit stays. *J Crit Care*. 2018; 46: 55–57. DOI: 10.1016/j.jcrc.2018.03.029. PMID: 29684773.
32. *Darvall J.N., Bellomo R., Bailey M., Young P.J., Rockwood K., Pilcher D.* Impact of frailty on persistent critical illness: a population-based cohort study. *Intensive Care Med*. 2022; 48 (3): 343–351. DOI: 10.1007/s00134-022-06617-0. PMID: 35119497.
33. *Rockwood K., Song X., MacKnight C., Bergman H., Hogan D.B., McDowell I., Mitnitski A.* A global clinical measure of fitness and frailty in elderly people. *CMAJ*. 2005; 173 (5): 489–495. DOI: 10.1503/cmaj.050051. PMID: 16129869.
34. *Okahara S., Subramaniam A., Darvall J.N. , Ryo Ueno R., Bailey M.M., David V. Pilcher D.V.* The relationship between frailty and mechanical ventilation: a population-based cohort study. *Ann Am Thorac Soc*. 2022; 19 (2): 264–271. DOI: 10.1513/AnnalsATS.202102-178OC. PMID: 34214022.

35. *Loss S.H., Marchese C.B., Boniatti M.M., Wawrzeniak I.C., Oliveira R.P., Nunes L.N., Victorino J.A.* Prediction of chronic critical illness in a general intensive care unit. *Rev Assoc Med Bras* (1992). 2013; 59 (3): 241–247. DOI: 10.1016/j.ramb.2012.12.002. PMID: 23680275.
36. *Jaiswal S., Sadacharam K., Shrestha R.R., Bhatta P., Ghimire R.K., Rimal A., Berhane Z., et al.* External validation of prognostic model of one-year mortality in patients requiring prolonged mechanical ventilation. *J Nepal Health Res Counc.* 2012; 10 (1): 47–51. PMID: 22929637.
37. *Feijó C.A.R., Borges A.E.P.P., da Cunha E.Q., de Meneses F.A., Albuquerque M.P., Natália LP Aragão N.L.P., Pinheiro T.O., et al.* Chronic critical illness: reason for concern during and after ICU admission!. *Crit Care.* 2015; 19 (Suppl 2): P20. DOI: 10.1186/cc14674.
38. *Mira J.C., Brakenridge S.C., Moldawer L.L., Moore F.A.* Persistent inflammation, immunosuppression and catabolism syndrome. *Crit Care Clin.* 2017; 33 (2): 245–258. DOI: 10.1016/j.ccc.2016.12.001. PMID: 28284293.
39. *Carson S.S., Garrett G., Hanson L.C., Lanier J., Govert J., Brake M.C., Landucci D.L., et al.* A prognostic model for one-year mortality in patients requiring prolonged mechanical ventilation *Crit Care Med.* 2008; 36 (7): 2061–9. DOI: 10.1097/CCM.0b013e31817b8925. PMID: 18552692.
40. *Udeh C.I., Hadder B., Udeh B.L.* Validation and extension of the prolonged mechanical ventilation prognostic Mmodel (ProVent) ccore for predicting 1-year mortality after prolonged mechanical ventilation. *Ann Am Thorac Soc.* 2015; 12 (12): 1845–51. DOI: 10.1513/AnnalsATS.201504-200OC. PMID: 26418231.
41. *Dibiasi C., Kimberger O., Bologheanu R., Staudinger T., Heinz G., Zauner C., G., et al.* External validation of the ProVent score for prognostication of 1-yearmortality of critically ill patients with prolonged mechanical ventilation: a single-centre, retrospective observational study in Austria. *BMJ Open.* 2022; 12 (9): e066197. DOI: 10.1136/bmjopen-2022-066197. PMID: 36127078.
42. *Hough C.L., Caldwell E.S., Cox C.E. ., Douglas I.S., Kahn J.M., White D.B., Seeley E.J.; the ProVent Investigators and the National Heart Lung and Blood Institute's Acute Respiratory Distress Syndrome Network.* Development and validation of a mortality prediction model for patients receiving 14 days of mechanical ventilation. *Crit Care Med.* 2015; 43 (11): 2339–2345. DOI: 10.1097/CCM.0000000000001205. PMID: 26247337.
43. *Darvall J.N., Boonstra T., Norman J., Murphy D., Bailey M., Iwashyna T.J., Bagshaw S.M., et al.* Persistent critical illness: baseline characteristics, intensive care course, and cause of death. *Crit Care Resusc.* 2019; 21 (2): 110–118. PMID: 31142241.
44. *Unroe M., Kahn J.M., Carson S.S., Govert J.A., Martinu T., Sathy S.J., Clay A.S., et al.* One year trajectories of care and resource utilization for recipients of prolonged mechanical ventilation: a cohort study. *Ann Intern Med.* 2010; 153 (3): 167–175. DOI: 10.7326/0003-4819-153-3-201008030-00007. PMID: 20679561.
45. *Marchioni A., Tonelli R., Sdanganelli A., Gozzi F., Musaro L.,Fantini R., Tabbi L., et al.* Prevalence and development of chronic critical illness in acute patients admitted to a respiratory intensive care setting. *Pulmonology.* 2020; 26 (3): 151–158. DOI: 10.1016/j.pulmoe.2019.09.006. PMID: 31672594.
46. *Ершов В.И., Белкин А.А., Горбачев В.И., Грицан А.И., Заболотских И.Б., Лебединский К.М., Лейдерман И.Н., с совт.* Российское многоцентровое обсервационное клиническое исследование «Регистр респираторной терапии у пациентов с ОНМК (RETAS)»: инфекционные осложнения при искусственной вентиляции легких. *Анестезиология и реаниматология.* 2023; 1: 19–25. *Ershov V.I., Belkin A.A., Gorbachev V.I., Gritsan A.I., Zabolotskikh I.B., Lebedinsky K.M., Leyderman I.N., et al.* Russian multicenter observational clinical study «Register of Respiratory Therapy in Patients with Ischemic Stroke (RETAS)»: infectious complications of mechanical ventilation. *Russian Journal of Anaesthesiology and Reanimatology = Anesteziologiya i Reanimatologiya.* 2023; 1: 19–25. (in Russ.). DOI: 10.17116/anaesthesiology202301119.
47. *Ершов В.И., Лейдерман И.Н., Белкин А.А., Горбачев В.И., Грицан А.И., Лебединский К.М., Петриков С.С., с совт* Распространенность и влияние белково-энергетической недостаточности на осложнения и исход тяжелого инсульта, требующего респираторной поддержки: многоцентровое проспективное наблюдательное исследование. *Вестник интенсивной терапии им. А. И. Салтанова.* 2024; 1: 58–68. *Ershov V.I., Leyderman I.N., Belkin A.A., Gorbachev V.I., Gritsan A.I., Lebedinsky K.M., Petrikov S.S., et al.* Protein-energy malnutrition prevalence and influence on complications and outcome of severe stroke requiring mechanical ventilation: a multicenter prospective observational trial. *Ann Crit Care= Vestnik Intensivnoy Terapii im. A. I. Saltanova.* 2024; 1: 58–68. (in Russ.). DOI: 10.21320/1818-474X-2024-1-58-68.

48. *Téblick A., Langouche L., Van den Berghe G.* Anterior pituitary function in critical illness. *Endocr Connect*. 2019; 8 (8): R131– R143. DOI: 10.1530/EC-19-0318. PMID: 31340197.
49. *Boonen E., van den Berghe G.* Endocrine responses to critical illness: novel insights and therapeutic implications. *J Clin Endocrinol Metab*. 2014; 99 (5): 1569–1582. DOI: 10.1210/jc.2013-4115. PMID: 24517153.
50. *Schmidt H., Hoyer D., Wilhelm J., Söffker G., Heinroth K., Hottenrott K., Said S.M., et al.* The alteration of autonomic function in multiple organ dysfunction syndrome. *Crit Care Clin*. 2008; 24 (1): 149–163,ix. DOI: 10.1016/j.ccc.2007.10.003. PMID: 18241783.
51. *Wang W., Xu C., Ma X., Zhang X., Xie P.* Intensive care unit-acquired weakness: a review of recent progress with a look toward the future. *Front Med (Lausanne)*. 2020; 7: 559789. DOI: 10.3389/fmed.2020.559789. PMID: 33330523.
52. *Macintyre N.R.* Chronic critical illness: the growing challenge to health care. *Respir Care*. 2012; 57 (6): 1021–1027. DOI: 10.4187/respcare.01768. PMID: 22663975.
53. *Pandharipande P.P., Girard T.D., Jackson J.C, Morandi A., Thompson J.L., Pun B.T., Brummel N.E., et al.; BRAIN-ICU Study Investigators.* Long-term cognitive impairment after critical illness. *N Engl J Med*. 2013; 369 (14): 1306–1316. DOI: 10.1056/NEJMoa1301372. PMID: 24088092.
54. *Cox C.E.* Persistent systemic inflammation in chronic critical illness. *Respir Care*. 2012; 57 (6): 859–864. DOI: 10.4187/respcare.01719. PMID: 22663963.
55. *Gentile L.F., Cuenca A.G., Efron P.A., Ang D., Bihorac A., McKinley B.A., Moldawer L.L., et al.* Persistent inflammation and immunosuppression: a common syndrome and new horizon for surgical intensive care. *J Trauma Acute Care Surg*. 2012; 72 (6): 1491–1501. DOI: 10.1097/TA.0b013e318256e000. PMID: 22695412.
56. *Hawkins R.B., Raymond S.L., Stortz J.A., Hiroguchi H., Brakenridge S.C., Gardner A., Efron P.A., et al.* Chronic critical illness and the persistent inflammation, immunosuppression, and catabolism syndrome. *Front Immunol*. 2018; 9: 1511. DOI: 10.3389/fimmu.2018.01511. PMID: 30013565.
57. *Zhou Q., Qian H., Yang A., Lu J., Liu J.* Clinical and prognostic features of chronic critical illness/persistent inflammation immunosuppression and catabolism patients: a prospective observational clinical study. *Shock*. 2023; 59 (1): 5–11. DOI: 10.1097/SHK.0000000000002035. PMID: 36383370.
58. *Likhvantsev V.V., Berikashvili L.B., Yadgarov M.Y., Yakovlev A.A., Kuzovlev A.N.* The tri-steps model of critical conditions in intensive care: introducing a new paradigm for chronic critical illness. *J Clin Med*. 2024; 13: 3683. DOI: 10.3390/jcm13133683. PMID: 38999249.
59. *Hesselink L., Hoepelman R.J., Spijkerman R., de Groot M.C.H., van Wessem K.J.P., Koenderman L., Leenen L.P.H., et al.* Persistent inflammation, immunosuppression and catabolism syndrome (PICS) after polytrauma: a rare syndrome with major consequences. *J Clin Med*. 2020; 9 (1): 191. DOI: 10.3390/jcm9010191. PMID: 31936748.
60. *Berikashvili L.B., Shestopalov A.E., Polyakov P.A., Yakovleva A.V., Yadgarov M.Y., Kuznetsov I.V., Said M.T.S.M., et al.* The neurological metabolic phenotype in prolonged/chronic critical illness: propensity score matched analysis of nutrition and outcomes. *Nutrients*. 2025; 17 (14): 2302. DOI: 10.3390/nu17142302. PMID: 40732927.

Received 11.02.2026
Accepted 13.05.2026
Online First 15.06.2026

The Instructions for Authors on the Design of References Sections (Updated 2025.04.21)

Novelty of sources

The discussion of research findings and the formulation of conclusions must be based on current scientific evidence. Therefore, it is recommended that at least 70% of the sources cited be published within the last five years, and no less than 30% within the last three years. An over-reliance on references older than ten years diminishes the relevance of the article and may significantly reduce its citation potential, as the analysis may not reflect current scientific perspectives.

Diversity and quantity of sources

A comprehensive and impartial discussion of the topic requires a broad and diverse range of sources, including both domestic and international publications. This diversity enhances the analytical depth and objectivity of the manuscript. Authors are encouraged to include references from a wide range of leading national journals in the relevant field to avoid bias resulting from the editorial policies of individual publications. The same recommendation applies to the international literature.

The suggested number of references is based on expert consensus regarding the amount of material necessary to adequately present the topic in the introduction, support a thorough discussion of the results, and justify the conclusions.

Recommended number of references by article type

- Original research articles: 25–45 references
- Short communications: 10–25 references
- Review articles: 80–120 references

Unacceptable sources

The following types of references are not permitted in the bibliography:

- Dissertations and dissertation abstracts whose main content is presented in the publications listed in the bibliography of the abstract. References to these published works are considered more appropriate. An exception is made for dissertations that include unpublished parts of the research. In such cases, when citing the dissertation, the author must clearly indicate that the referenced material has not been previously published.
- Conference abstracts that are generally considered preliminary or final summaries of work in progress unless they present original results that have not been published elsewhere or contain substantial preliminary results that are later developed in the article.
- Textbooks and dictionaries because they are educational rather than scientific in nature, synthesize data from individual articles and monographs without incorporating the most recent scientific findings. *Citing the original sources referenced in textbooks is a more accurate and effective way to support scientific claims and allows for more precise topic-specific literature searches.*

These guidelines are consistent with internationally accepted standards for scholarly referencing.

The ***reference list*** should follow all sections of the manuscript and be preceded by two line breaks. Each source must begin on a new line and be numbered consecutively in the order in which it is cited in the text — not alphabetically by author's last name.

When individual authors are mentioned in the text, their initials should precede their surnames. In-text citations should be indicated by Arabic numerals in square brackets (e. g., [1], [2]). For online sources, the full URL (Uniform Resource Locator) must be provided in the following format: protocol://hostname/filename.

The ***format for each reference*** should follow this order:

- Author(s): if there are seven or fewer, list all authors; if there are more than seven, list the first seven followed by et al.
- Title of the article or book.
- Publication details.
- If editors or compilers are cited instead of authors, their names should be followed by (ed.).

Here are specific formats for citing various types of references.

When citing a book:

Author(s). Title of the Book. Edition (if not the first). Place of publication: Publisher; Year: page range. ISBN.

Example: Murray PR, Rosenthal KS, Pfaller MA. Medical Microbiology. 9th ed. Philadelphia: Elsevier; 2020:15–35. ISBN: 9780323674508.

When citing a book chapter:

Author(s) of the chapter. Title of the chapter. In: Editor(s), ed(s). Title of the Book. Edition (if applicable). Place of publication: Publisher; Year: page range. ISBN.

Example: Kumar V, Abbas AK, Aster JC. Inflammation and Repair. In: Kumar V, Abbas AK, Aster JC, eds. Robbins and Cotran Pathologic Basis of Disease. 10th ed. Philadelphia: Elsevier; 2021:69–110. ISBN: 9780323531139.

When citing an electronic book:

Author(s). Title of the Book. Edition. [eBook]. Place of publication: Publisher; Year. Available from: URL. Accessed [date].

Example: Hall JE. Guyton and Hall Textbook of Medical Physiology. 14th ed. [eBook]. Philadelphia: Elsevier; 2020. Available from: https://www.clinicalkey.com. Accessed April 15, 2025.

For non-English works, provide transliterated title (italicized) and add translation in brackets if necessary.

In references to journal articles, the authors' last names and initials must be italicized (see the rules described above for listing authors by number). The article title is followed by the journal title — also italicized — then the year, volume (using Arabic numerals only), issue number, and page range (from-to). Each of the following elements — article title and journal title — should be followed by a period.

Abbreviated titles of international journals should follow the nomenclature used in PubMed (see examples). At the end of each reference, include the article's DOI and PMID (if available). These identifiers provide access to the original source with a full list of authors and can be obtained from the PubMed website: http://www.ncbi.nlm.nih.gov/pubmed/.

If the identifiers are not listed in PubMed, they can be found at: http://www.ncbi.nih.gov/entrez/query.fcgi?db

http://www.crossref.org/guestquery/

Example: Brunkhorst F.M., Engel C., Bloos F., Meier-Hellmann A., Ragaller M., Weiler N., Moerer O., Gruendling M., Oppert M., Grond S., Olthoff D., Jaschinski U., John S., Rossaint R., Welte T., Schaefer M., Kern P., Kuhnt E., Kiehntopf M., Hartog C., Natanson C., Loeffler M., Reinhart K. German Competence Network Sepsis (SepNet). Intensive insulin therapy and pentastarch resuscitation in severe sepsis. N Engl J Med. 2008; 358 (2): 125–139. http://dx.doi.org/10.1056/NEJMoa070716. PMID: 1818495

The Instructions for Authors on the Materials and Methods Sections (Updated 2026.06.22)

This section should contain the inclusion and exclusion criteria for the study material and a rationale for the research methods chosen. If the study was conducted as part of a specific program, the name of the program should be provided. If the clinical and research components were conducted in different institutions, the name of the institution from which the research material was obtained must be provided.

Information on the informed consent of patients to participate in the study and to the publication of anonymized results must be provided. References to documents that regulate the use of laboratory animals and the conduct of experiments with them should be provided. In addition, the quantitative and qualitative characteristics of the patients/subjects or laboratory animals included in the study, the study design, and the clinical, laboratory, instrumental, experimental, and other methods used, including statistical methods for data analysis, should be described. If artificial intelligence (AI) was used in the preparation of the material, the name and version of the AI model(s) should be provided, along with details of the parts of the study to which the AI contributed.

When describing the research methods, the following should be included:

- **Research design:** Provide a detailed description of the study design.
- **Location and duration:** Indicate the location and time period during which the study was conducted.
- **Inclusion and exclusion criteria:** Include criteria for selection and exclusion of participants (for clinical trials).
- **Randomization and blinding:** If applicable, describe the randomization and blinding methods used (for randomized trials).
- **Patient selection flowchart:** Include a flowchart outlining the process for selecting patients for the study (for clinical trials).
- **Statistical Methods:** Provide sufficient detail about the statistical tests used, including the name and version of the statistical software package used, so that readers can reproduce the results using the original data.
- **Study aim and hypothesis:** Clearly state the research aim and hypothesis, as well as the endpoints of the study.
- **Normality Test:** State the method used to test the normality of the data distribution. For parametric methods, state whether the major statistical assumptions were met.
- **Analysis of categorical variables:** For low-frequency events, use Fisher's exact test or the asymptotic chi-squared test with appropriate corrections (e. g., Yates' correction). The standard chi-squared test should only be performed with a sufficiently large sample size and number of events.
- **P Values:** Report exact *P* values for statistical tests (for values less than 0.001, use the format «$P > 0.001$»). Report *P* values in figure or table legends, clearly indicating the control groups.
- **Sample size calculation:** For prospective studies, describe the a priori sample size calculation. Power should be at least 80%.
- **Reporting of quantitative variables:** For the presentation of values of quantitative (continuous) variables, it is recommended to use the format mean ± *SD* (for normally distributed parameters) or medians and quartiles (*Q1*, *Q3*).

Information on the use/non-use of artificial intelligence (AI) should be included at the end of the «Materials and Methods» section (following the statistical data processing description) as a subsection «Information on the Use of Artificial Intelligence» The subsection should include:

- name of the AI model(s) and version(s);
- list of the article sections (including illustrations, bibliography) and technical operations (style improvement, translation, etc.) in which AI was used;
- key queries in the AI instructions(s) (the basis of the prompt(s).

A copy(s) of the full prompt(s) should be provided upon request by the reviewer or editor if clarification of the semantic logic of the text generated using AI may be required.

The use of AI is not permitted in the formulation of the research and/or practical goals of the work, the discussion of the results, and the drawing of conclusions.

If the authors prepared the article materials without the help of AI, then the corresponding subsection notes: «Artificial intelligence was not used in the preparation of the article».

Basic information for the manuscript submission (v. Jule 22, 2026)

1. Initial submission

Authors should submit a single Word file containing the complete manuscript. Language of submission: Russian — for Russian-speaking authors. English — for non-Russian-speaking authors.

The file must include the following components:

- Title of the paper
- Full names of all authors
- Institutional affiliations of all authors
- Full manuscript text, including all sections
- Tables, figures, and photographs with captions and explanatory note
- Reference list

2. File Naming Format

Name the file using the first author's last name and the submission date in the format: LastName_YYYYMMDD.docx . For revised versions, only the date should be updated.

3. Manuscript Length

Original article: approximately 40,000 characters with spaces

Short communication: no more than 2,500 words

Review or meta-analysis: between 25,000 and 40,000 characters with spaces

4. Title Page Information

Title: must not exceed 12 words

Authors: full names (e. g., Peter A. Johnson)

Affiliations: full institutional names and postal addresses with zip code

Corresponding author: full name, email address, and phone number

5. Structure of summary, body text, References

Summary (Abstract): must be between 250 and 300 words and structured into the following sections:

- Introduction (background / scope of the problem)
- Aim
- Materials and Methods
- Results
- Conclusion

Highlights (optional): one to three main messages may be presented either in textual or infographic form. Text highlights should not exceed 40 words each.

Keywords: 6–8 keywords, separated by semicolons (;). Do not place a period at the end.

Post-keyword Informational Sections:

- Conflict of interest
- Study funding
- Acknowledgements (optional)
- Information about the Authors (ID, contributions)

Body text:

- Introduction (Background)
- Materials and Methods (information on the use / non-use of artificial intelligence must be included)
- Results
- Discussion
- Conclusion

References: at least 70% of the references should be published within the last 5 years, and at least 30% within the last 3 years. Number of references: original articles — 25 to 45; short communications — 10 to 25; reviews — 80 to 120. Formatting: must comply with the Author Guidelines «3.14. References» section.

Illustrations (including tables): for original articles — up to 8; for short communications — up to 3; for reviews — up to 8.

6. Formatting

Font: Times New Roman, 12 pt. Section headings: bold. Line spacing: 5. Paragraph formatting: no extra space before or after paragraphs; one additional line between sections. First-line indent: 1.25 cm. Margins: 2.5 cm on all sides. Page numbers: bottom right corner of each page

2231 десятилетие науки и технологий

Министерство науки и высшего образования Российской Федерации

Российская Академия Наук

ФНКЦ РР

1936 2026 90 ЛЕТ
Федеральный научно-клинический центр реаниматологии и реабилитологии (ФНКЦ РР)
Научно-исследовательский институт общей реаниматологии имени В.А. Неговского ФНКЦ РР

Федерация анестезиологов и реаниматологов

XXVIII Всероссийская конференция с международным участием

ЖИЗНЕОБЕСПЕЧЕНИЕ ПРИ КРИТИЧЕСКИХ СОСТОЯНИЯХ

16-17 октября 2026 г. | Москва

ТЕМАТИКИ КОНФЕРЕНЦИИ

- Доказательная медицина критических состояний
- Дыхательная недостаточность и респираторная поддержка
- Иммунология и генетика критических состояний
- Искусственный интеллект и цифровая трансформация в реаниматологии
- Критические состояния в акушерстве
- Критические состояния в педиатрии
- Метаболизм и нутритивная поддержка при критических состояниях
- Мониторинг микроциркуляции при критических состояниях
- Нейроанестезиология, нейрореаниматология
- Неотложная кардиология и неврология
- Общая патология хронических критических состояний
- Организация медицинской помощи в экстремальных условиях удаленных промышленных объектов
- Органопротекция при критических состояниях
- Остановка кровообращения и сердечно-легочная реанимация
- Персонализация в медицине критических состояний
- Ранняя нейрореабилитация пациентов в критических состояниях
- Сепсис
- Сестринское дело в анестезиологии-реаниматологии
- Экспериментальные исследования в реаниматологии
- Экстракорпоральная мембранная оксигенация

ФОРМАТ И МЕСТО ПРОВЕДЕНИЯ

Очно — Международный мультимедийный пресс-центр «РИА Новости», г. Москва, Зубовский бульвар, 4

CRITICALCONF.RU

Тел.: +7 (499) 390 34 38
E-mail: criticalconf@confreg.org

Научно-исследовательский институт общей реаниматологии им. В.А. Неговского ФНКЦ РР

Ассоциация анестезиологов-реаниматологов

Ассоциация детских анестезиологов-реаниматологов России
Russian Pediatric Anesthesiologists and Reanimatologists Association

Региональная общественная организация медицинских сестер г. Москва

Ассоциация анестезиологов и реаниматологов Узбекистана

Фонд «Медицина критических состояний»

НСР Национальный совет по реанимации

Общество по изучению шока (России) SSS(R) Society for Shock Studies (Russia)